REPORT DOCUMENTATION PAGE

1a Report Security Classification: Unclassified		1b Restrictive Markings	
2a Security Classification Authority		3 Distribution/Availability of Report	
2b Declassification/Downgrading Schedule		Approved for public release; distribution is unlimited.	
4 Performing Organization Report Number(s)		5 Monitoring Organization Report Number(s)	
6a Name of Performing Organization Naval Postgraduate School	6b Office Symbol *(if applicable)* MR	7a Name of Monitoring Organization Naval Postgraduate School	
6c Address *(city, state, and ZIP code)* Monterey CA 93943-5000		7b Address *(city, state, and ZIP code)* Monterey CA 93943-5000	
8a Name of Funding/Sponsoring Organization	6b Office Symbol *(if applicable)*	9 Procurement Instrument Identification Number	
Address *(city, state, and ZIP code)*		10 Source of Funding Numbers	
		Program Element No / Project No / Task No / Work Unit Accession No	

11 Title *(include security classification)* AN INVESTIGATION OF THE ERICA IOP-5A CYCLONE

12 Personal Author(s) Spinelli, Julia M.

13a Type of Report	13b Time Covered From To	14 Date of Report *(year, month, day)*	15 Page Count
Master's Thesis		December 1992	114

16 Supplementary Notation The views expressed in this thesis are those of the author and do not reflect the official policy or position of the Department of Defense or the U.S. Government.

17 Cosati Codes			18 Subject Terms *(continue on reverse if necessary and identify by block number)*
Field	Group	Subgroup	Experiment on Rapidly Intensifying Cyclones over the Atlantic (ERICA) IOP-5A, rapid cyclogenesis, NORAPS, mesoscale coastal cyclogenesis.

19 Abstract *(continue on reverse if necessary and identify by block number)*

A synoptic investigation was conducted of the rapid coastal cyclogenesis event that occurred during Intensive Observation Period (IOP) 5A of the Experiment on Rapidly Intensifying Cyclones over the Atlantic (ERICA). Navy Operational Regional Analysis and Prediction System (NORAPS) objective analyses, utilizing operationally available and some special ERICA data, were examined in order to study the environment in which rapid development took place and to determine key synoptic and subsynoptic features important in the evolution of this storm. Additionally, the ability of NORAPS to accurately simulate the rapid cyclogenesis was investigated.

Several processes contributed to the storm's intense development including strong low tropospheric temperature advection and upper-level cyclonic vorticity advection and divergence associated with a mobile trough and jet streak. NORAPS forecasts initialized 12 h prior to the explosive deepening phase of the IOP-5A cyclone provided a reasonably accurate simulation of the event. However, subjective hand analyses of hourly data for the period surrounding the onset of rapid deepening revealed the presence of a mesoscale coastal cyclone, which influenced the development of the storm. The development of this separate cyclone was not resolved by the model, resulting in a forecast track north of the actual storm's path.

20 Distribution/Availability of Abstract	21 Abstract Security Classification	
xx unclassified/unlimited __ same as report __ DTIC users	Unclassified	
22a Name of Responsible Individual Wash, Carlyle H.	22b Telephone *(include Area Code)* (408) 656-2295	22c Office Symbol MR/Wx

DD FORM 1473,84 MAR 83 APR edition may be used until exhausted
All other editions are obsolete

Approved for public release; distribution is unlimited.

An Investigation of the ERICA IOP-5A Cyclone

by

Julia M. Spinelli
Lieutenant, United States Navy
B.S., United States Naval Academy, 1985

Submitted in partial fulfillment
of the requirements for the degree of

MASTER OF SCIENCE IN METEOROLOGY AND PHYSICAL OCEANOGRAPHY

from the

NAVAL POSTGRADUATE SCHOOL
December 1992

ABSTRACT

A synoptic investigation was conducted of the rapid coastal cyclogenesis event that occurred during Intensive Observation Period (IOP) 5A of the Experiment on Rapidly Intensifying Cyclones over the Atlantic (ERICA). Navy Operational Regional Analysis and Prediction System (NORAPS) objective analyses, utilizing operationally available and some special ERICA data, were examined in order to study the environment in which rapid development took place and to determine key synoptic and subsynoptic features important in the evolution of this storm. Additionally, the ability of NORAPS to accurately simulate the rapid cyclogenesis was investigated.

Several processes contributed to the storm's intense development including strong low tropospheric temperature advection and upper-level cyclonic vorticity advection and divergence associated with a mobile trough and jet streak. NORAPS forecasts initialized 12 h prior to the explosive deepening phase of the IOP-5A cyclone provided a reasonably accurate simulation of the event. However, subjective hand analyses of hourly data for the period surrounding the onset of rapid deepening revealed the presence of a mesoscale coastal cyclone, which influenced the development of the storm. The development of this separate cyclone was not

resolved by the model, resulting in a forecast track north of the actual storm's path.

TABLE OF CONTENTS

LIST OF FIGURES

ACKNOWLEDGMENTS

I would like to extend my most sincere thanks to Professor Carlyle Wash for sharing his wisdom and experience with me and for the guidance he provided in support of my thesis research. I also want to thank Professor Paul Hirschberg for his technical expertise, constructive criticism and assistance in this study. Additionally, thanks are due to Mr. Rolf Langland (and the Naval Research Laboratory Monterey in general) for preparing the ERICA IOP-5A NORAPS analyses and NORAPS forecasts studied in this thesis.

Finally, I would like to express my appreciation to Ms. Mary Jordan for her tireless efforts in cataloging the ERICA data, accessing the observations and providing answers to all of my questions concerning the data set with which I was working.

I. INTRODUCTION

A. THE SIGNIFICANCE OF RAPID CYCLOGENESIS

Extratropical cyclones that undergo explosive development can pose significant hazards to seagoing vessels. Thus, they represent a critical forecast problem for meteorologists in maritime and coastal areas. Because of their unusual nature, these extreme weather events pique the interest of meteorologists, mariners and the general public alike. Without adequate early warning of the storm's approach, damage to property and loss of life can result.

Explosive cyclogenesis remains a challenging forecast for numerical weather prediction due to limitations in our understanding of the physical processes (and their complex interactions) that lead to such rapidly developing storms. The reasons for forecast difficulty include problems with model parameterization of surface and boundary layer fluxes and effects of cumulus convection, inadequate model resolution and poor initial conditions. Also the lack of maritime observations significantly hinders the analysis and prediction of oceanic rapid cyclogenesis.

B. RECENT CLIMATOLOGICAL STUDIES/RESEARCH PROJECTS

While the fundamental cyclogenetic processes are generally well documented and recognized (e.g., Uccellini 1990), the

manner in which they combine to produce a rapidly deepening cyclone is still uncertain. Thus, numerous case studies and model sensitivity studies have been conducted in an effort to further our comprehension of those physical and dynamical atmospheric processes responsible for rapid cyclogenesis. The climatological, synoptic study of explosively deepening systems by Sanders and Gyakum (1980) sparked the recent interest in this area. They defined the meteorological "bomb" or explosively developing storm as one that experiences a fall in sea level pressure at a rate of at least 1 mb h^{-1} for 24 h (a definition attributed to Tor Bergeron). This rate was based on a latitude of 60N. Multiplying by a factor of sin ϕ/sin 60 geostrophically adjusts this deepening rate for any latitude ϕ.

Using this rate to classify storms as explosive or nonexplosive deepeners, Sanders and Gyakum (1980) found that the explosive cyclogenesis events occurred primarily during the cold season (September through April in the Northern Hemisphere) and were most likely to develop over or just north of the Kuroshio Current (western Pacific Ocean) and Gulf Stream (western Atlantic Ocean). Another climatological study done by Rogers and Bosart (1986) used data from 328 storms to create three-dimensional composites of the development stages of Atlantic explosive cyclones and a composite sounding of the environment near Pacific Ocean rapid deepeners. They found that strong baroclinicity, low-level conditional instability

and intense upward motion are characteristics of the intense development.

Several large-scale field experiments focusing on rapid cyclogenesis have been conducted in recent years. These efforts include the Genesis of Atlantic Lows Experiment (GALE), the Canadian Atlantic Storms Program (CASP) and the Experiment on Rapidly Intensifying Cyclones over the Atlantic (ERICA). GALE was conducted from 15 January to 15 March 1986 and concentrated on studying East Coast winter storms, their heavy precipitation systems and mesoscale structure and numerical simulation and prediction models (Dirks et al. 1988). CASP was conducted parallel to GALE, but over the Canadian Atlantic Provinces. It also emphasized the oceanic response to intense low pressure systems on the synoptic and mesoscale (Stewart et al. 1987).

C. THE EXPERIMENT ON RAPIDLY INTENSIFYING CYCLONES OVER THE ATLANTIC (ERICA)

The ERICA study was concentrated over the data-sparse oceanic region of the western North Atlantic Ocean, and was conducted during December 1988 through February 1989 (Hadlock et al. 1989). A complex, multi-platform, multi-agency observing system was employed in order to maximize the data set obtained during the field phase of the study. Special observation platforms utilized in the experiment include research aircraft provided by the U.S. Air Force, U.S. Navy,

the National Center for Atmospheric Research (NCAR) and the National Oceanic and Atmospheric Agency (NOAA), moored and air-deployed drifting buoys, coastal marine (C-man) stations, ships of opportunity and supplemental rawinsonde soundings.

Hadlock and Kreitzberg (1988) stated that the ERICA objectives were to:

(i) Understand the fundamental physical processes occurring in the atmosphere during rapid intensification of cyclones at sea;

(ii) Determine those physical processes that need to be incorporated into dynamical prediction models through efficient parameterization if necessary; and

(iii) Identify measurable precursors that must be incorporated into the initial analysis for accurate and detailed operational model predictions.

To accomplish these objectives, data was collected during eight Intensive Observation Periods (IOP's) that lasted approximately 36 h each. The area for the ERICA study was chosen to encompass the climatologically preferred area for rapid cyclogenesis as determined by Sanders and Gyakum (1980), Roebber (1984) and Hadlock and Kreitzberg (1988) (Figure 1). An IOP was considered when storms within the study area were predicted to meet the criterion of explosive deepening of at least 10 mb $(6\ h)^{-1}$ for at least 6 h.

During the course of the experiment, an extensive data base detailing rapid cyclogenesis was amassed. Following the ERICA objectives, the focus of this thesis is to examine the data collected during IOP-5A in order to gain insight as to the processes contributing to the rapid development of this

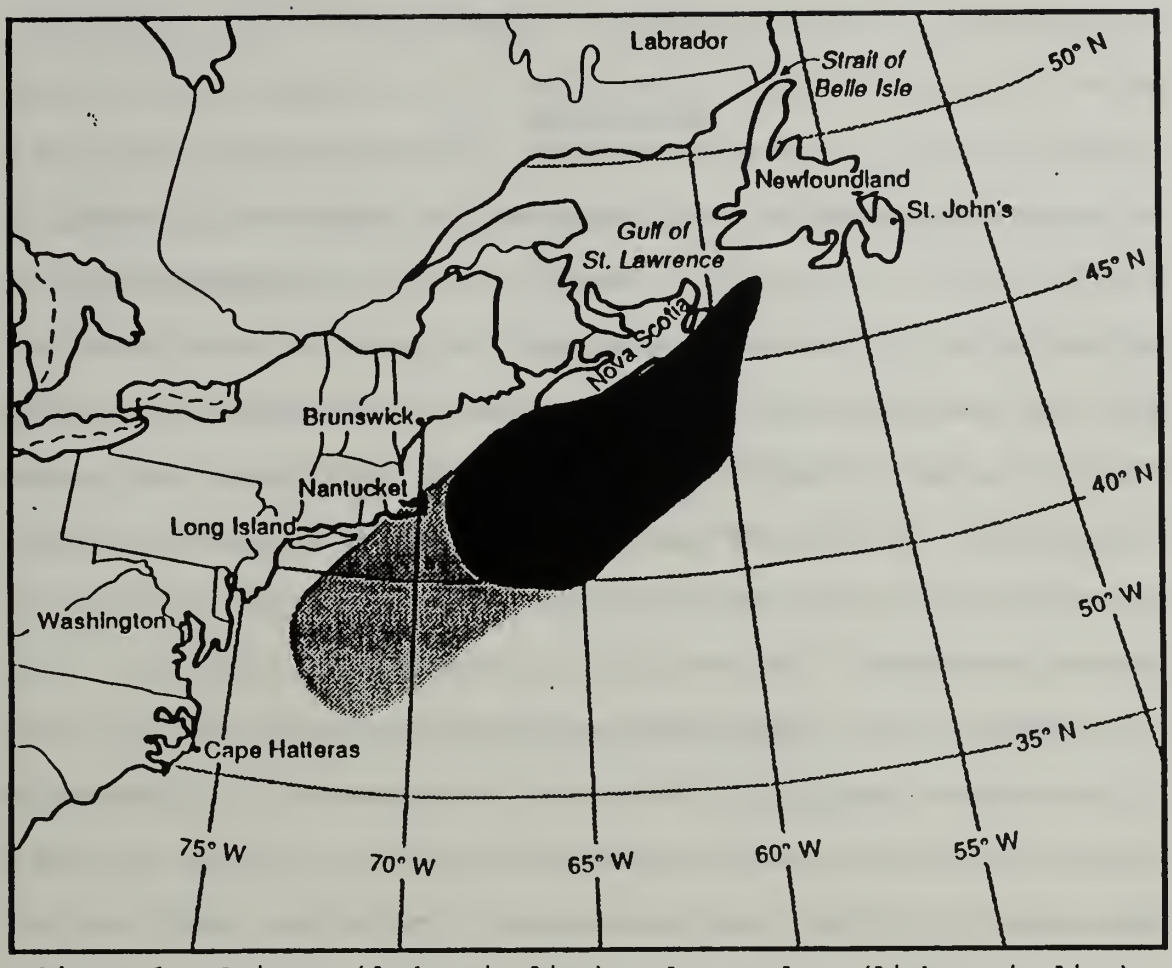

Figure 1. Primary (dark stippling) and secondary (light stippling) areas where rapidly developing storms are most likely to occur (from Hadlock et al. 1989).

coastal storm.

D. THESIS OBJECTIVES

The specific goals of this thesis are to determine what processes were important in the development of the IOP-5A cyclone, and to assess the capability of the Navy Operational Regional Atmospheric Prediction System (NORAPS) model to accurately simulate this rapid cyclogenesis event.

An examination of NORAPS analyses at all levels prior to,

during and following explosive deepening will be conducted. Observations and satellite imagery will be used to aid in the interpretation of these analyses. Subjective manual analysis of observed data will be performed in order to investigate coastal and/or topographic mesoscale influences on the storm system prior to and at the onset of rapid intensification. Next, a comparison of model forecasts and analyses will be done to assess NORAPS performance in depicting the rapid cyclogenesis of the IOP-5A storm. Finally, vertical motions associated with the system will be studied as a means to better understand the evolution of the IOP-5A storm.

Chapter II of this thesis provides background on rapid cyclogenesis events. Chapter III presents the synoptic discussion and mesoscale investigation of the IOP-5A cyclone. Assessment of NORAPS performance in simulating this case of coastal rapid cyclogenesis is discussed in Chapter IV, using a comparison of forecasts and analyses. Chapter V presents the procedural details and the examination of vertical motions associated with the IOP-5A cyclone, while the final section contains conclusions and recommendations.

II. BACKGROUND

A. PREVIOUS STUDIES OF THE PROCESSES CONTRIBUTING TO RAPID CYCLOGENESIS

There are a variety of processes believed to contribute to rapid cyclogenesis (Uccellini 1990). Although most rapidly deepening cyclones do exhibit several common characteristics, they also display large case-to-case variability. According to Uccellini (1990), it is probable that some processes are more important than others in individual storms, and that individual processes may be necessary for developing extratropical cyclones but are not sufficient when acting alone to produce rapid cyclogenesis. Uccellini (1990) contends that rapid cyclogenesis results from an interaction of many factors, and that the relative importance of each contributing factor is still a matter of debate within the meteorological community.

It has been shown that upper-level forcing is an essential ingredient in producing explosive cyclogenesis. As described in Uccellini (1990), in the early to mid-1900's Margueles, Dines and Scherhag promoted the concept that sea-level cyclonic development requires upper-level divergence so as to yield a net reduction of mass in the air column and a sea-level pressure decrease in a region where the low-level wind

field is generally convergent. Hence, forcing at upper-levels, e.g., associated with the ageostrophic circulations accompanying a jet streak or the cyclonic vorticity advection accompanying a mid-tropospheric short wave trough, must be manifested as divergence above the surface cyclone.

The Sanders and Gyakum (1980) study and more recent studies by Sanders (1986a, 1987) confirm that rapid cyclogenesis often commences as the 500 mb trough/ridge system, with its associated region of positive vorticity advection, moves to within 500 km upstream of a surface disturbance. Uccellini et al. (1984) and Wash et al. (1988) found that jet streaks can provide significant divergence aloft, even if the jets exhibit little or no curvature. There is growing recognition that the circulations associated with the entrance and exit regions of jet streaks are important in rapid cyclogenesis, as concluded by Sinclair and Elsberry (1986).

The evolution of tropopause potential vorticity anomalies may also affect the development of these storms. Several works provide supporting evidence of the importance of these anomalies to the development of surface cyclones (e.g., Hoskins et al. 1985; Boyle and Bosart 1986; Hirschberg and Fritsch 1991a, 1991b). Hirschberg and Langland (1992) conducted a numerical model-based diagnostic study of the ERICA IOP-5A rapid cyclogenesis event, focusing on a tropopause undulation and the coupling mechanisms between the

upper- and lower-atmosphere. Their preliminary findings suggest that strong lower-stratospheric warm advection associated with the tropopause undulation played a part in the development and evolution of the rapidly intensifying cyclone system. Other studies (e.g., Uccellini et al. 1984) have shown upper-level frontogenesis and tropopause folding to be important in explosive cyclogenesis.

In addition to these upper-level processes, several low-level processes have been shown to play an important role in contributing to explosive cyclogenesis. Four such processes are listed by Uccellini (1990):

(i) The thermal advection pattern in the lower troposphere in conjunction with the presence of low-level baroclinic zones and strong low-level winds;

(ii) Sensible and latent heat fluxes in the boundary layer;

(iii) Decrease of static stability in the lower troposphere; and

(iv) Terrain effects.

Lower-tropospheric thermal advections have been widely recognized as being important to the formation and subsequent intensification of cyclone systems (e.g., Petterssen 1956). During the period of most rapid development, the thermal field in the lower troposphere typically evolves into an "S-shaped" pattern. As confirmed by Kocin and Uccellini (1990), this pattern is evident in a wide variety of East Coast storms. The "S" pattern arises from warm air advection east of the cyclone and cold air advection west of the cyclone. This

couplet of cold and warm advections yields a pattern favorable for cyclone development.

Sensible and latent fluxes of heat and moisture also appear to play a role in fueling rapid cyclogenesis. Numerous diagnostic and model sensitivity studies have shown that heat fluxes due to cold air flowing over a warmer ocean surface contribute to rapid deepening. However, numerous studies have also shown the opposite result. Uccellini (1990) discusses the conflicting findings and offers an explanation for the differences. He believes the contradiction may be due to the large case-to-case variability of the extent to which surface fluxes influence storm development, or to differences in various model boundary layer parameterization schemes. Differing degrees of preconditioning of the atmosphere through warming and moistening processes prior to rapid cyclogenesis may also account for the opposing results. Studies by Nuss and Kamikawa (1990) and Kuo et al. (1991) suggest that early surface fluxes (e.g., from the cold air outbreak of a previous storm) may increase the potential for explosive deepening at a later time by preconditioning the atmosphere.

Sensible and latent heat fluxes into the lower troposphere act to decrease the low-level static stability. As discussed in Bosart's (1981) study of the President's Day storm, static stability is an important factor in controlling the strength of the secondary circulations associated with fronts and jets. Many studies, starting with Petterssen (1956) have indicated

that reduced lower-tropospheric static stability decreased the braking tendency of vertical motion on cyclogenesis, allowing intensification of low-level convergence and upper-level divergence during rapid deepening.

Emanuel (1983) showed that sensible and latent heat fluxes can also decrease the symmetric stability and thus lead to conditional symmetric instability (CSI) in the vicinity of strong frontal zones. This is a process by which the combination of gravity acting in the vertical and centrifugal forces acting radially result in slantwise convective motion. Hence, an atmosphere that is stable to vertical displacements can be unstable to slantwise displacement, and convection could thus occur in a "traditionally" stable region.

Although debate may exist as to the role of surface fluxes in contributing to rapid cyclogenesis, it is generally accepted that latent heat release (LHR) plays a significant role. In their study of nine Western Atlantic explosive cyclones, Kuo and Low-Nam (1990) determined LHR to be an important factor in cyclone intensification. Results of their study indicate precipitation parameterization is the most important factor necessary for accurate modelling of rapid cyclogenesis. Several other studies (e.g., Anthes et al. 1983; Pauley and Smith 1988) contend that LHR can strongly influence the intensity, wind speed and movement of developing storm systems.

B. NUMERICAL MODELLING OF RAPID CYCLOGENESIS

Assessing the accuracy of numerical model simulations of explosive development is the focus of many researchers' attention. While early operational numerical models experienced difficulties in predicting rapid cyclogenesis, the general skill of numerical weather prediction models has been steadily improving.

1. National Meteorological Center Models

Sanders (1986b, 1987) suggests several reasons for the recent improvements in the National Meteorological Center's (NMC) operational models. The latest operational regional NMC model, the Nested Grid Model (NGM), has shown improved forecast skill due to better resolution, improved analyses and better treatment of boundary-layer fluxes than the previous Limited-area Fine Mesh (LFM) model. Sanders (1987) asserts that the most important factor limiting prediction skill is now the problem of initial conditions associated with data limitations.

2. The Navy Operational Regional Atmospheric Prediction System (NORAPS)

The Navy's regional operational model, NORAPS, forecast skill in predicting rapid cyclogenesis has also improved in recent years. Hodur (1987) describes NORAPS and the modifications that were tested and implemented in response to cyclogenesis forecast problems. He showed that significant

improvements were accomplished by changing the wind and mass analysis procedures in the model and by the inclusion of a 12-h update cycle. NORAPS now utilizes an objective analysis scheme that allows the analysis to draw closer to the observations and discard duplicate reports. Additionally, first-guess fields used in the analyses are now produced from the NORAPS regional forecasts rather than from the coarser-resolution global model (the Navy Operational Global Atmospheric Prediction System, NOGAPS).

As NORAPS analyses and forecasts were utilized in conducting this thesis study, a brief description of important aspects of the NORAPS analysis scheme is presented. A description of important NORAPS forecast model parameters will be provided in the model performance discussion of Chapter IV.

For this study a "research version" of NORAPS was used, which included a number of modifications to the operational version. NORAPS is a relocatable regional mesoscale model. For this study, the horizontal domain consists of a 109 x 82 grid point array, with horizontal resolution of 60 km, centered at 45N 65W. The analysis portion of NORAPS performs a multi-variate optimum interpolation analysis on 16 standard pressure levels every 6 h. A NOGAPS analysis is used as the first-guess in this version. NORAPS uses a sigma vertical coordinate system with 24 levels. Thus, the first-guess fields must be interpolated onto the sigma levels prior to normal mode initialization.

The upper boundary of the model is at approximately 10 mb. Surface and upper-air data from ship, aircraft, radiosonde and pibal observations, as well as satellite soundings and cloud track winds are incorporated into the analyses. Additionally, some special ERICA data and the ERICA 50 km sea surface temperature analysis were also used in the analysis procedure. Additional details of the NORAPS analysis method used in this study are described by Hirschberg and Langland (1992).

III. SYNOPTIC DISCUSSION

The time period 18-22 January 1989 was one of the more interesting of ERICA. During this five day period, two rapidly intensifying cyclones developed within 36 h of each other over the western North Atlantic Ocean. The first cyclone, observed during IOP-5, developed off of the mid-Atlantic coast and tracked along the north wall of the Gulf Stream, reaching a maximum deepening rate of 18 mb $(6\ h)^{-1}$ (Hadlock et al. 1989). The second cyclone, observed during IOP-5A, developed northeast of Lake Ontario and tracked along the Canadian Maritimes coast, reaching a maximum deepening rate of 15 mb $(6\ h)^{-1}$ (Figure 2). This latter storm presents an opportunity to study a rapidly developing cyclone in a near-coastal environment with abundant land-based operational and special surface and upper-air data.

A. 1200 UTC 20 JANUARY 1989

The synoptic discussion of the ERICA IOP-5A cyclone begins at 1200 UTC 20 January 1989. Hereafter time and date will be denoted as hour/date (e.g., 1200/20). At this time, the surface low was located north of Lake Ontario with an analyzed central pressure of 1003 mb (Figure 3). The 1000 mb - 500 mb thickness pattern shows a strong baroclinic zone through the low center. The thickness gradient behind the cold front had

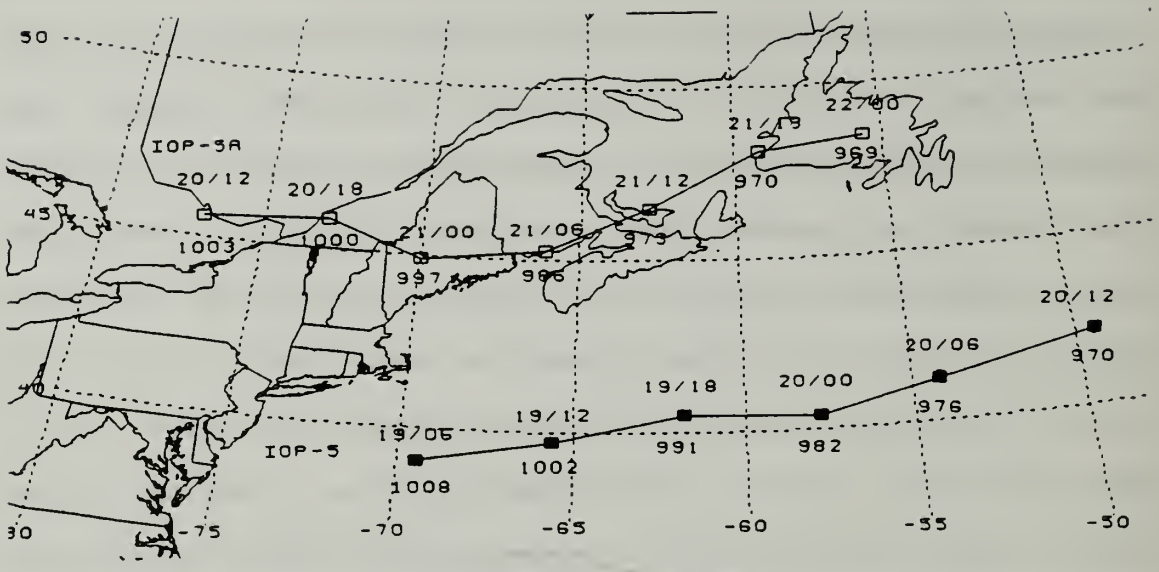

Figure 2. Tracks (solid) and central pressures (mb) of the IOP-5 (marked by solid squares) and IOP-5A (marked by open squares) storms. Time is day/hour UTC January 1989.

been tightening over the last 6 h. Areas of significant low-tropospheric warm and cold advection are evident east and southwest, respectively, of the cyclone center. The intense circulation of the IOP-5 storm is evident southeast of Newfoundland.

A 500 mb trough, which had intensified over the previous 12 h, was positioned upstream of the surface low (Figure 4). Positive vorticity advection (PVA) east of the 24×10^{-5} s^{-1} absolute vorticity center (located in the base of the 500 mb trough over northern Ohio and Indiana) was overtaking the surface low position.

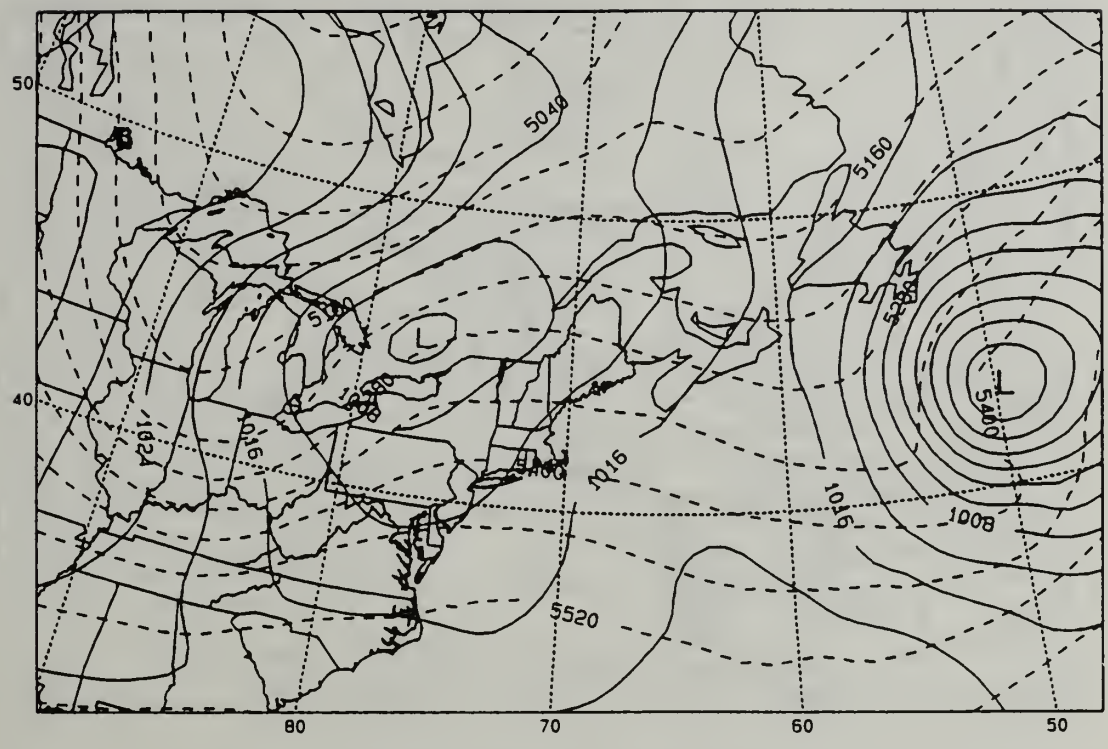

Figure 3. Surface pressure (solid, contour interval 4 mb) and 1000-500 mb thickness (dashed, contour interval 60 m) analysis at 1200 UTC 20 January 1989.

Further aloft at 300 mb, a jet streak (>60 m s^{-1}) was present on the eastern side of the upper-air trough, southwest of the surface low (Figure 5). The 300 mb divergence analysis (Figure 6) shows weak divergence over the surface low position, with a maximum $2x10^{-5}$ s^{-1} contour southwest of the surface low along 80W. Divergence is also indicated over the southeast and eastern U.S. which corresponds to the bright (cold) cloud areas depicted in the satellite imagery (Figure 7). The strong divergence area associated with the IOP-5A cyclone is analyzed east of the Canadian Maritime Provinces.

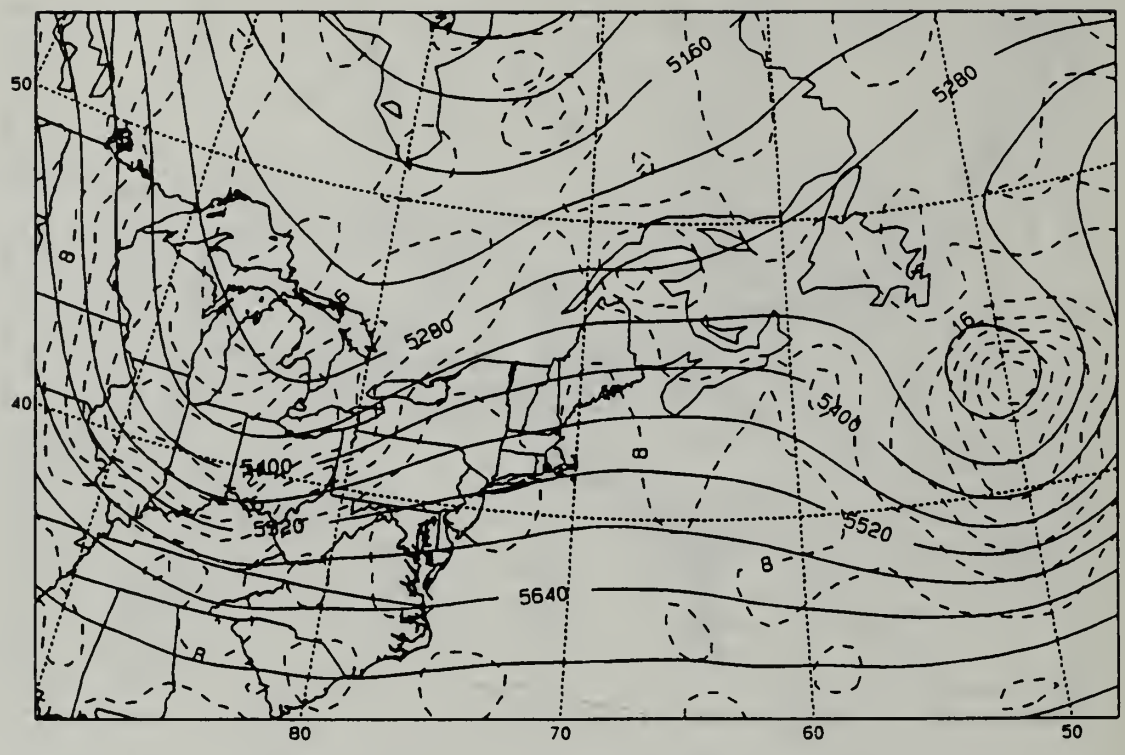

Figure 4. 500 mb height (solid, contour interval 60 m) and absolute vorticity (dashed, contour interval 4×10^{-5} s^{-1}) analysis at 1200 UTC 20 January 1989.

Geostationary Orbiting Environmental Satellite (GOES) enhanced infrared (IR) imagery at 1331/20 (Figure 7) shows an irregular comma-shaped area of cloudiness asssociated with the surface low center. This area extends from the eastern Great Lakes to the Maine coast. A break in the high clouds is present from Virginia to Massachusetts, south of the jet streak, which separates the IOP-5A cyclone from the extensive cloud area over the southeastern U.S. and Gulf of Mexico. The well-organized vortex associated with the IOP-5 cyclone is clearly evident over the western North Atlantic Ocean.

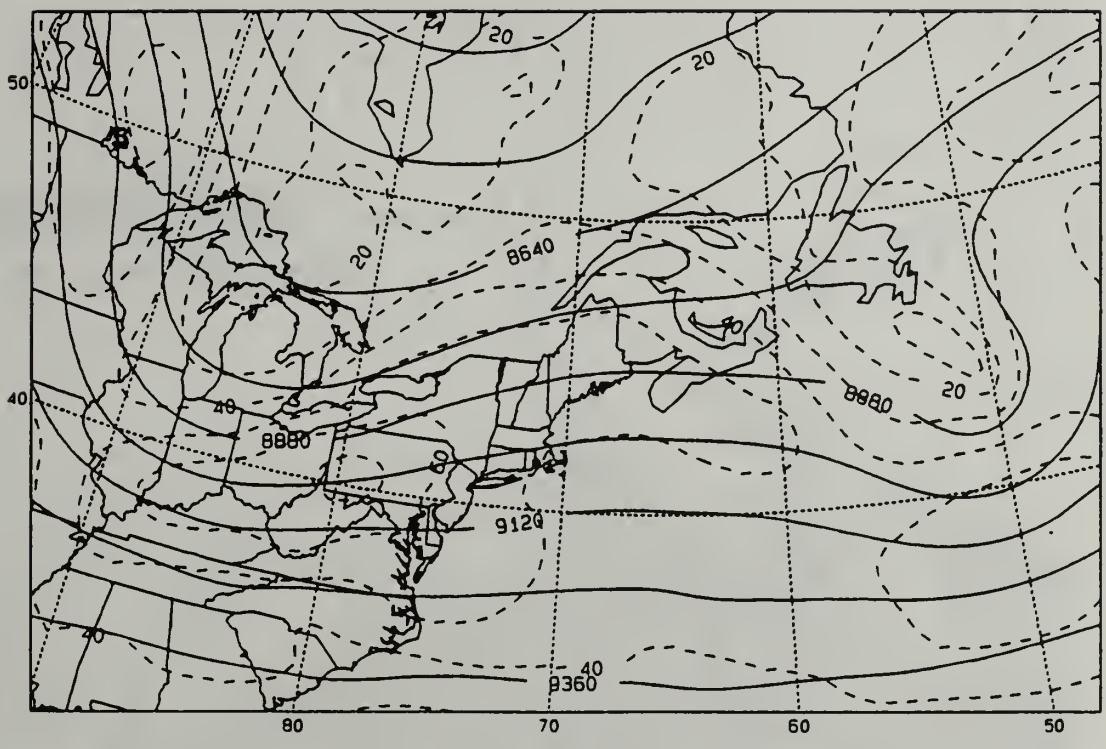

Figure 5. 300 mb height (solid, contour interval 120 m) and isotach (dashed, contour interval 10 m s^{-1}) analysis at 1200 UTC 20 January 1989.

It is apparent that the IOP-5A cyclone was in a very favorable environment for development. Several features expected to aid in deepening the low include the location of the incipient disturbance within a strengthening baroclinic zone, a 500 mb short wave with its associated cyclonic vorticity advection superimposed over the surface low, and a jet maximum with its upper-level divergence also favorably positioned with respect to the surface cyclone.

B. 1800 UTC 20 JANUARY 1989

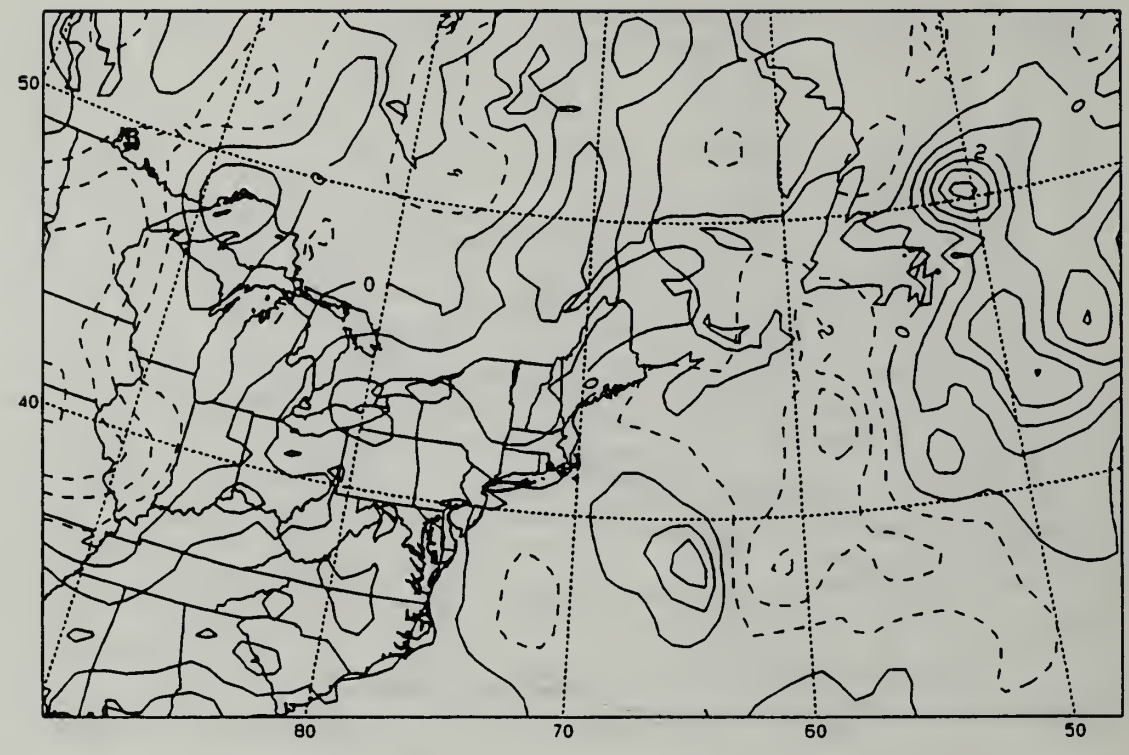

Figure 6. 300 mb divergence [solid (positive), contour interval $1x10^{-5}$ s^{-1}] analysis at 1200 UTC 20 January 1989. Negative values (dashed, contour interval $1x10^{-5}$ s^{-1}) are convergence.

By 1800/20, the surface low had deepened modestly by 3 mb to a central pressure of 1000 mb (Figure 8). The 1000 mb - 500 mb thickness gradient tightened primarily behind the cold front, and the thickness pattern exhibited the typical "S-shape" of a developing cyclone. A strong thermal advection pattern, especially evident over Pennsylvania, West Virginia, Maryland and Virginia, continued to support development of the IOP-5A cyclone.

Mid-level positive vorticity advection was evident over the surface low and cold front, projecting eastward from the $>20x10^{-5}$ s^{-1} absolute vorticity center that extended from north of Lake Ontario southwestward to Kentucky (Figure 9). The

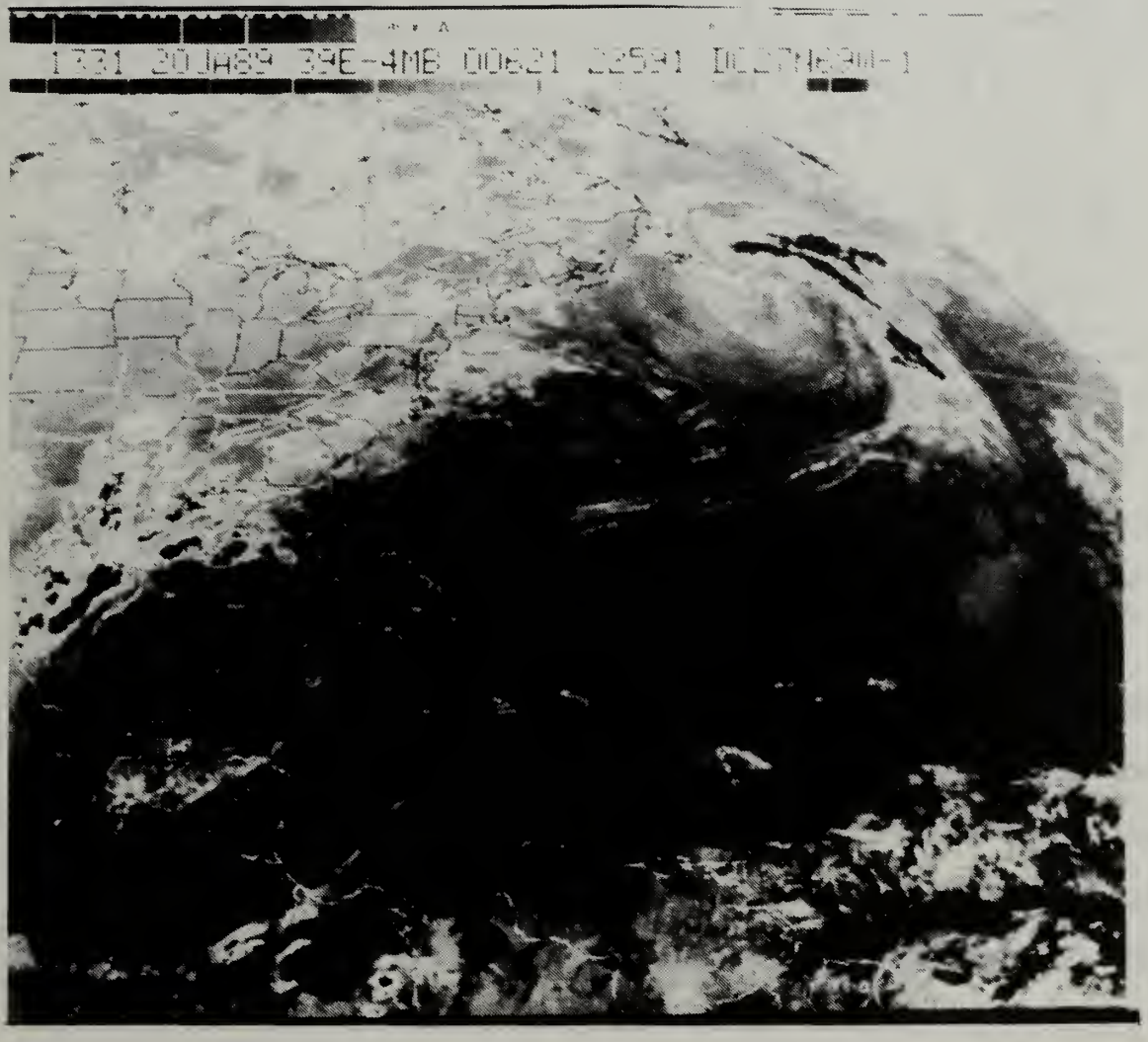

Figure 7. GOES enhanced IR imagery at 1331 UTC 20 January 1989.

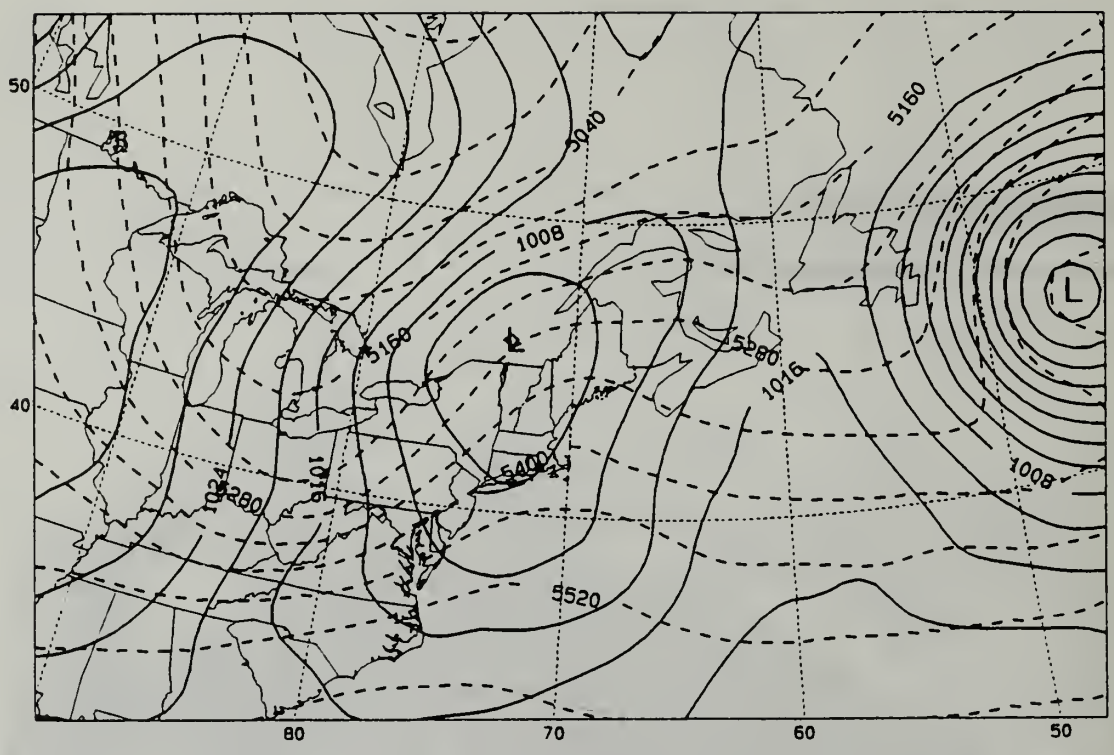

Figure 8. Surface pressure and 1000-500 mb thickness analysis as in Figure 3, except for 1800 UTC 20 January 1989.

southwestern portion of this vorticity area contained a maximum contour of 28×10^{-5} s^{-1}. A second vorticity center can be inferred from the analysis in the northeastern portion of the elongated lobe extending northeast from the primary center and is located west of the developing surface cyclone.

The 300 mb jet streak was positioned in the base of the trough (Figure 10), just south of its 1200/20 position and still on the eastern side of the trough axis. The size of the isotach maximum (70 m s^{-1}) contour had expanded over the last 6 h, and the eastern extent of the jet maximum had spread eastward to the U.S. mid-Atlantic coast.

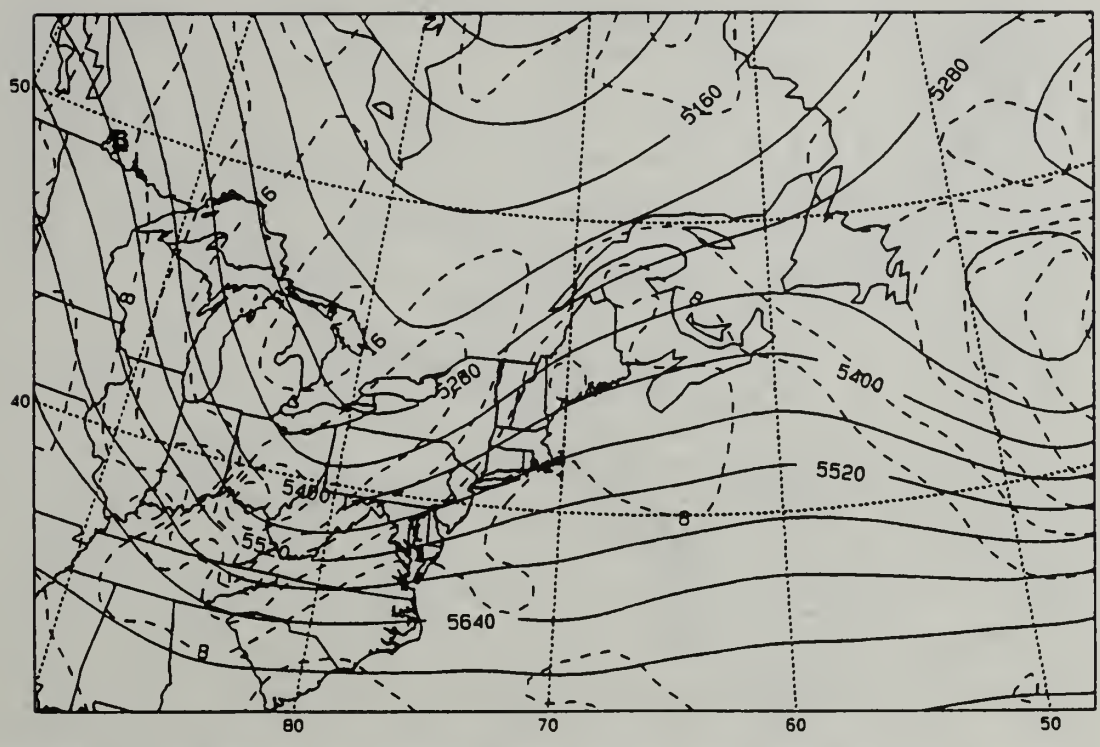

Figure 9. 500 mb height and absolute vorticity analysis as in Figure 4, except for 1800 UTC 20 January 1989.

The 300 mb divergence analysis (Figure 11) shows two maxima. The northern area of divergence is associated with the left exit region of the jet streak, just east of the surface low position. The southern area of divergence is associated with the upward vertical motion in the bright convective cloud mass (as seen in unenhanced IR and water vapor imagery, not shown) well south of the cyclone at this time.

GOES enhanced IR imagery (Figure 12) shows the region of 60 m s^{-1} and greater depicted in the 1800/20 300 mb isotach analysis coincided with a cloud-free area stretching from eastern Tennessee through Virginia, Maryland and Delaware.

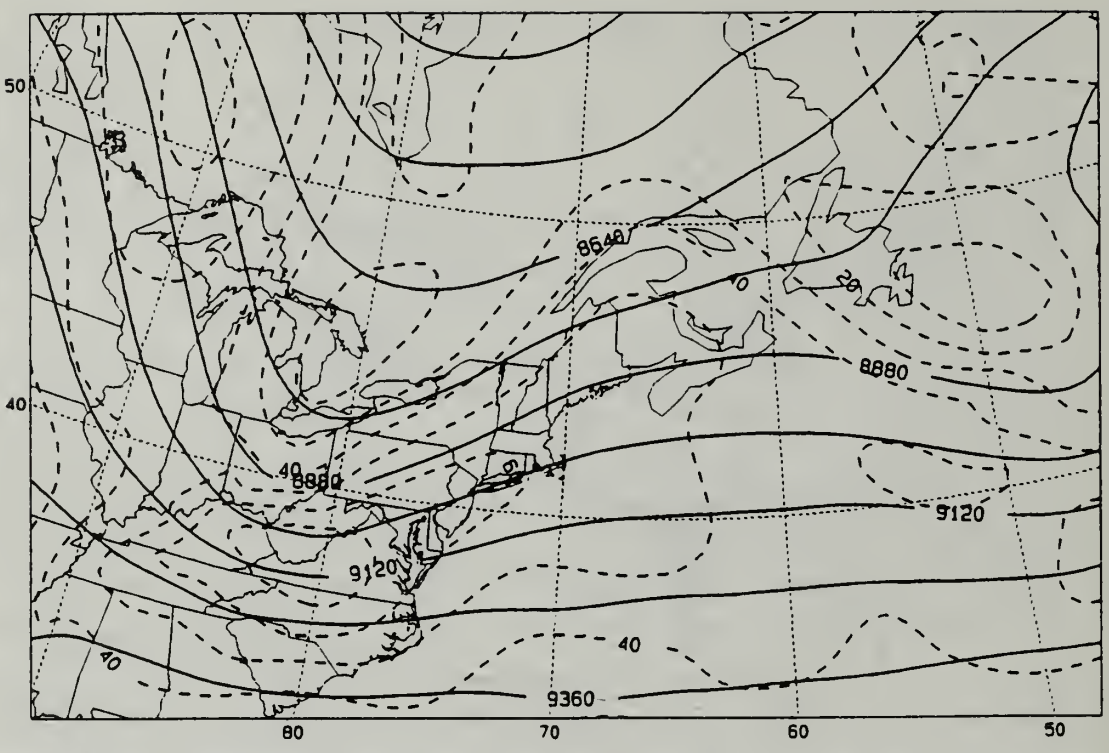

Figure 10. 300 mb height and isotach analysis as in Figure 5, except for 1800 UTC 20 January 1989.

This imagery also shows that the coldest cloud-top temperatures were approximately -40 to -50°C and located north and southeast of the surface low center. The extensive area of bright, high clouds continued to develop over the southeastern U.S. and northern Gulf of Mexico and remained separate from the cloud band associated with the IOP-5A cyclone.

C. 0000 UTC 21 JANUARY 1989

The IOP-5A cyclone's rapid intensification stage began at 0000/21 and continued for the next 12 h. The NORAPS mean sea level pressure (MSLP) analysis at 0000/21 depicted an oblong

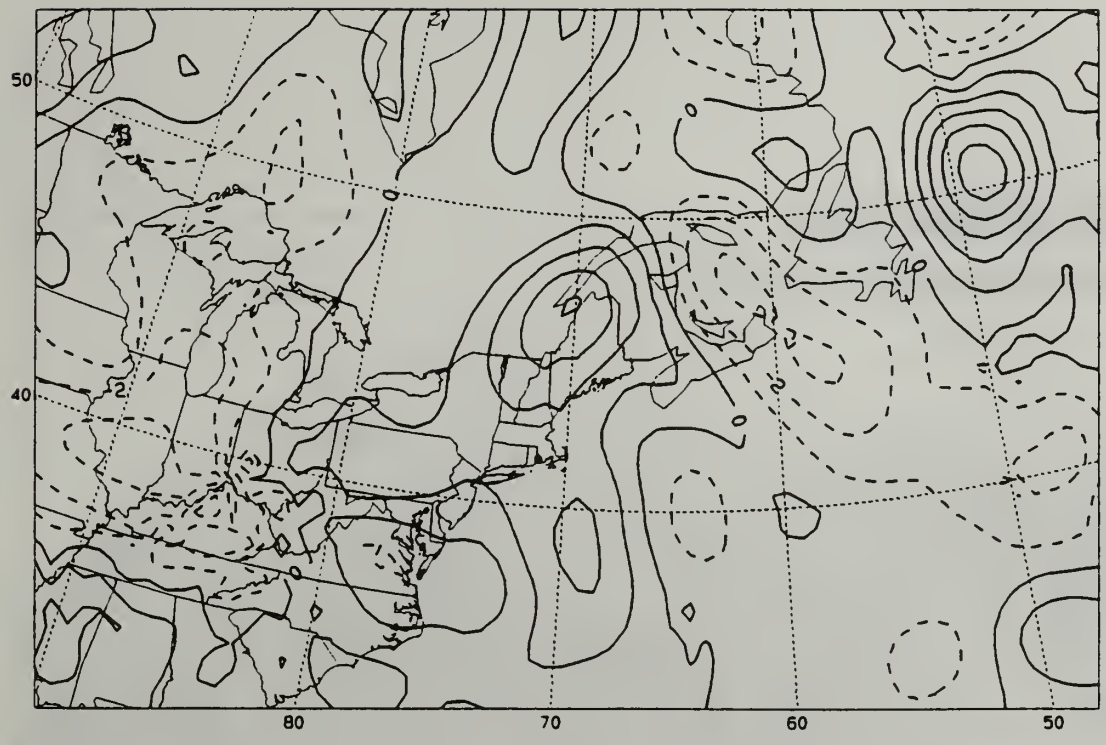

Figure 11. 300 mb divergence analysis as in Figure 6, except for 1800 UTC 20 January 1989.

1000 mb isobar center, with the 997 mb low indicated over the mountainous interior of Maine near 45N 70W (Figure 13).

By this time, the cold front had moved offshore east of the Eastern Seaboard states from the Maine coast southward to east of North Carolina. Cold air advection associated with this system continued to intensify in conjunction with the increased pressure gradient. This is especially evident in the offshore region from 35N to 41N.

The 500 mb analysis at 0000/21 (Figure 14) shows that the absolute vorticity maximum, roughly 200 nm southwest of the surface low position, intensified dramatically and was associated with strong PVA over the surface low and northward,

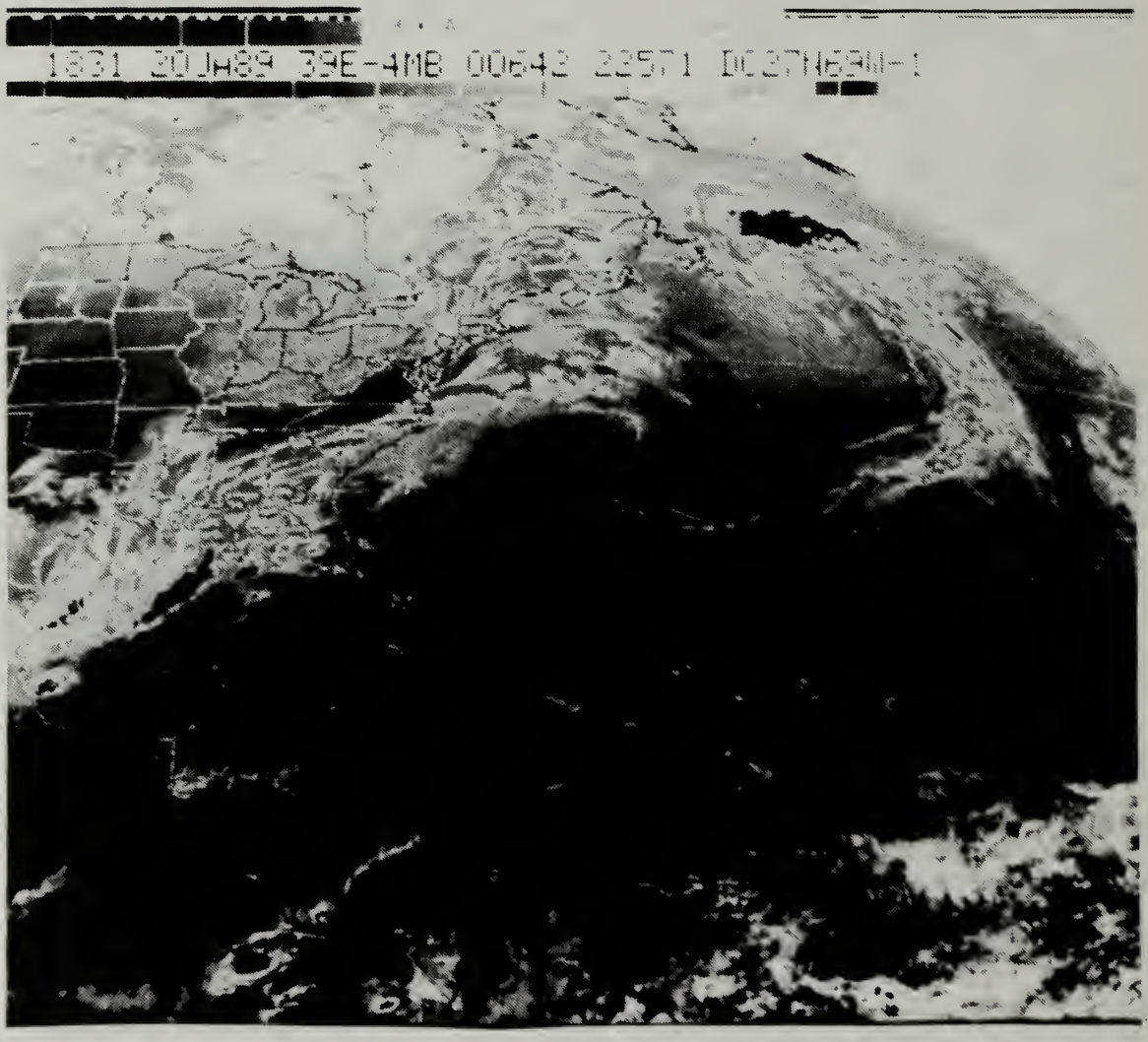

Figure 12. GOES enhanced IR imagery at 1831 UTC 20 January 1989.

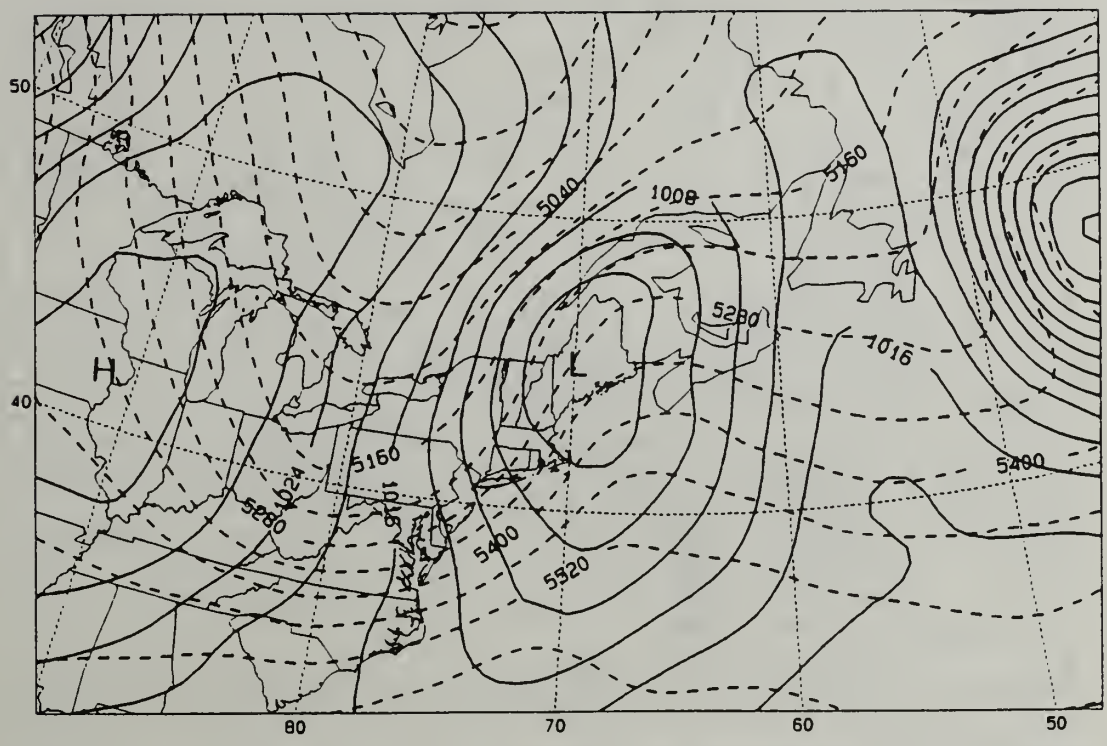

Figure 13. Surface pressure and 1000-500 mb thickness analysis as in Figure 3, except for 0000 UTC 21 January 1989.

as well as to the offshore region from 37N to 42N in the cold air behind the cold front. There was also a small but intense (32×10^{-5} s^{-1}) absolute vorticity maximum analyzed over the Ohio/West Virginia border at 0000/21. This maximum was the southern part of the elongated lobe of vorticity in the base of and along the eastern side of the 500 mb trough at 1800/20 (see Figure 9).

Figure 15 depicts the 300 mb trough and jet streak at 0000/21. The jet had continued to progress northeastward with the intensifying upper-air trough. The maximum isotach analyzed was a small 80 m s^{-1} contour over the Delmarva peninsula. Also, a new small 70 m s^{-1} contour appeared

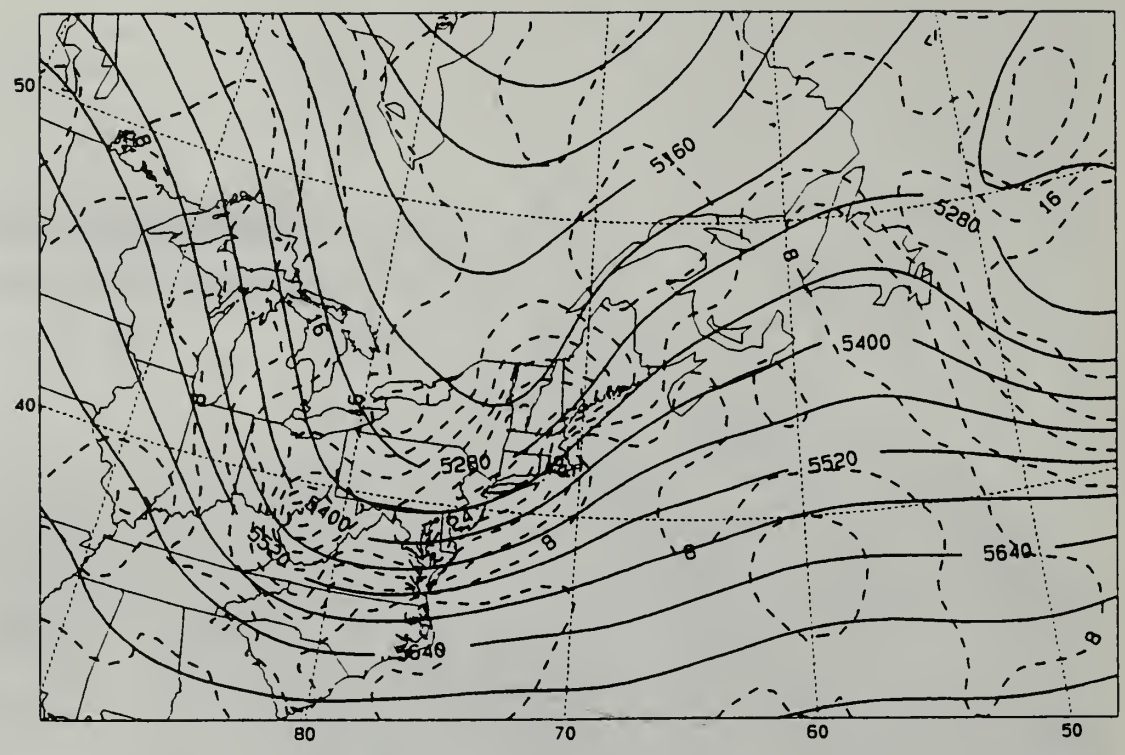

Figure 14. 500 mb height and absolute vorticity analysis as in Figure 4, except for 0000 UTC 21 January 1989.

approximately 120 nm south of the surface low position, about halfway between the 300 mb trough and downstream ridge. The wind speed over the surface low had increased by 20 m s^{-1} over the last 6 h to 50 m s^{-1}.

Figure 16 shows that the surface cyclone was still under divergence associated with the left exit region of the jet, but the maximum areas of divergence were analyzed east-northeast and south of the surface low position.

GOES infrared satellite imagery at 0001/21 (Figure 17) shows the brightest (coldest) mass of clouds east through south of the surface cyclone center. The dark area of the enhancement indicates cloud-top temperatures of <-60°C in the

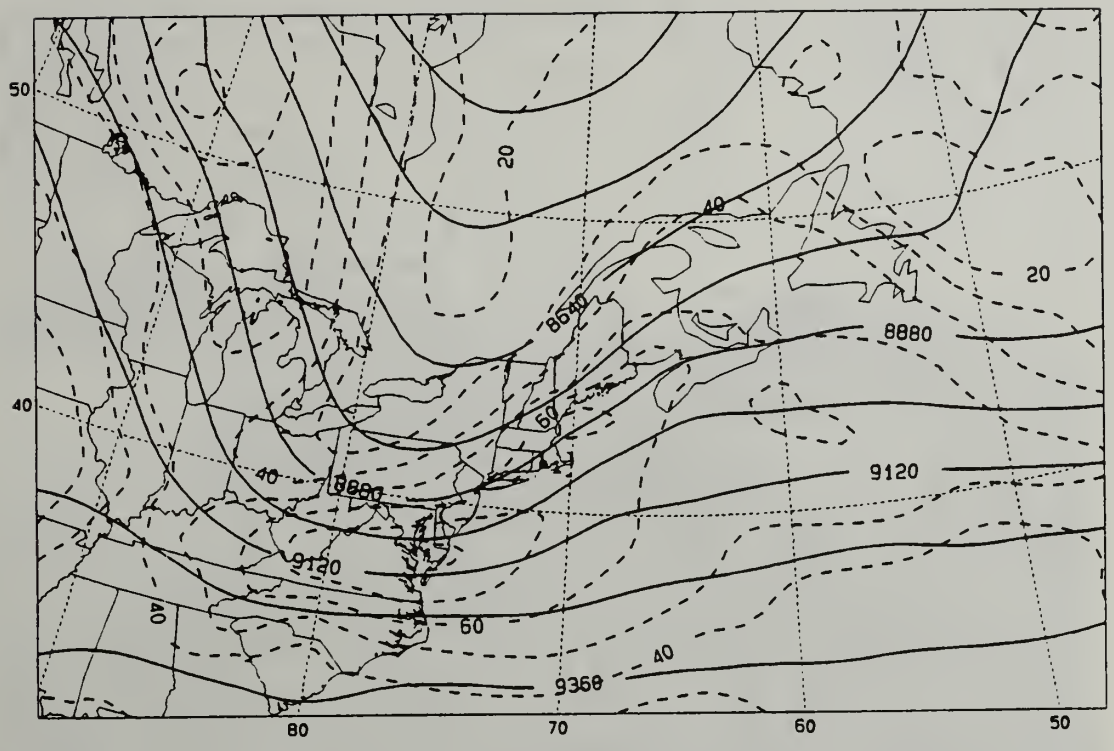

Figure 15. 300 mb height and isotach analysis as in Figure 5, except for 0000 UTC 21 January 1989.

vicinity of Nova Scotia, east of the surface low position. This correlates fairly well with the analyzed divergence maximum.

D. 0600 UTC 21 JANUARY 1989

By 0600/21, rapid development of the IOP-5A cyclone was underway. Over the previous 6 h the system deepened 11 mb to 986 mb (Figure 18) as it tracked along the northern coast of the Bay of Fundy. Low-level thermal advections remained very pronounced.

The 500 mb geopotential height and absolute vorticity analysis (Figure 19) indicated that strong positive vorticity

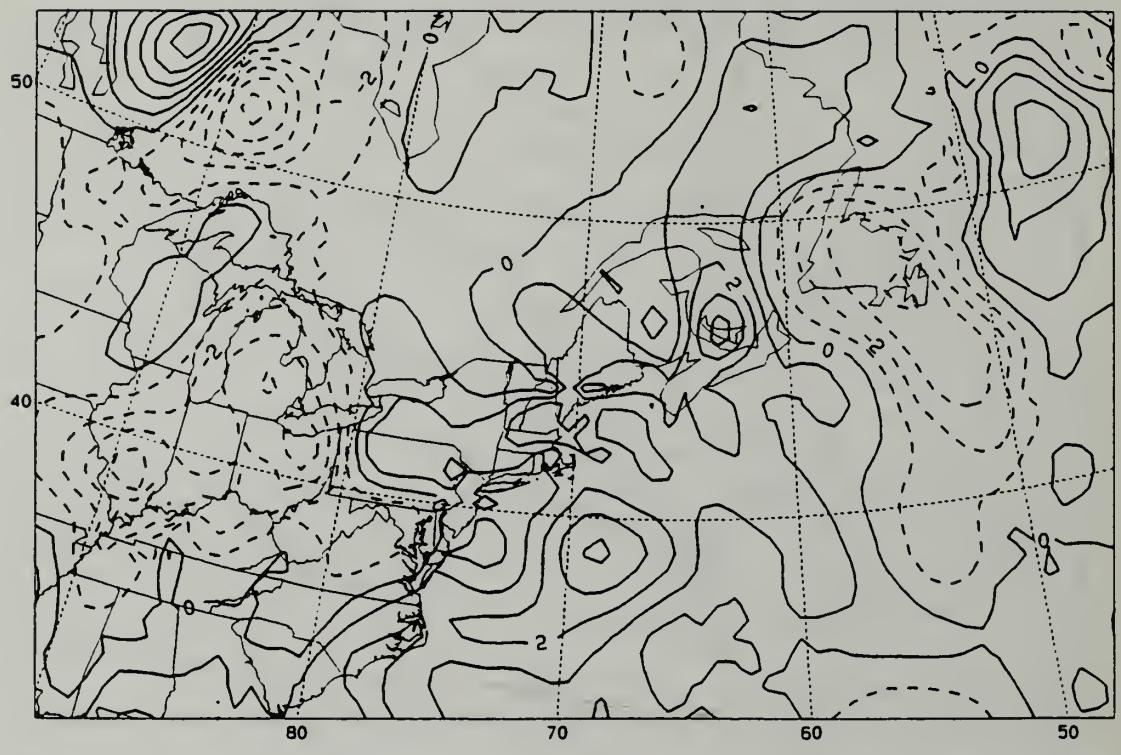

Figure 16. 300 mb divergence analysis as in Figure 6, except for 0000 UTC 21 January 1989.

advection continued to occur over the surface low position and northward, as well as behind the cold front southward to 35N.

Very strong cold air advection accompanied by convective cloud lines in the satellite imagery (Figure 20) were present offshore from North Carolina to Massachusetts in the cold air behind the cold front. Rapid expansion of the area of coldest cloud-top temperatures was clearly evident from the enhanced IR imagery (cf. Figures 17 and 20). This rapid cloud growth is indicative of the explosive development the system was experiencing.

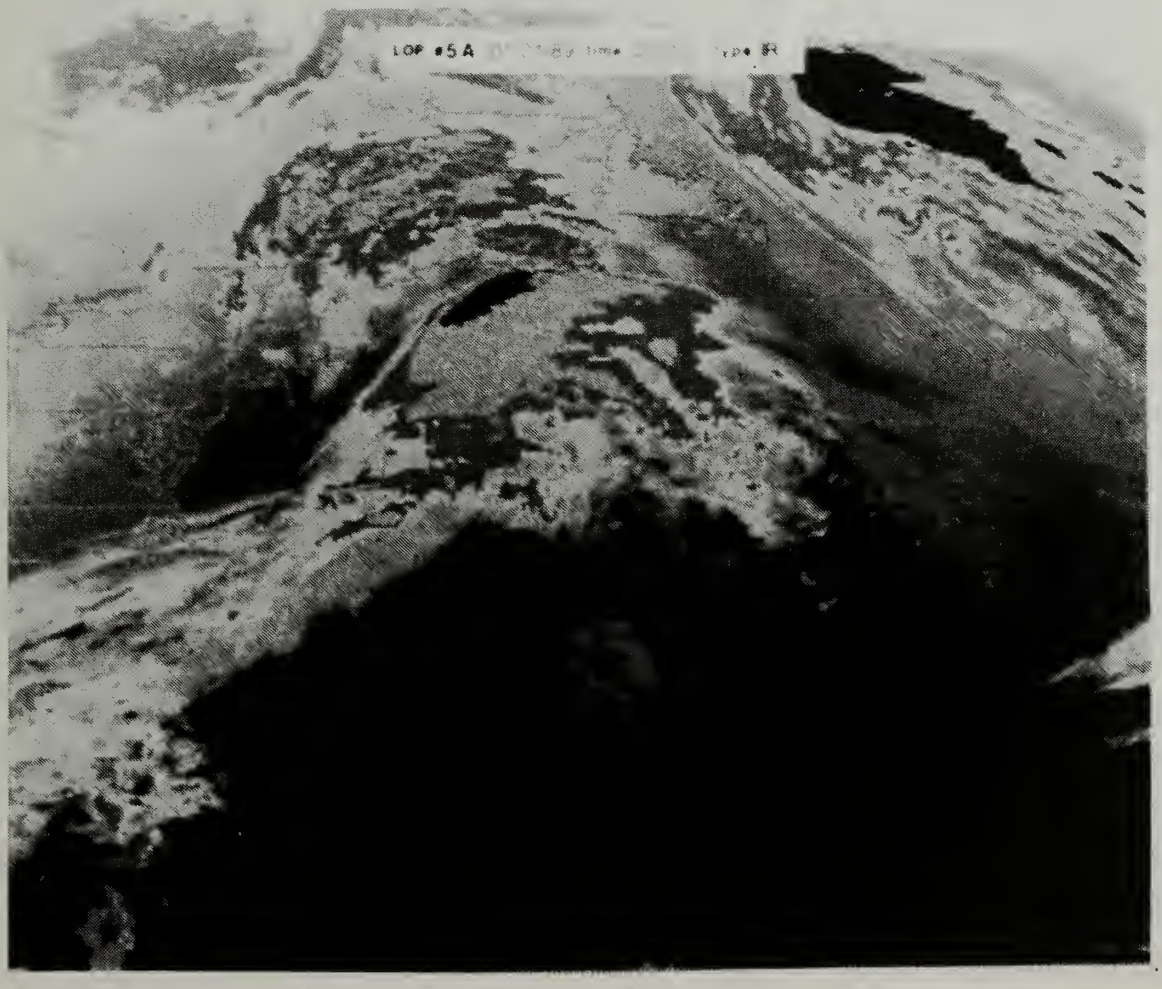

Figure 17. GOES enhanced IR imagery at 0001 UTC 21 January 1989.

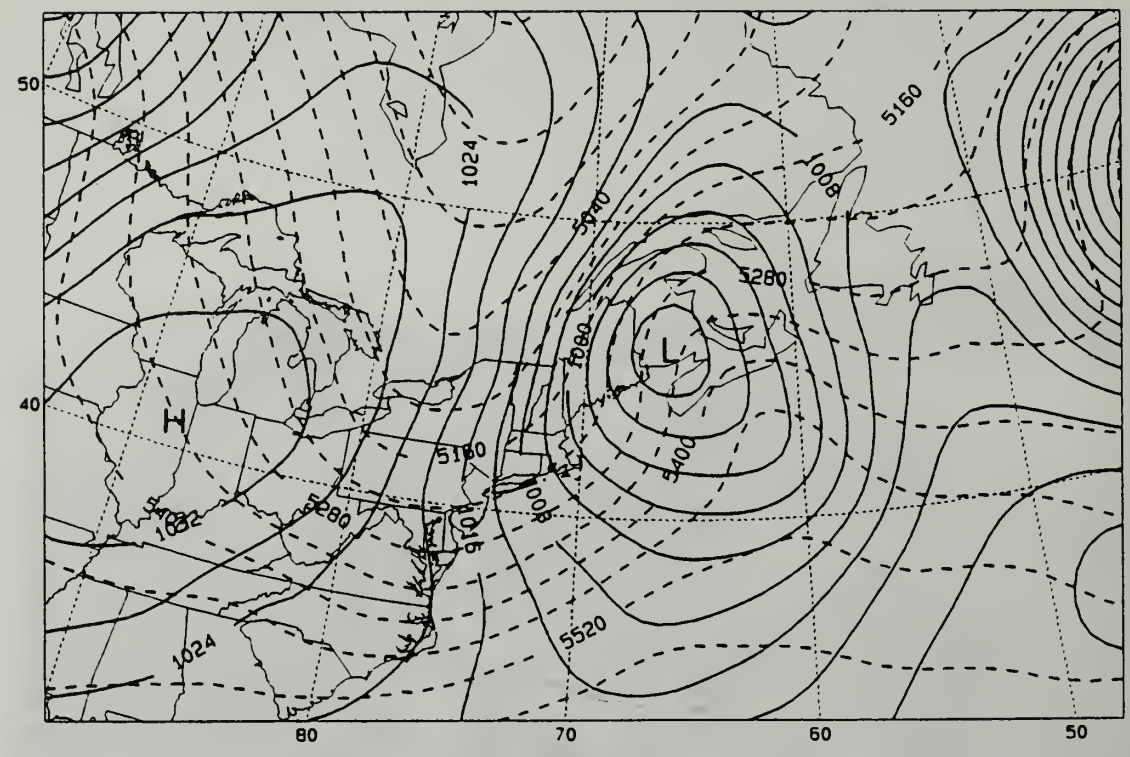

Figure 18. Surface pressure and 1000-500 mb thickness analysis as in Figure 3, except for 0600 UTC 21 January 1989.

Note that there still appears to be a distinct separation between the "comma head" cloud mass and the larger, more vertically developed cloud mass south of Nova Scotia centered along 60W. An interesting aspect of this case is the northward movement of this cloud band, which resembles the warm conveyor belt as described by Carlson (1980).

As discussed in Hirschberg and Langland (1992), the IOP-5A cyclone's evolution was associated with an upper-level potential vorticity anomaly and mesoscale tropopause undulation. A large (360 nm radius) pool of relatively warm (>-46 °C) stratospheric air at 200 mb was centered 300 nm west of the surface low position (Figure 21), while a 300 mb

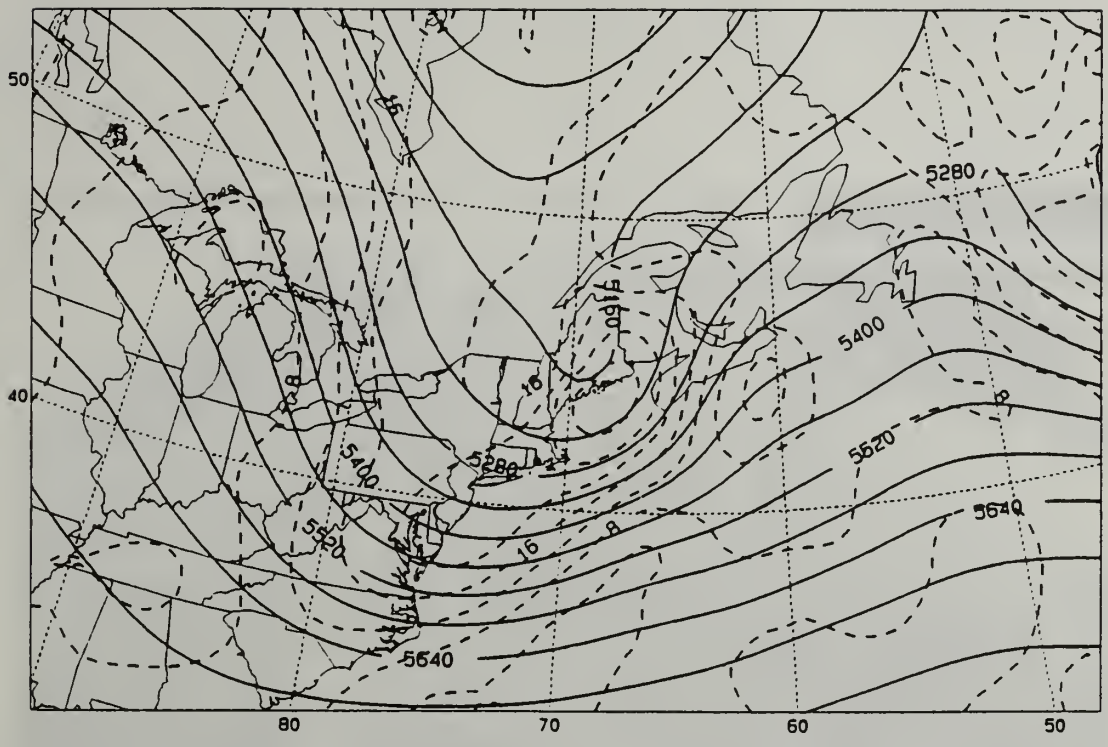

Figure 19. 500 mb height and absolute vorticity analysis as in Figure 4, except for 0600 UTC 21 January 1989.

potential vorticity value of $>30x10^{-5}$ m^2 s^{-1} K kg^{-1} existed within a closed contour in the same area (Figure 22). The isolines of potential vorticity were approximately in phase with the 300 mb trough at this time (0600/21).

The jet streak at 300 mb (not shown) weakened to a maximum of 60 m s^{-1}, and stretched completely over the ocean from the coasts of North Carolina and Virginia to south and east of Nova Scotia. It is likely that there was an area of stronger winds within this contour that was not resolved by the analysis and the observations.

The divergence analysis (Figure 23) now shows a single, greatly expanded $4x10^{-5}$ s^{-1} contour just east of the surface

Figure 20. GOES enhanced IR imagery at 0601 UTC 21 January 1989.

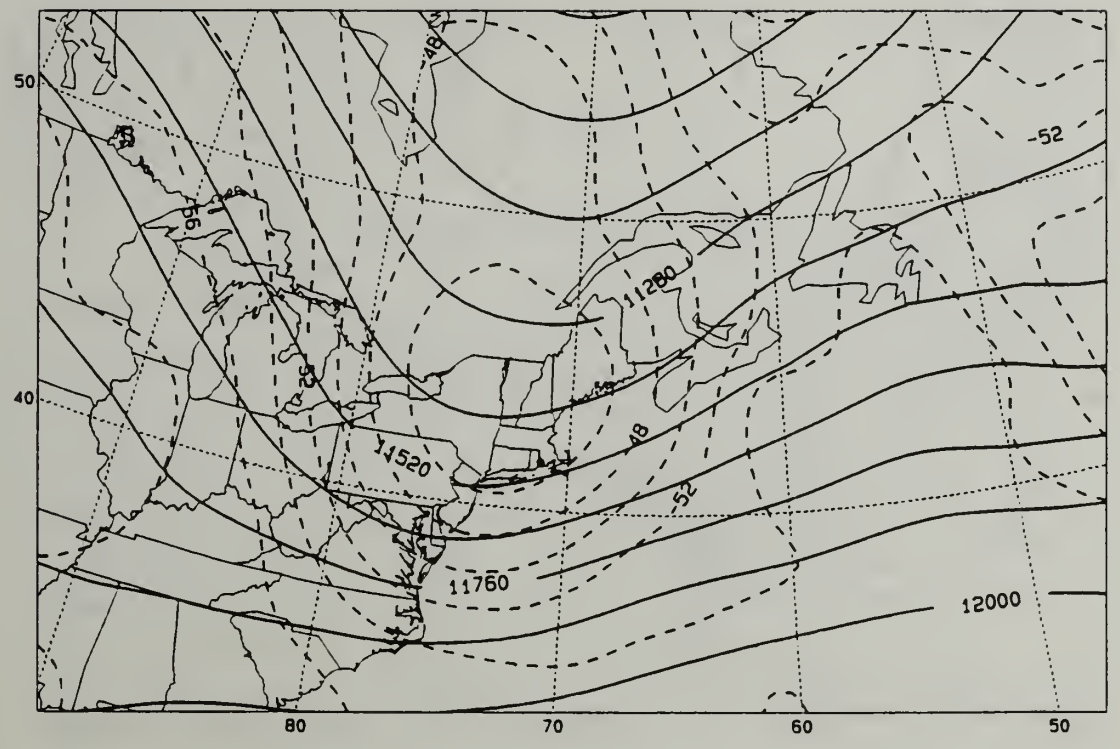

Figure 21. 200 mb height (solid, contour interval 120 m) and temperature (dashed, contour interval 2°C) analysis at 0600 UTC 21 January 1989.

low position (over Nova Scotia and southward). The divergence pattern is consistent with the satellite imagery, showing a large divergence region extending southward in the same location of the "warm conveyor belt" cloud band (Figure 20).

E. 1200 UTC 21 JANUARY 1989

The IOP-5A cyclone's most intense development occurred between 0300/21 and 0900/21, during which time a deepening rate of 15 mb $(6\ h)^{-1}$ was observed (Hirschberg and Langland 1992). A deepening rate of 13 mb $(6\ h)^{-1}$ was indicated in the NORAPS analyses from 0600/21 to 1200/21. During that time,

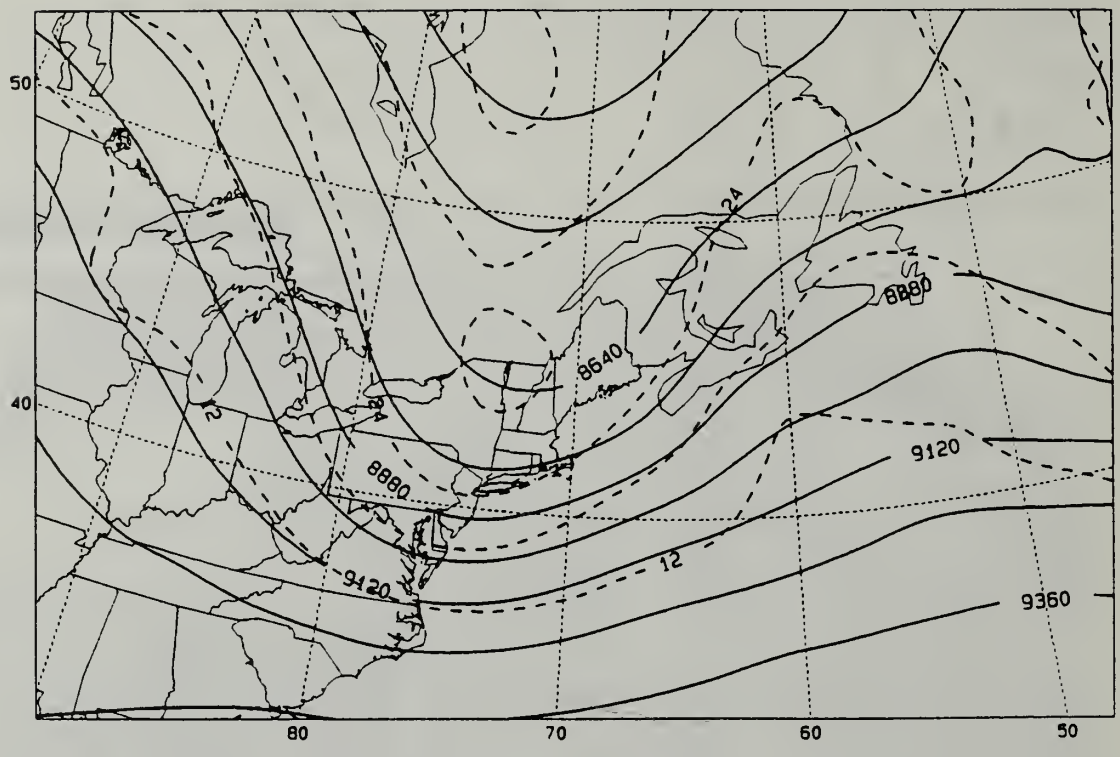

Figure 22. 300 mb height (solid, contour interval 120 m) and potential vorticity (dashed, contour interval $6x10^{-5}$ m^2 s^{-1} K kg^{-1}) analysis at 0600 UTC 21 January 1989.

the cyclone tracked north of Nova Scotia to the western Gulf of Saint Lawrence.

The IR satellite data (Figure 24) shows that the IOP-5A cyclone has developed the cloud signature of a mature, deep marine cyclone at 1201/21. The coldest cloud tops remain east of the cyclone surface center in the intense cloud band that has now merged with the northern cyclone cloud area. The GOES IR imagery also shows the cold front extending over 600 nm southward from the low. A pronounced thickness ridge east of 60W (Figure 25) is evidence that the system was occluding, and that the thermal advection pattern had shifted so that major

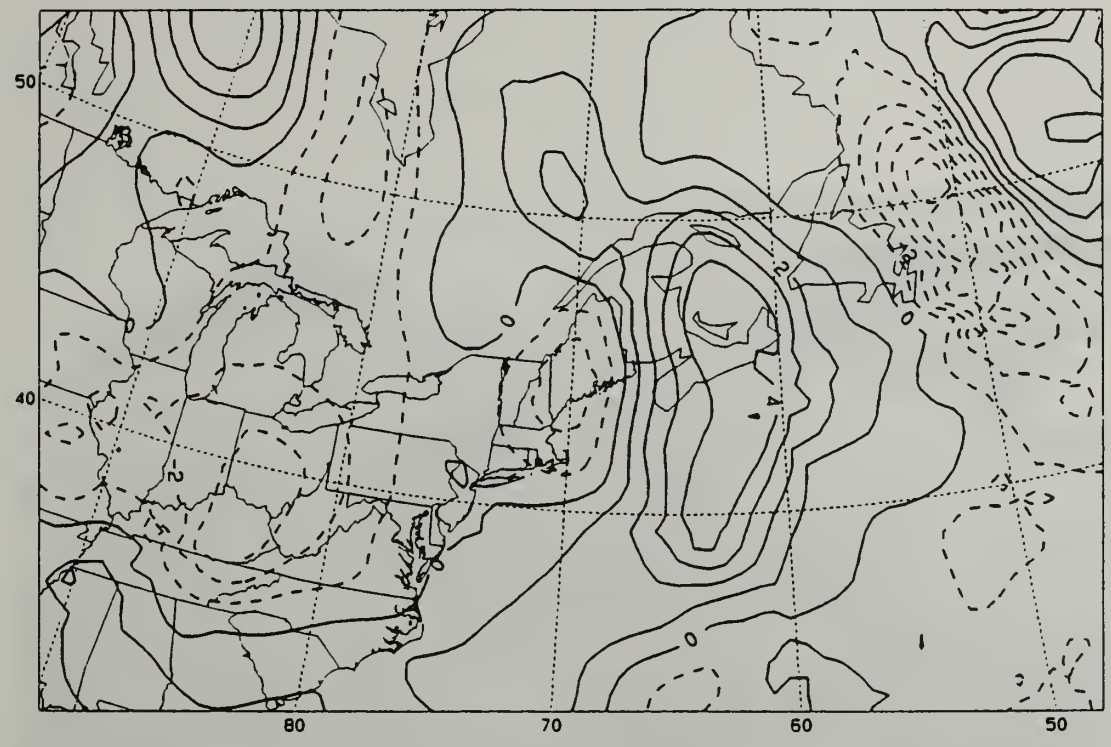

Figure 23. 300 mb divergence analysis as in Figure 6, except for 0600 UTC 21 January 1989.

cold air advection was south of the low and warm air advection was north of the low center.

By 1200/21, mid-level support for development was becoming less vigorous. In fact, positive vorticity advection over the surface low decreased substantially over the last 6 h, due to the appearance of the closed 5100 m 500 mb geopotential height center (Figure 26). However, PVA was still evident north and east of the surface low position from a strong (32×10^{-5} s^{-1}) absolute vorticity center over Nova Scotia.

At upper levels, the 60 m s^{-1} isotach contour at 300 mb (Figure 27) was quite extensive, covering most of the eastern side of the upper-air trough. It had expanded greatly from

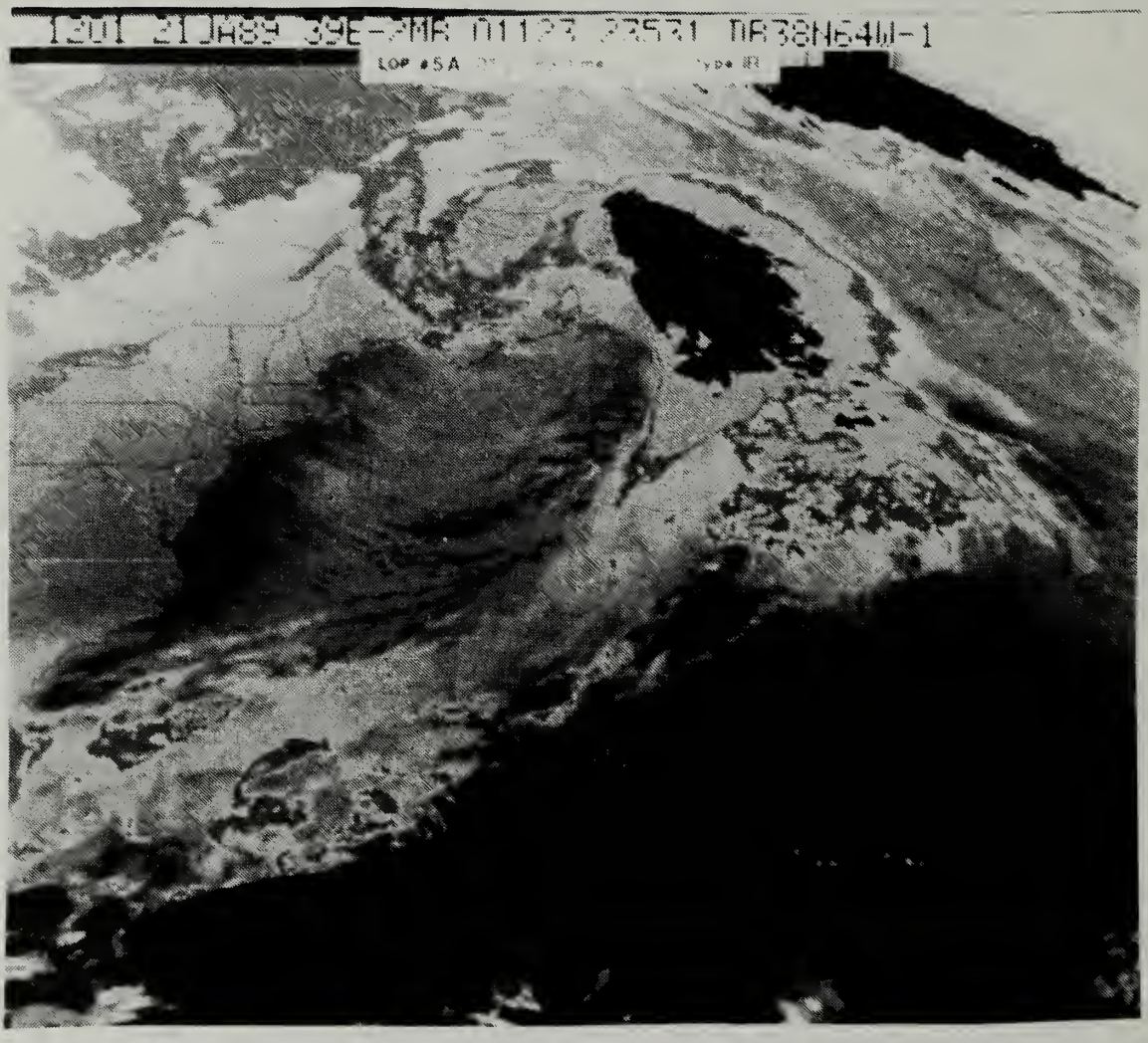

Figure 24. GOES enhanced IR imagery at 1201 UTC 21 January 1989.

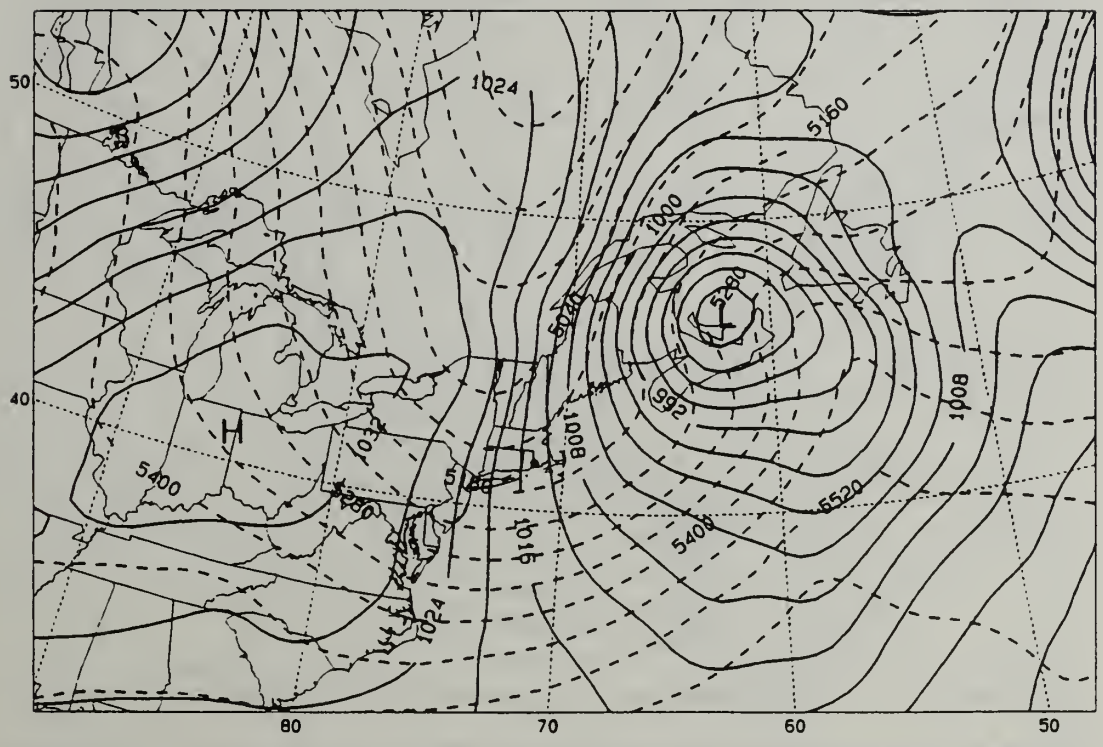

Figure 25. Surface pressure and 1000-500 mb thickness analysis as in Figure 3, except for 1200 UTC 21 January 1989.

its analyzed size 6 h earlier (not shown). The analysis for 1200/21 also indicates a stronger maximum contour of 70 m s^{-1} than at the previous time.

The maximum in the 300 mb divergence field (Figure 28) is northeast of the surface low position, due to the jet and trough locations. The analyzed divergence field continues to correlate well with satellite cloud imagery of the system (Figure 24). The maximum divergence contour ($9x10^{-5}$ s^{-1}) increased dramatically over the last 6 h and is located over Newfoundland, in the vicinity of the coldest cloud-top temperatures.

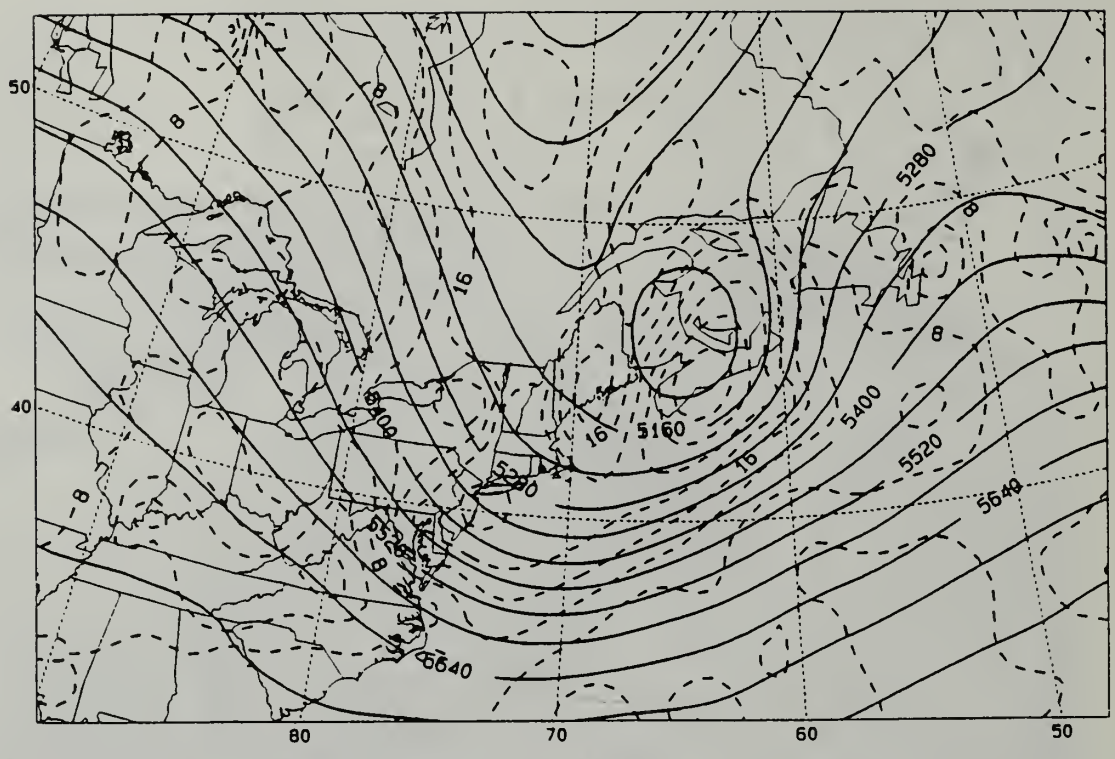

Figure 26. 500 mb height and absolute vorticity analysis as in Figure 4, except for 1200 UTC 21 January 1989.

The 200 mb temperature analysis (Figure 29) indicates that the warm pool of stratospheric air had warmed and expanded greatly, suggesting that the tropopause had lowered to well below the 200 mb level. At 300 mb, the high values of potential vorticity were west and northwest of the surface cyclone position (Figure 30); and now a relative minimum in the field appeared with values of $<10 \times 10^{-5}$ m^2 s^{-1} K kg^{-1} to the southeast of the surface low within the cold-frontal cloud band.

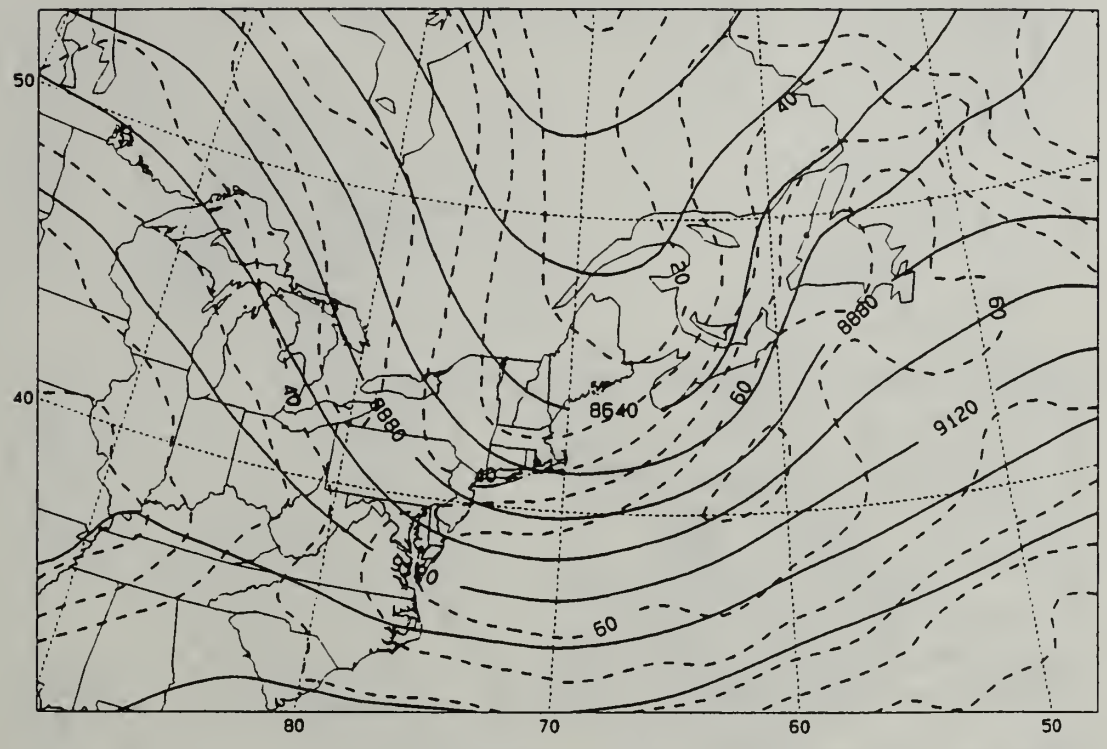

Figure 27. 300 mb height and isotach analysis as in Figure 5, except for 1200 UTC 21 January 1989.

F. 1800 UTC 21 JANUARY 1989

The IOP-5A cyclone continued to deepen from 1200/21 to 1800/21, but only at a rate of 3 mb $(6\ h)^{-1}$. During that time, the 970 mb center moved across the Gulf of Saint Lawrence at a speed of 25 kts. Thermal advections remained strong, especially north and south of the low (Figure 31).

The 500 mb support for this system continued to weaken as the low became more vertical (Figure 32). The maximum vorticity center had weakened from a value of 32 to $28 \times 10^{-5}\ s^{-1}$ and rotated around the 500 mb trough over the last 6 h.

Satellite imagery for 1801/21 still shows the classic signature of a well-developed, deep marine system (Figure 33).

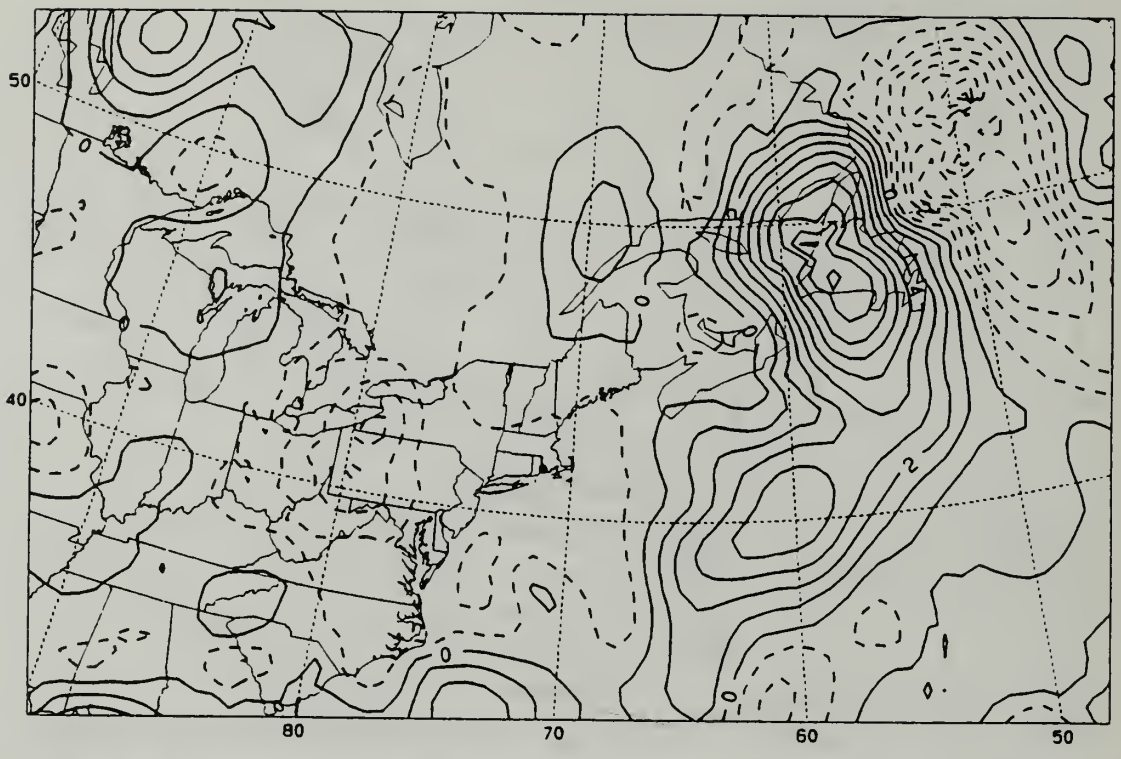

Figure 28. 300 mb divergence analysis as in Figure 6, except for 1200 UTC 21 January 1989.

The area of coldest cloud-top temperatures remained east of Newfoundland, and the frontal band was moving eastward away from the low center.

Significant divergence was indicated east of the cyclone (Figure 34), although the analyzed divergence maximum had weakened to 7×10^{-5} s^{-1}. Divergence directly above the surface cyclone decreased to near zero.

G. 0000 UTC 22 JANUARY 1989

The IOP-5A cyclone stopped deepening by 0000/22, reaching a central pressure of 969 mb (Figure 35). The system tracked east-northeast over land at 21 kts during the last 6 h. The

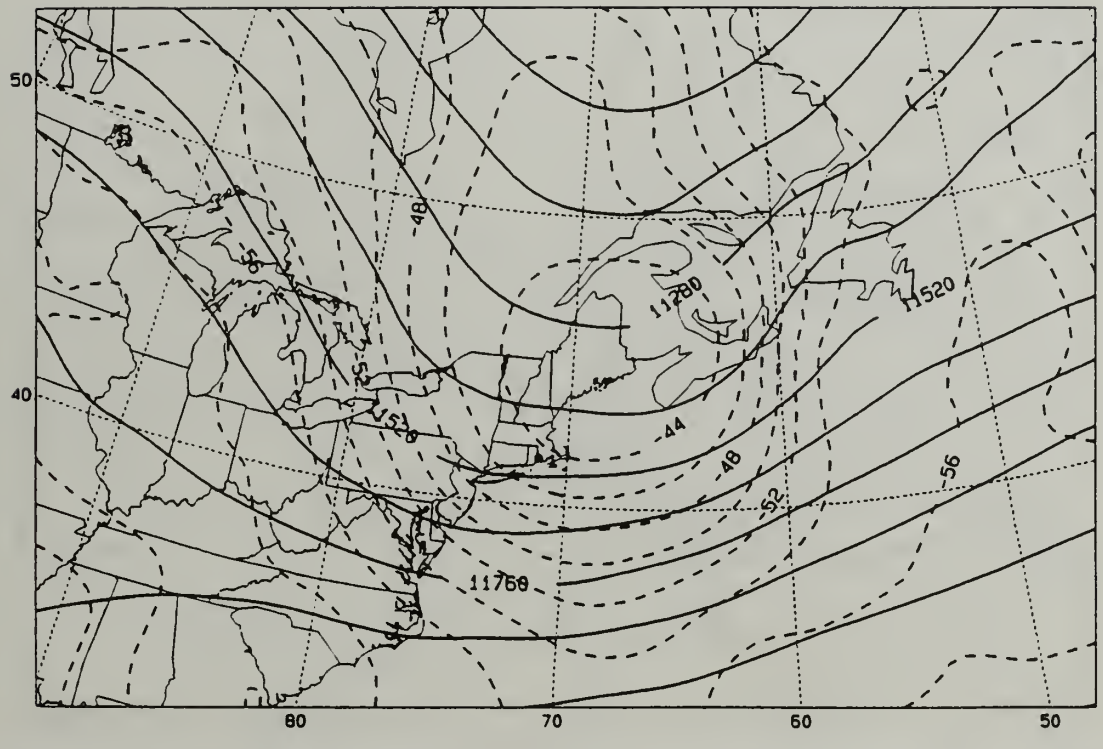

Figure 29. 200 mb height and temperature analysis as in Figure 21, except for 1200 UTC 21 January 1989.

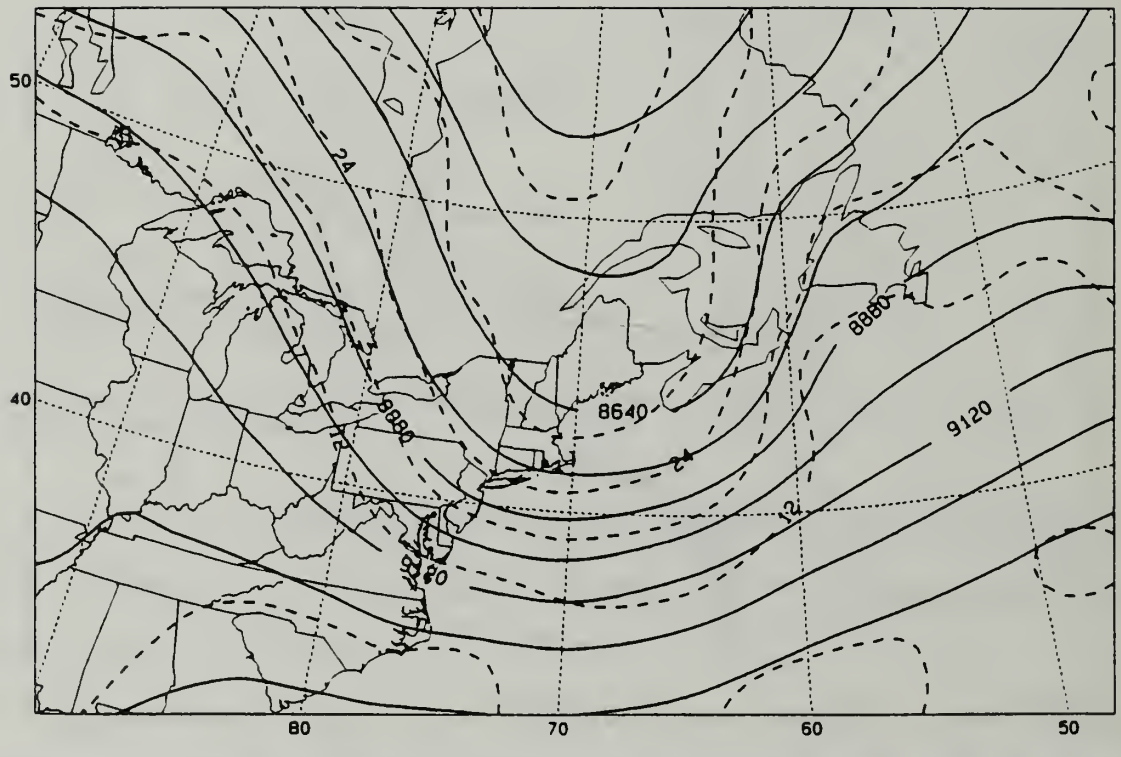

Figure 30. 300 mb height and potential vorticity analysis as in Figure 22, except for 1200 UTC 21 January 1989.

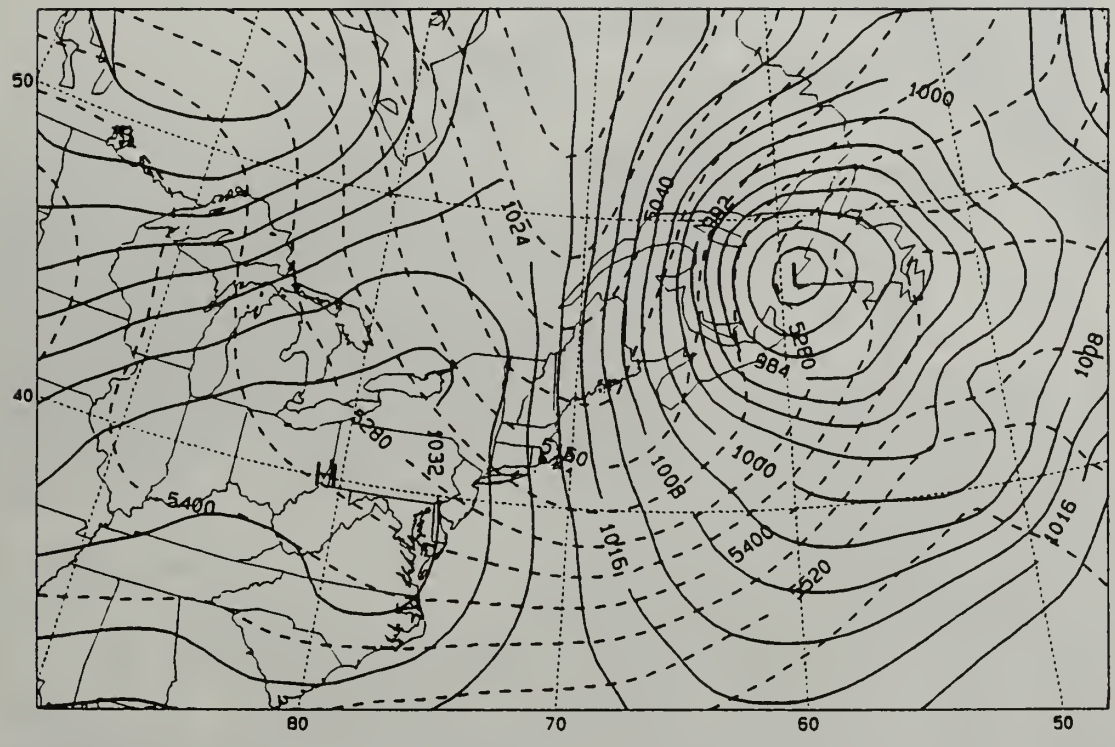

Figure 31. Surface pressure and 1000-500 mb thickness analysis as in Figure 3, except for 1800 UTC 21 January 1989.

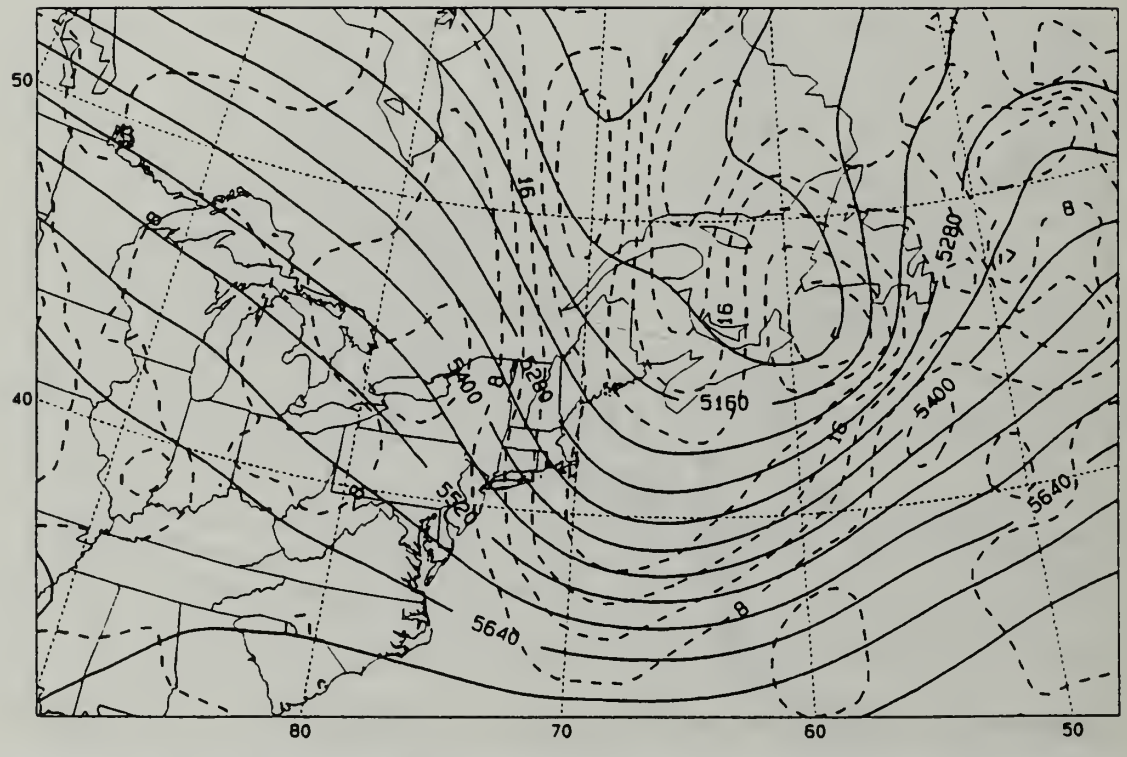

Figure 32. 500 mb height and absolute vorticity analysis as in Figure 4, except for 1800 UTC 21 January 1989.

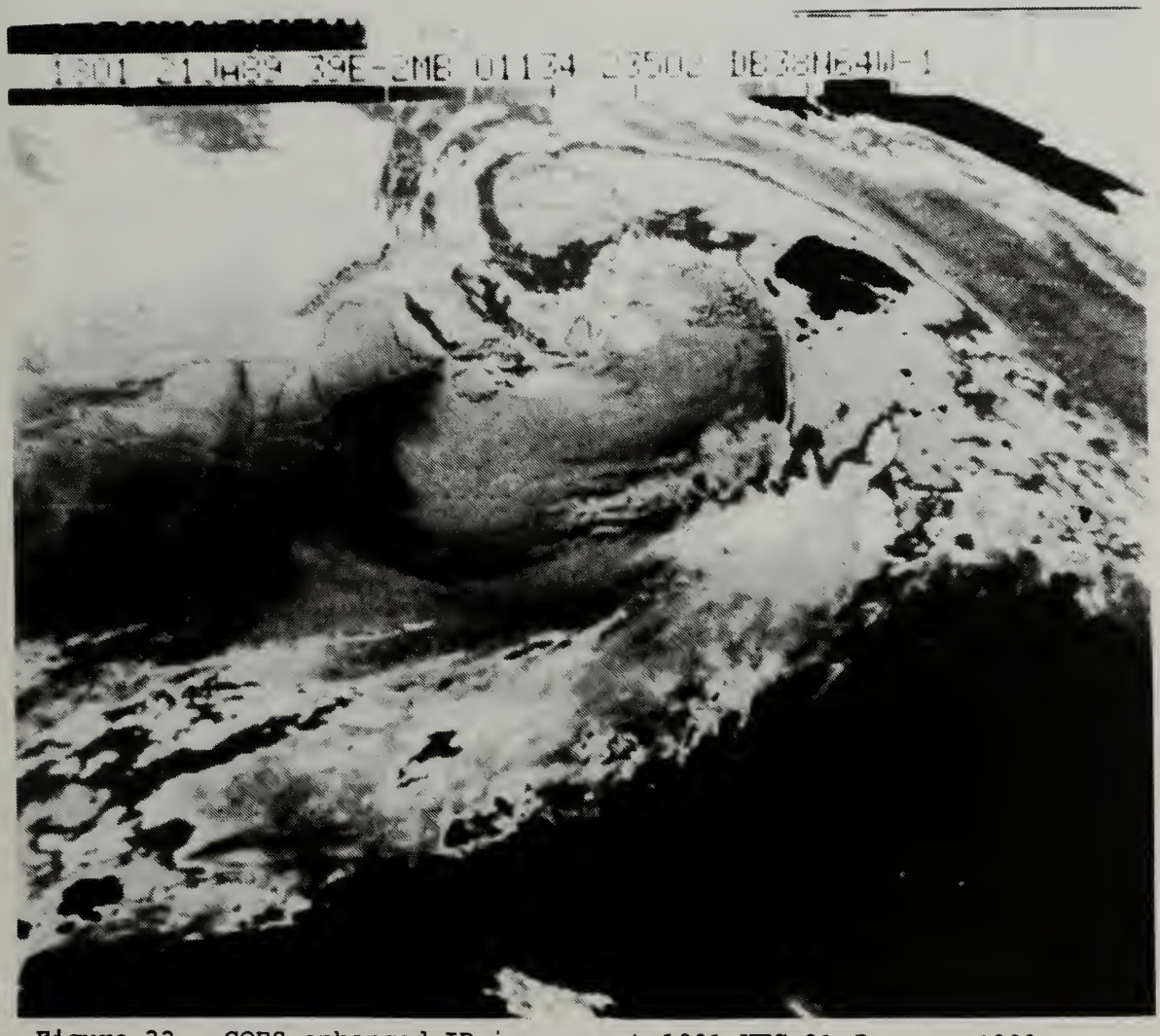

Figure 33. GOES enhanced IR imagery at 1801 UTC 21 January 1989.

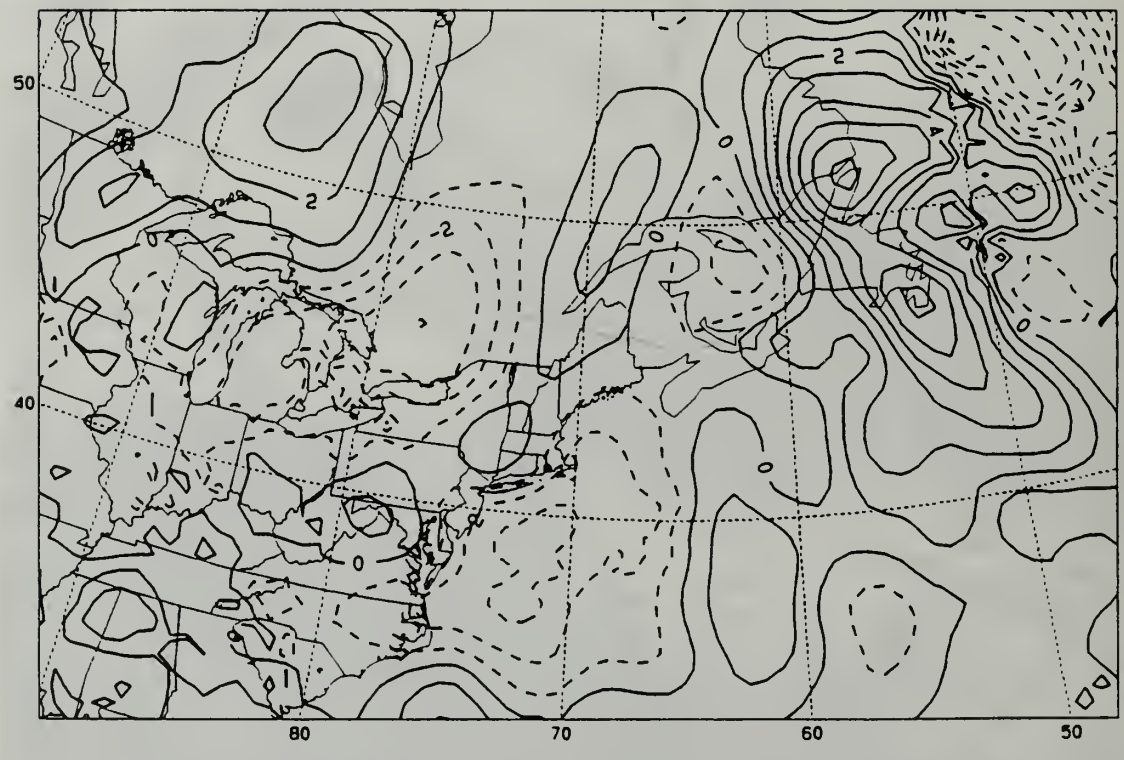

Figure 34. 300 mb divergence analysis as in Figure 6, except for 1800 UTC 21 January 1989.

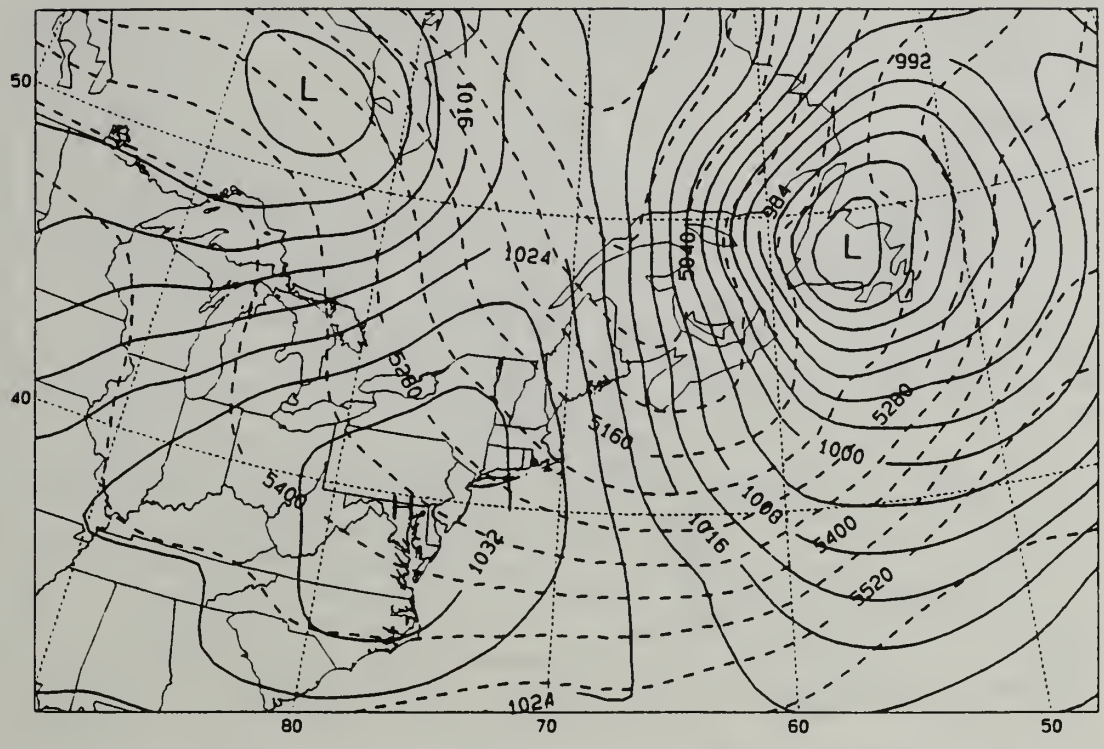

Figure 35. Surface pressure and 1000-500 mb thickness analysis as in Figure 3, except for 0000 UTC 22 January 1989.

MSLP and thickness analyses show a weakening of the thermal advection pattern with warm air advection to the north and cold air advection to the south of the low.

The system was now fully mature and vertical at 0000/22, as shown by the 500 mb analysis (Figure 36). The main cloud band to the east of the low moved away from the cyclone center toward the east (not shown). Positive vorticity advection was small at this time as the 4980 m closed 500 mb height center was almost directly over the surface low. There was a closed 8460 m height contour indicated on the 300 mb analysis as well (Figure 37). Consequently, the system began to fill as it moved over the North Atlantic Ocean thereafter.

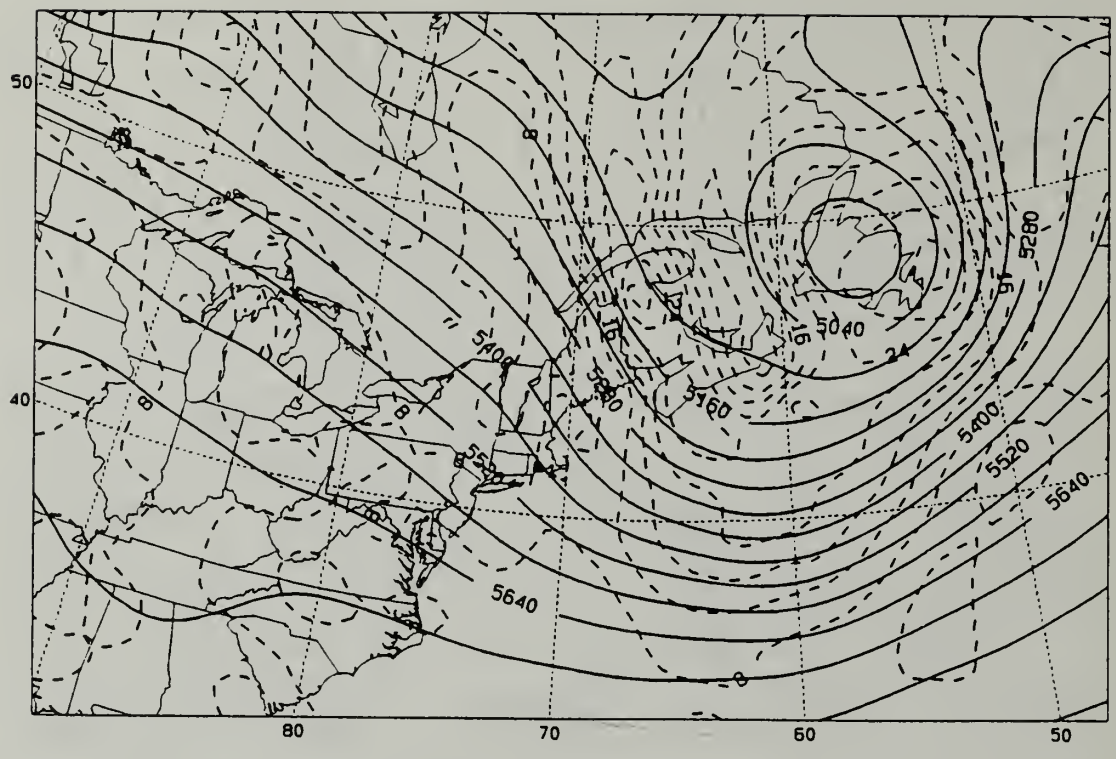

Figure 36. 500 mb height and absolute vorticity analysis as in Figure 4, except for 0000 UTC 22 January 1989.

H. MESOSCALE ANALYSES AND THE EXAMINATION OF TOPOGRAPHIC/COASTAL INFLUENCES

The 6-hourly, 60 km NORAPS analyses are too coarse to resolve mesoscale features that may have played an important role in the rapid development of the IOP-5A cyclone. In this section, a detailed, subjective hand analysis of all available data for each hour from 1500/20 to 0300/21 is described in order to examine the mesoscale processes taking place as the cyclone interacted with the topography enroute to the coast of Maine. The data utilized for these analyses include operational surface and upper-air observations and special ERICA data from land stations, buoys and ships.

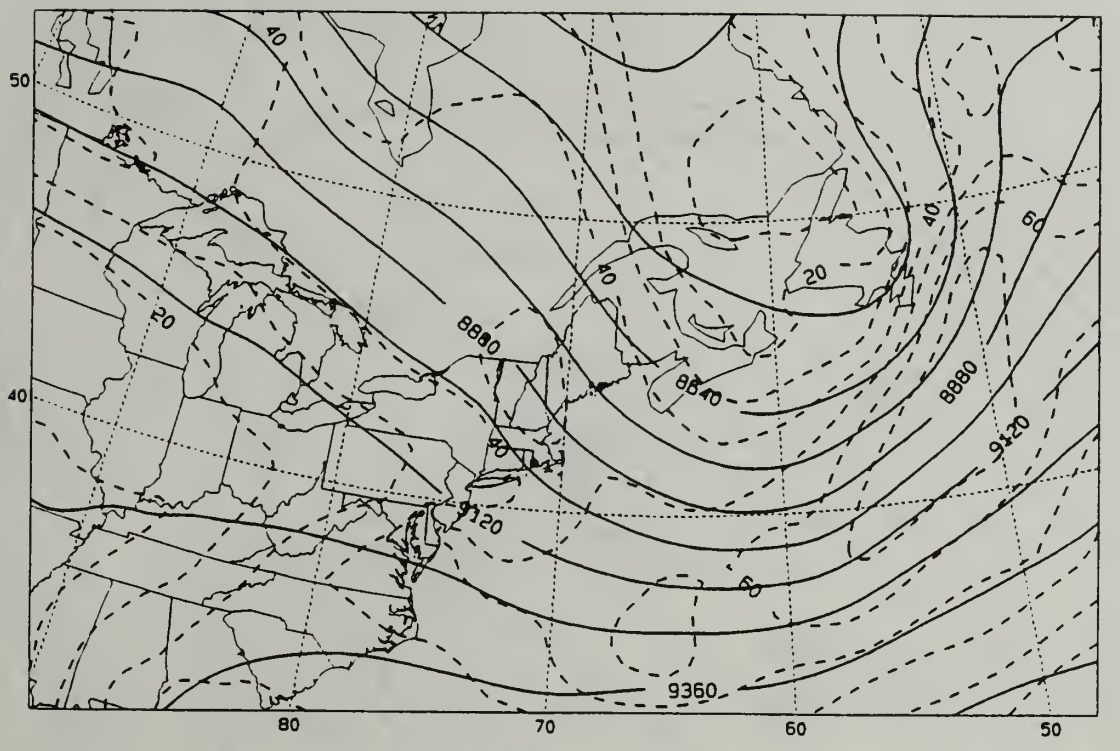

Figure 37. 300 mb height and isotach analysis as in Figure 5, except for 0000 UTC 22 January 1989.

The investigation focused on an area from 41N to 48N and 75W to 65W. Synoptically, the IOP-5A cyclone was approaching the mountains of New England from the west at the beginning of the period (1500/20). On a smaller scale, local terrain effects and distinctly different stability characteristics near the coast could have played significant roles in influencing the cyclone's evolution.

Most significantly, the hand analyses reveal the development of a secondary low pressure center well to the southeast of the primary low. This second low was never indicated in the synoptic NORAPS analyses.

Figure 38 shows the isobaric hand analysis for 1500/20.

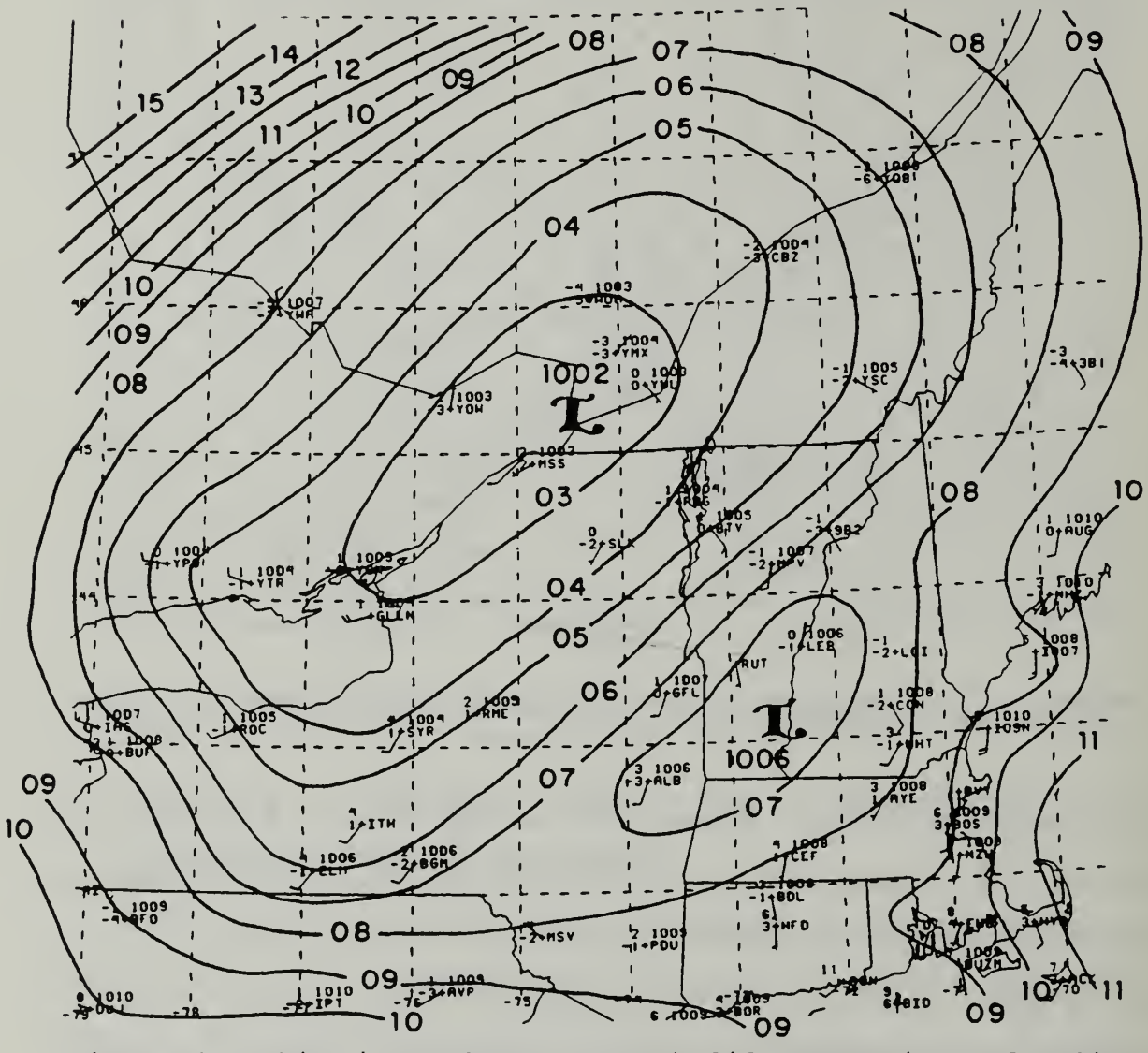

Figure 38. Subjective surface pressure (solid, contour interval 1 mb) analysis at 1500 UTC 20 January 1989.

At this time, a new low develops near 43.2N 72.6W (southeast Vermont) southeast of the primary IOP-5A cyclone, located near 45.3N 74.5W (vicinity of Montreal).

Based on the topography of the region (Figure 39), it is conceivable that the secondary low pressure area is the result of lee cyclogenesis on the downwind (eastern) side of the

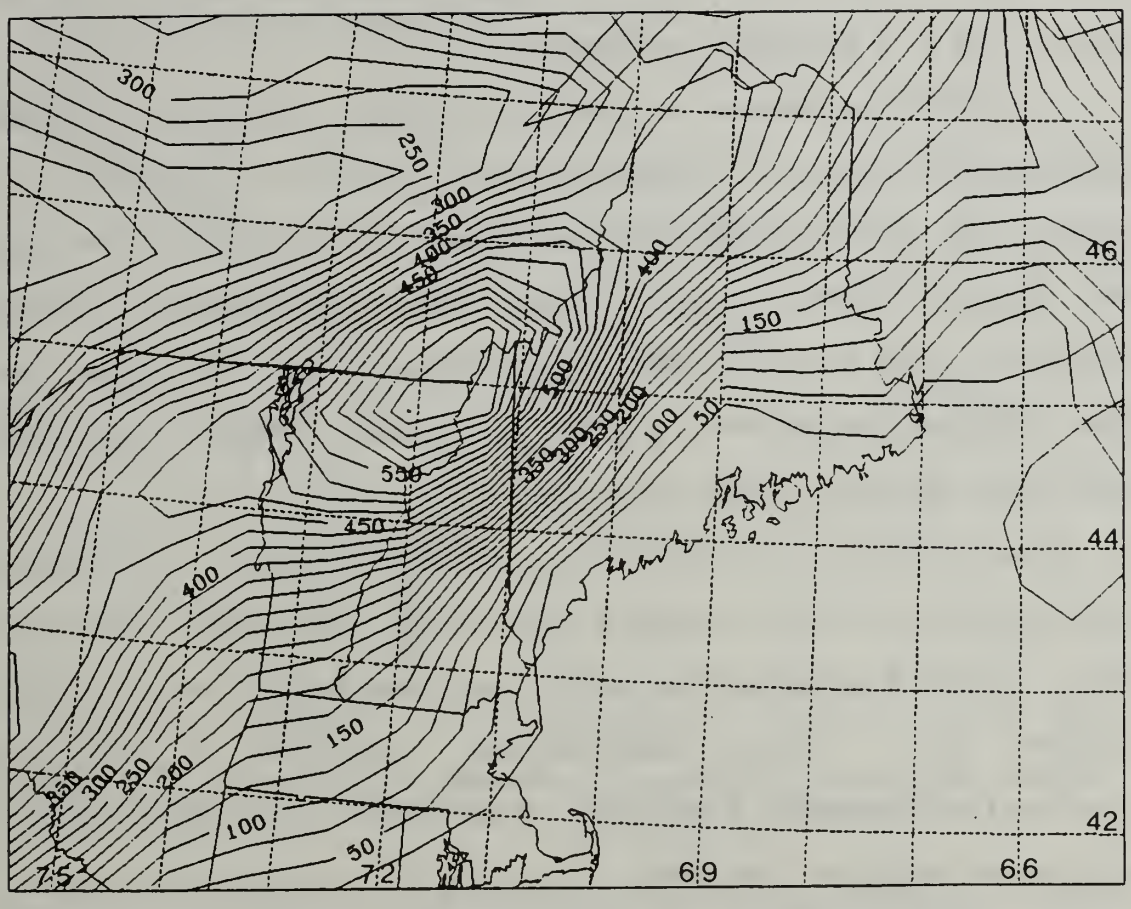

Figure 39. NORAPS surface terrain height (solid, contour interval 25 m) for January 1989.

northern Appalachian Mountains.

From 1500/20 to 1800/20 (not shown), the primary IOP-5A cyclone moved to the northeast (initially along the Saint Lawrence River) at an average of 21 kts and deepened from 1002 mb to 998 mb. At the same time the southern low pressure area moved southeast and then northeast, and was located near 42.9N 71.8W (southern New Hampshire) at 1800/20. While the wind pattern still did not indicate a cyclonic circulation, the

minimum pressure in the area dropped from 1006 mb to 1001 mb during the 3-h period (not shown).

The NORAPS analyses of the difference of 500 mb - 1000 mb equivalent potential temperature at 1800/20 (Figure 40), showed that static stability was significantly lower over the New England coastal region than over the primary IOP-5A cyclone's path north of New York, Vermont and New Hampshire. This reduced stability along the coast favors continued deepening of the coastal cyclone.

From 1800/20 to 2100/20, the secondary low tracked northeast at 19 kts to near 43.3N 70.7W (southwest corner of Maine, about 5 nm from the coast) and deepened 3 mb to 998 mb (Figure 41). The observations indicate a cyclonic circulation, showing a distinct wind shift from northerly at Manchester Airpark, NH (MHT) to westerly at Beverly Municipal, MA (BVY) and southerly at the buoy IOSN, with lowest pressures reported by the coastal stations. The primary cyclone maintained an average movement of northeasterly at 21 kts from 1800/20 to 2100/20, but only deepened 1 mb to 997 mb (Figure 41).

The ridge-line of the mountain range runs from southwest to northeast along the northwest Maine border. In the time period from 2100/20 to 0000/21, the primary cyclone appeared to "jump" across the mountains to the southeastern side of the ridge near 45.2N 69.5W (central Maine) by 0000/21 (not shown). This indicates a speed of movement of approximately 33 kts.

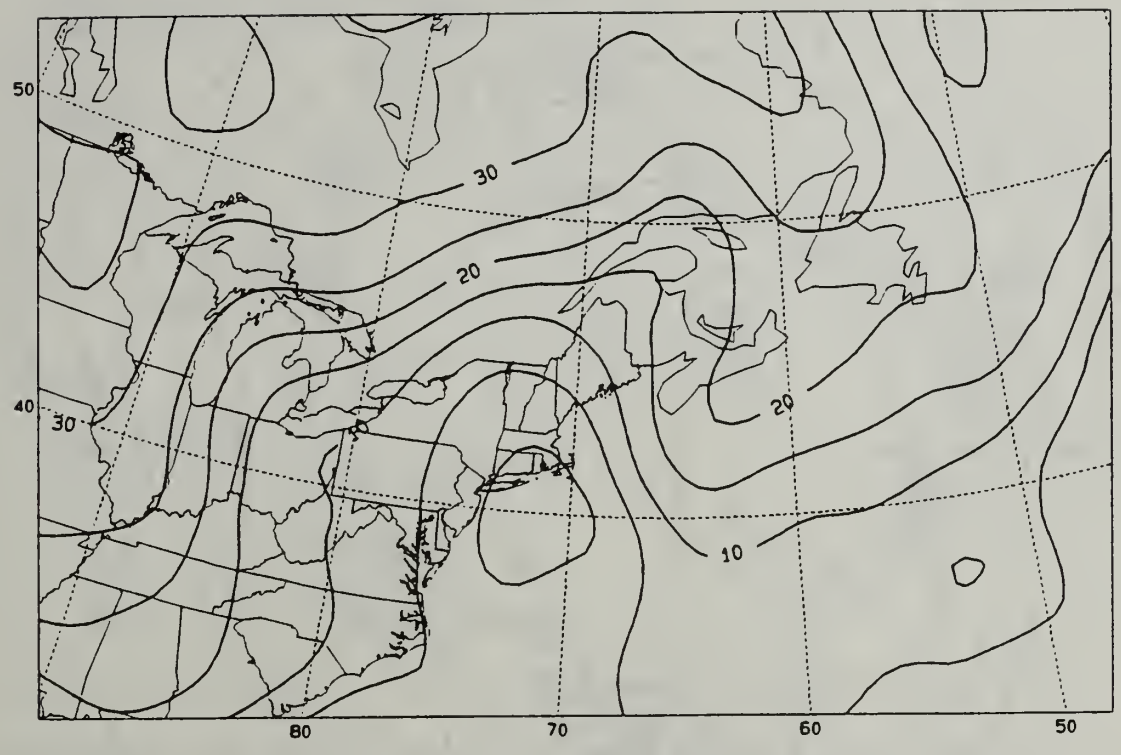

Figure 40. 500-1000 mb equivalent potential temperature (solid, contour interval 5°K) analysis at 0000 UTC 21 January 1989.

The central pressure was analyzed as having dropped 2 mb to 995 mb at that time.

Meanwhile, the coastal low continued to progress northeastward at 21 kts along the southern coast of Maine, and deepened 3 mb to 995 mb, near 43.9N 69.5W at 0000/21 (not shown).

The 500 mb - 1000 mb equivalent potential temperature analysis at 0000/21 (Figure 42) shows the coastal area of weak stability had persisted and moved to the northeast, over southern Maine.

From 0000/21 to 0300/21, the primary low moved northeast then southeast to approximately 45.3N 68.4W and deepened 4 mb

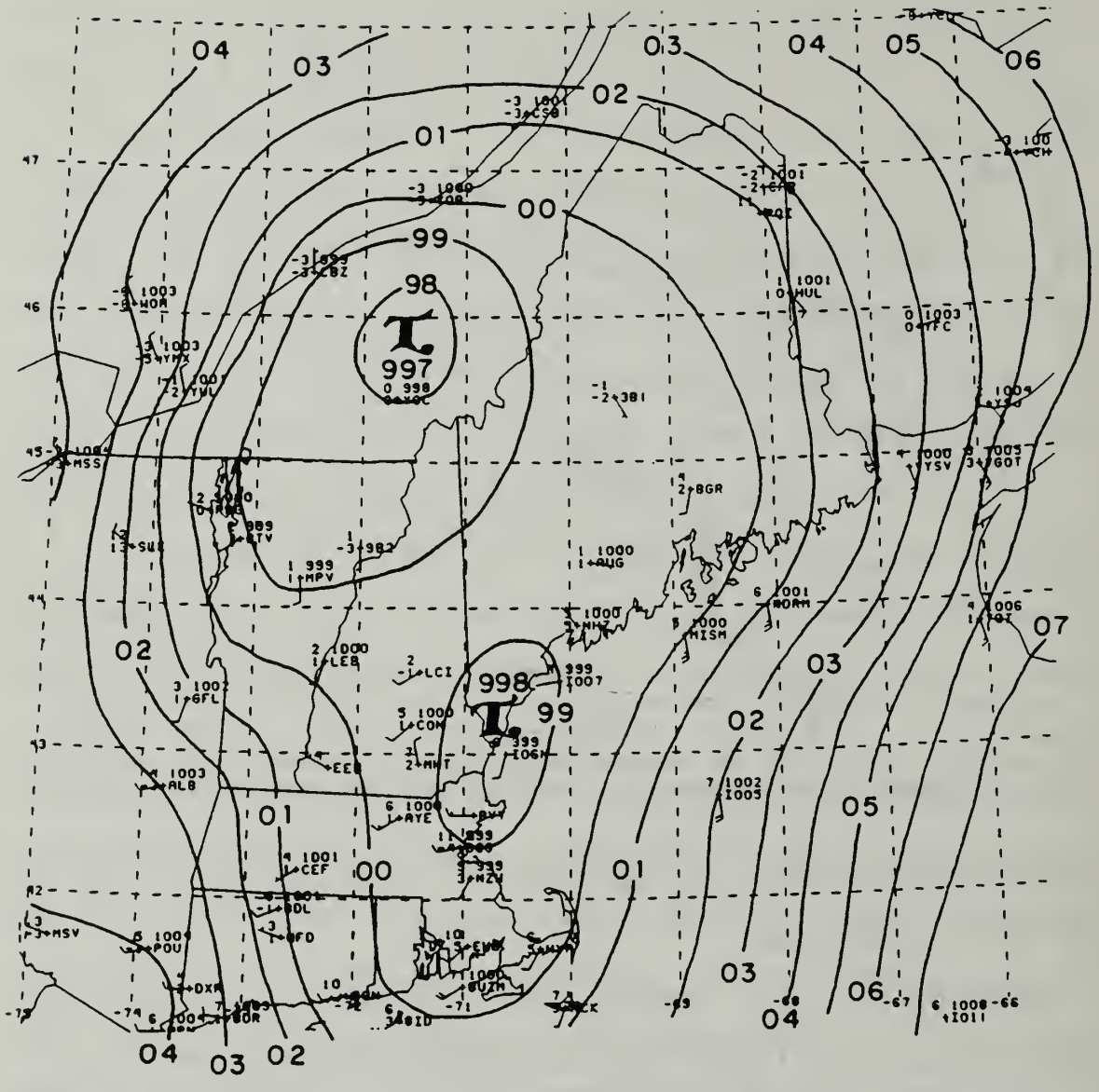

Figure 41. Subjective surface pressure analysis as in Figure 38, except for 2100 UTC 20 January 1989.

to an analyzed central pressure of 991 mb (not shown). The coastal low continued to move northeast along the southern coast of Maine during this time while it intensified to 990 mb, a drop of 5 mb in 3 h (not shown).

Figure 43 shows the tracks of the two separate lows from 1500/20 to 0300/21 as derived from the hourly hand analyses.

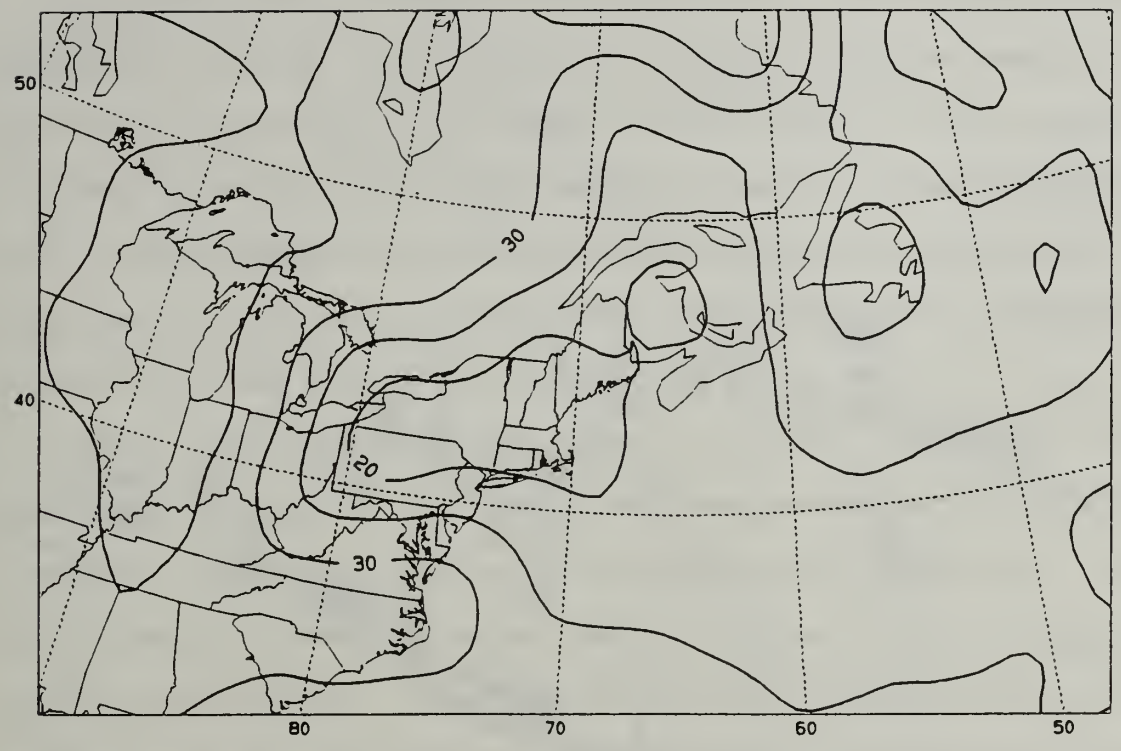

Figure 42. 500-1000 mb equivalent potential temperature analysis as in Figure 40, except for 0000 UTC 21 January 1989.

The hour and last two digits of the central pressure are shown above and below the position markers (open circles). The 6-h positions of the IOP-5A cyclone as analyzed by NORAPS are represented by the open square symbols.

Notice that the NORAPS position at 1800/20 is about 20 nm north of the manually analyzed position of the primary cyclone at that time. The NORAPS analysis at 0000/21 shows a position at a latitude between the two manually analyzed separate low centers, and 30 nm further west. The 0600/21 NORAPS position would be fairly accurate as compared with the projected hand analyses, except perhaps further west.

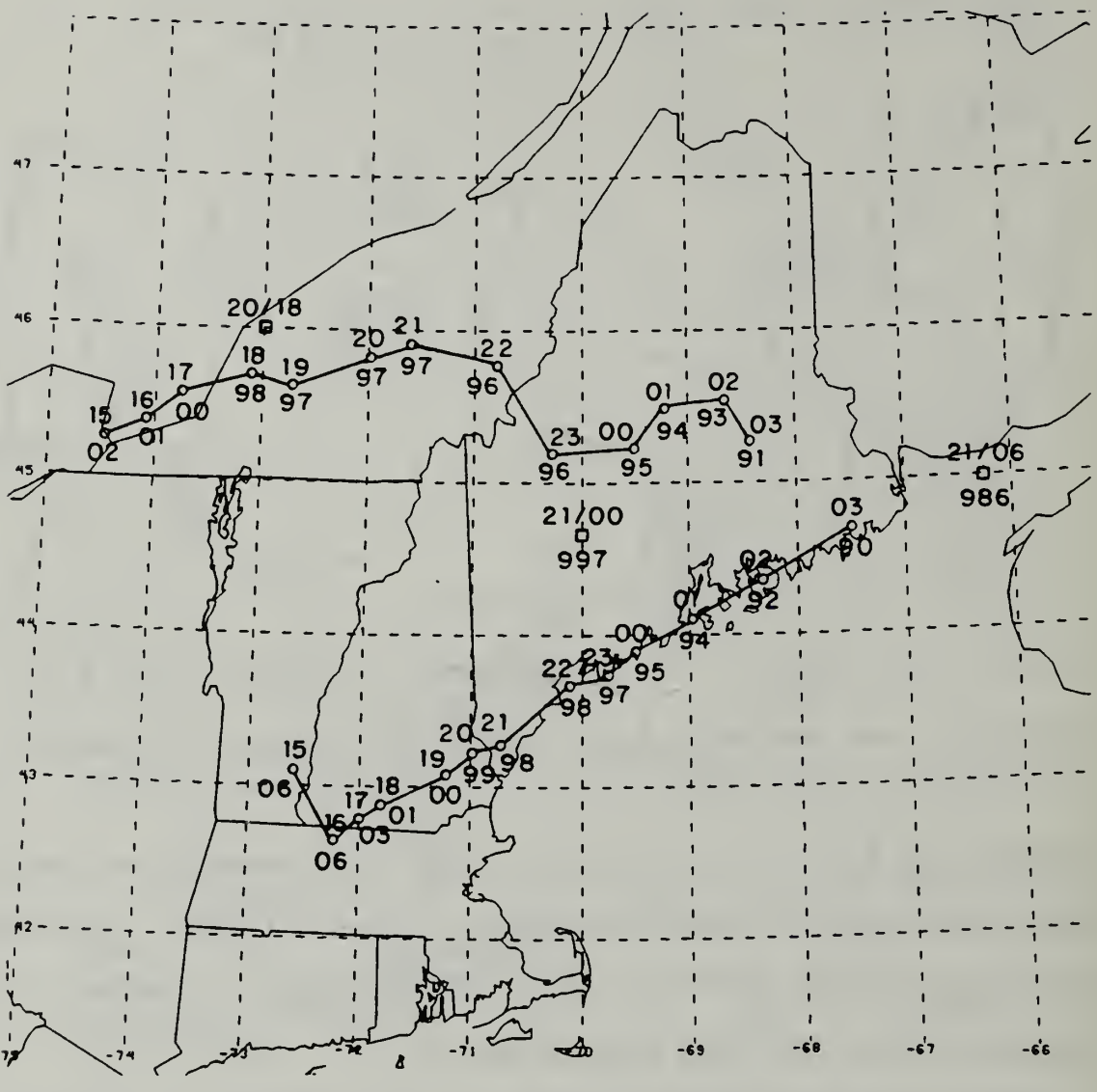

Figure 43. Tracks (solid lines connecting open circles) and central pressures (mb) of primary and secondary lows from 1500/20 to 0300/21. Open squares are positions of main low from NORAPS analyses.

The NORAPS central pressure analyses indicate consistently higher central pressure values of 2 mb greater than what the hand analyses show. This is probably due to inadequate resolution and/or problems with the optimum interpolation scheme not drawing to the observations.

The motivation behind performing the subjective hourly analyses was the desire to gain insight into the mesoscale details of the IOP-5A cyclone's development in the period leading up to its explosive deepening stage. The intention was to accurately delineate a higher resolution portrayal of the area of interest than the NORAPS analyses could represent, during the time period in question.

These detailed analyses give a clear indication that mesoscale processes not necessarily captured by the NORAPS analyses were occurring during the time period examined. Lee side coastal mesoscale development occurred to the southeast of the existing low. This new low deepened rapidly and likely became the primary center. Unfortunately, at this time the quantitative impact of these processes on the track and intensity of the IOP-5A cyclone remains a matter of speculation.

IV. NORAPS MODEL PERFORMANCE

A. MODEL DESCRIPTION

The model used in this study is a modified version of the Navy Operational Regional Atmospheric Prediction System (NORAPS). NORAPS is a relocatable regional mesoscale model that solves the hydrostatic primitive equations on an Arakawa C-grid of 109 x 82 grid points. It has a horizontal resolution of 60 km and uses a sigma vertical coordinate system with 24 sigma levels. A detailed model description is provided in Hodur (1987), and a summary of the salient characteristics of the NORAPS model version used in this study is given in Hirschberg and Langland (1992).

NORAPS cumulus parameterization uses a modified Kuo approach in which convection is linked to the planetary boundary layer (PBL). When the environmental moisture exceeds 100% relative humidity, condensation is assumed to occur and precipitation is allowed to fall until reaching an unsaturated layer. NORAPS uses one-way interactive boundary conditions that are obtained from NOGAPS analyses at 6-h intervals. The U.S. Navy's 10 minute data base provides the terrain fields used by the NORAPS model. The model terrain height has been enhanced to account for the highest peaks' effect on the flow.

A NORAPS 36-h forecast series initialized at 1200/20 (12 h prior to the IOP-5A cyclone's rapid intensification phase) will now be compared to the NORAPS analyses. In this manner, the model performance in predicting the evolution of the IOP-5A cyclone will be evaluated.

B. POSITION AND INTENSITY

NORAPS fairly accurately forecasted the rapid development of the IOP-5A cyclone. While the 6-h forecast central pressure of the low was 2 mb too high (as compared to the NORAPS analysis valid at the same time, 1800/20), the 12-h forecast intensity was the same as the analyzed intensity. The forecast positions were correct for both times. The 18-h forecast had a position error of 20 nm too far north, with the central pressure 3 mb too high. This trend by the model to insufficiently deepen the storm and to move it north-northwest of the analyzed position continued thereafter. By the 24-h point (1200/21), the MSLP forecast was 5 mb too high, and the forecast position was approximately 60 nm north of the analysis position. The 30- and 36-h forecasts were more accurate in terms of the predicted central pressures, but the position errors increased. The 30-h forecast indicated that the low was 1 mb more than analyzed and approximately 90 nm too far northwest. At 0000/22 (the 36-h forecast time), the forecast low was again too weak (central pressure was 2 mb too high) and approximately 160 nm northwest of the analyzed low.

Table 1 summarizes the results of the central pressure and position error comparison of the NORAPS forecasts and objective analyses from 1200/20 to 0000/22. Considering the magnitude of the IOP-5A cyclone's deepening (34 mb (36 h)$^{-1}$ and 24 mb (12 h)$^{-1}$), the NORAPS forecasts were quite successful.

Table 1. COMPARISON OF NORAPS FORECAST CENTRAL PRESSURE AND POSITION WITH ANALYSES FROM 1200/20 TO 0000/22.

	analysis	forecast	pressure error	position error	direction
20/12	1003mb	1003mb	0 mb	0 nm	none
20/18	1000mb	1002mb	+2 mb	0 nm	none
21/00	997mb	997mb	0 mb	0 nm	none
21/06	970mb	970mb	+3 mb	20 nm	north
21/12	973mb	973mb	+5 mb	90 nm	north
21/18	970mb	971mb	+1 mb	90 nm	northwest
22/00	969mb	971mb	+2 mb	160 nm	northwest

C. LOW-LEVEL THICKNESS/THERMAL FEATURES

The NORAPS forecasts of 1000 mb - 500 mb thickness and mean sea level pressure from 1200/20 to 0000/21 (0-h to 24-h forecasts) exhibited very similar patterns to those of the analyses with respect to their gradients, magnitudes and orientation; thus the forecasts are not shown. The 18-h forecast (valid at 0600/21) did differ in some respects from the analysis at that time. For example, the forecast (Figure 44) shows both the cold tongue over New York and the thermal ridge southwest of the low center were more pronounced than in

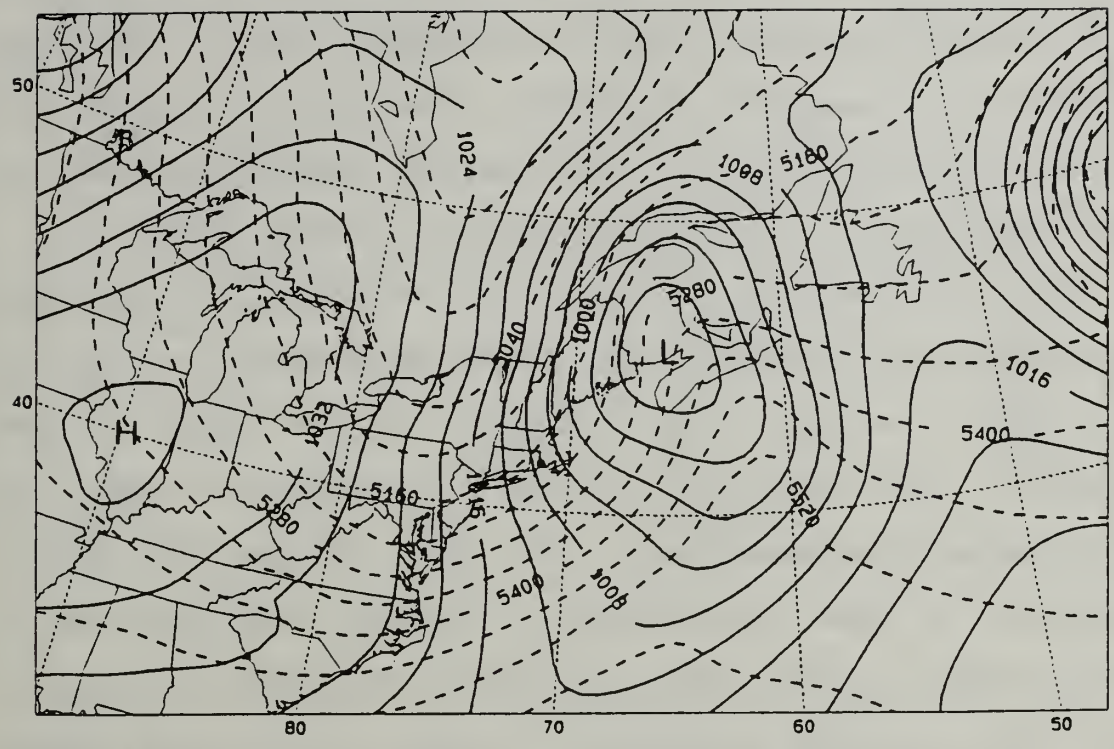

Figure 44. Surface pressure (solid, contour interval 4 mb) and 1000-500 mb thickness (dashed, contour interval 60 m) forecast valid at 0600 UTC 21 January 1989.

the analysis (Figure 18). Also, the thickness gradient behind the cold front appeared tighter in the forecast. The strength of these simulated features may have been at least partly responsible for the model 11 mb $(6\ h)^{-1}$ MSLP deepening rate from 0600/21 to 1200/21. Although the analyzed intensification was slightly greater (13 mb) during that time, NORAPS performance in predicting explosive deepening was quite respectable.

The 24-h forecast (not shown), valid at 1200/21, continued to display a stronger thermal ridge than the analysis. Additionally, the forecast thickness gradient and cold air

advection were stronger than analyzed. Thus, NORAPS predicted 7 mb deepening between 1200/21 and 1800/21, while only 3 mb deepening was analyzed. In effect, the forecast "caught up" to the analysis at the 30-h time period, possibly because of overpredicting the strength of the 24-h thermal ridge.

The 30-h forecast (Figure 45), valid at 1800/21, did reasonably well in predicting an open wave forming along the cold front near 42N 55W (indicated by the "gap" in the isobars). The analysis (Figure 31) depicted a wave in approximately the same place. The 36-h forecast (not shown) continued to show very strong cold air advection and a significantly tighter thickness gradient behind the cold front than the analysis indicated. True to its well-known characteristics, NORAPS was slow to deepen the IOP-5A cyclone in the early portion of the forecast, and slow to fill it once it had reached maturity and its maximum intensity.

D. MID-LEVEL VORTICITY FEATURES

Comparison of the analyzed and forecasted 500 mb absolute vorticity/geopotential height fields indicates that NORAPS simulated the mid-level wave associated with this case well. While the forecast depictions of the vorticity maxima were not always identical to the analyzed locations, the general PVA and NVA patterns were quite similar. The basic characteristics of the height and vorticity fields were generally good at each forecast hour.

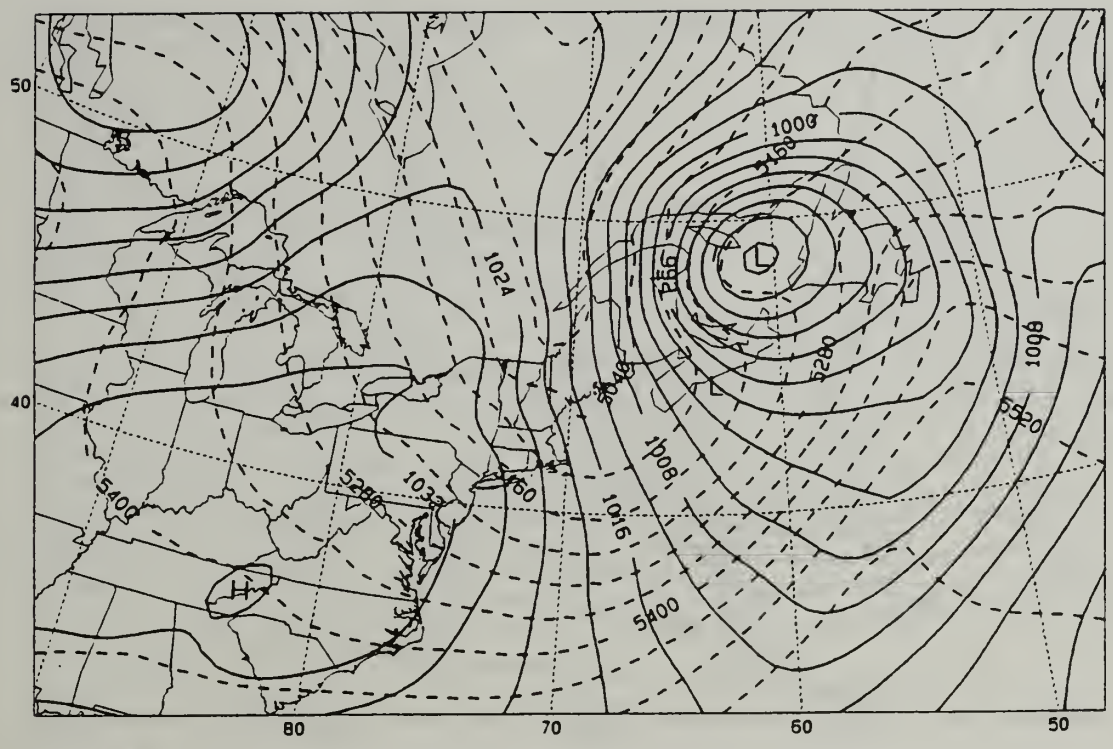

Figure 45. Surface pressure and 1000-500 mb thickness forecast as in Figure 44, except for 1800 UTC 21 January 1989.

The 6-h forecast (Figure 46), valid at 1800/20, shows a large $20x10^{-5}$ s^{-1} contour extending from Lake Ontario to Kentucky, similar to the analysis (Figure 9). The difference is that the simulation shows a maximum value of 24 centered northeast of the maximum of 28 over southern Ohio in the analysis. The forecast and analysis height fields are very similar at both the 6-h and 12-h valid times. The 12-h forecast (not shown) is slightly weak on the intensity of the maximum vorticity center as well, indicating one 28 contour in the center of the 20 vorticity lobe, while the analysis (Figure 14) shows separate 32 centers at each end of the lobe.

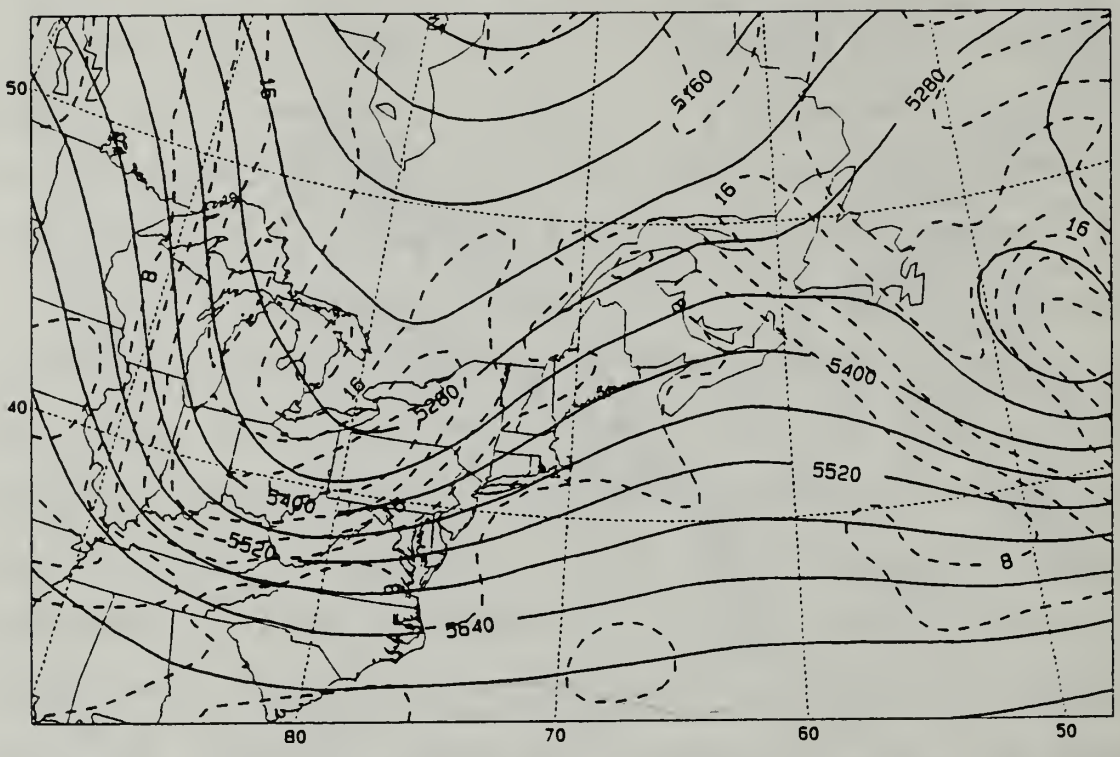

Figure 46. 500 mb height (solid, contour interval 60 m) and absolute vorticity (dashed, contour interval $4x10^{-5}$ s^{-1}) forecast valid at 1800 UTC 20 January 1989.

The 18-h forecast, valid at 0600/21, accurately depicts the deepening and shift of the 500 mb trough axis over New England (Figure 47). It also shows the northeastern edge of the $24x10^{-5}$ s^{-1} absolute vorticity center directly over the surface low position, just as the analysis (Figure 19) indicates. However, the analyzed vorticity maximum is stronger and does not extend as far to the southwest as depicted in the forecast.

At 1200/21, the 24-h forecast (Figure 48) and the analysis (Figure 26) both show the double vorticity maxima in approximately the same manner. Slight differences in the

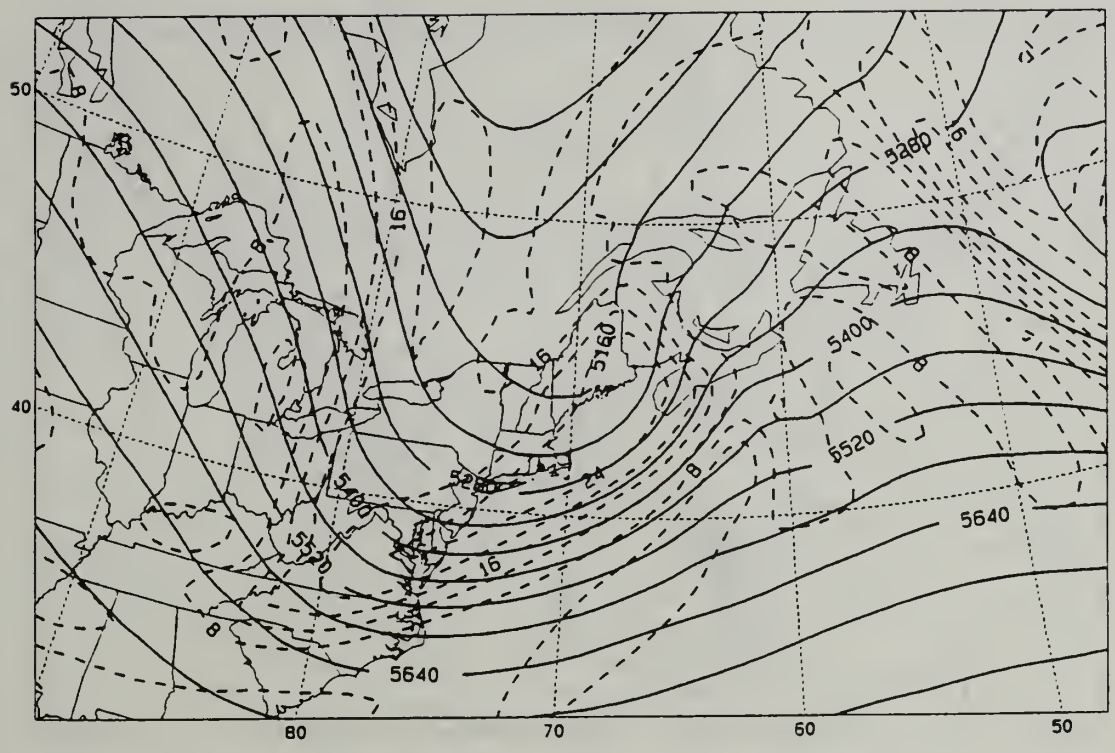

Figure 47. 500 mb height and absolute vorticity forecast as in Figure 46, except for 0600 UTC 21 January 1989.

forecast versus the analyzed height fields occur at 1200/21 (24-h forecast) and 1800/21 (30-h forecast, not shown). At the former time, the analysis shows a closed 5100 m height center (while the forecast does not), and at the latter time the forecast shows the closed height contour (while the analysis does not). The closing of the centers at different times led to differences in the times of zero or near-zero vorticity advection over the surface low. The 30-h forecast indicates stronger PVA behind the cold front than does the analysis. At the 36-h forecast time (0000/22), both fields display similar areas of PVA and NVA around the IOP-5A cyclone (not shown).

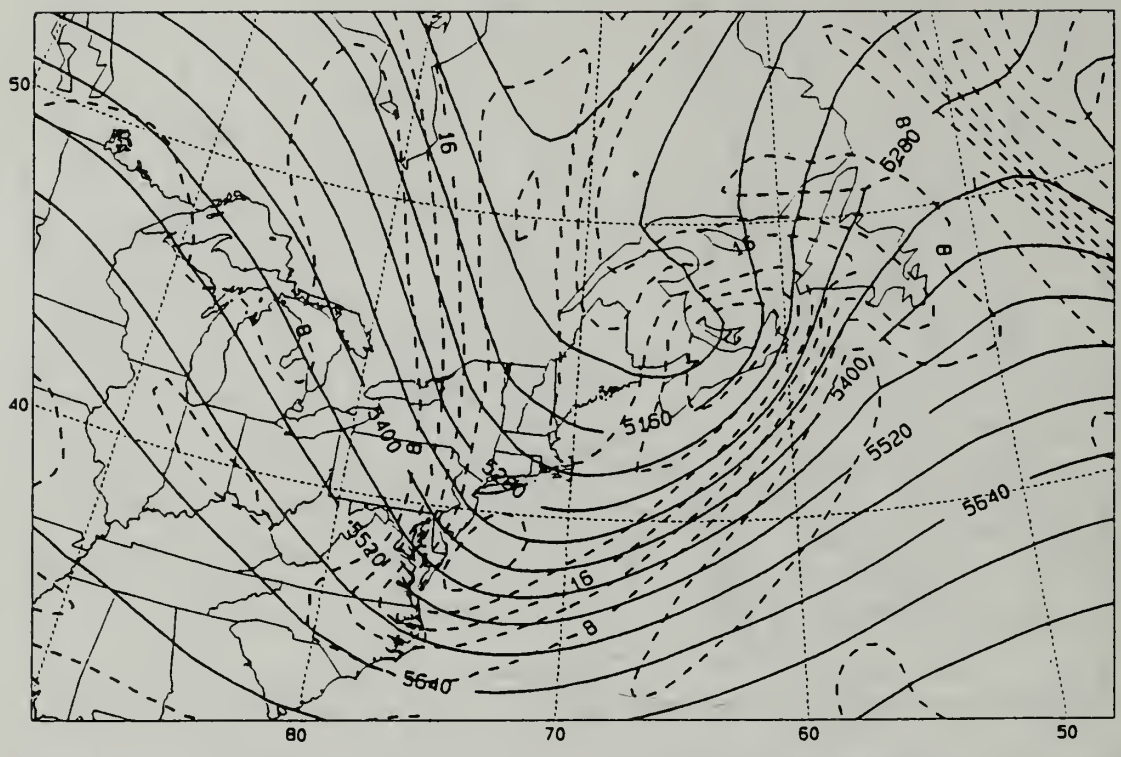

Figure 48. 500 mb height and absolute vorticity forecast as in Figure 46, except for 1200 UTC 21 January 1989.

E. UPPER-LEVEL JET AND DIVERGENCE FEATURES

There are only very minor differences in the forecast versus analyzed 300 mb geopotential height/isotach series. Throughout the entire comparison, maximum jet intensities differ by 10 m s^{-1} or less. The forecasts and analyses closely resemble each other at 1800/20 (the 6-h forecast time, forecast not shown). The location of the 60 m s^{-1} isotach was predicted very accurately, and the jet maximum was forecast only 10 m s^{-1} weaker than the analysis (Figure 10). The 12-h forecast (not shown) indicates less curvature of the jet around the base of the 300 mb trough than was analyzed (Figure 15), but overall location and intensity are still very good.

Figure 49 shows the 18-h forecast, valid at 0600/21, and

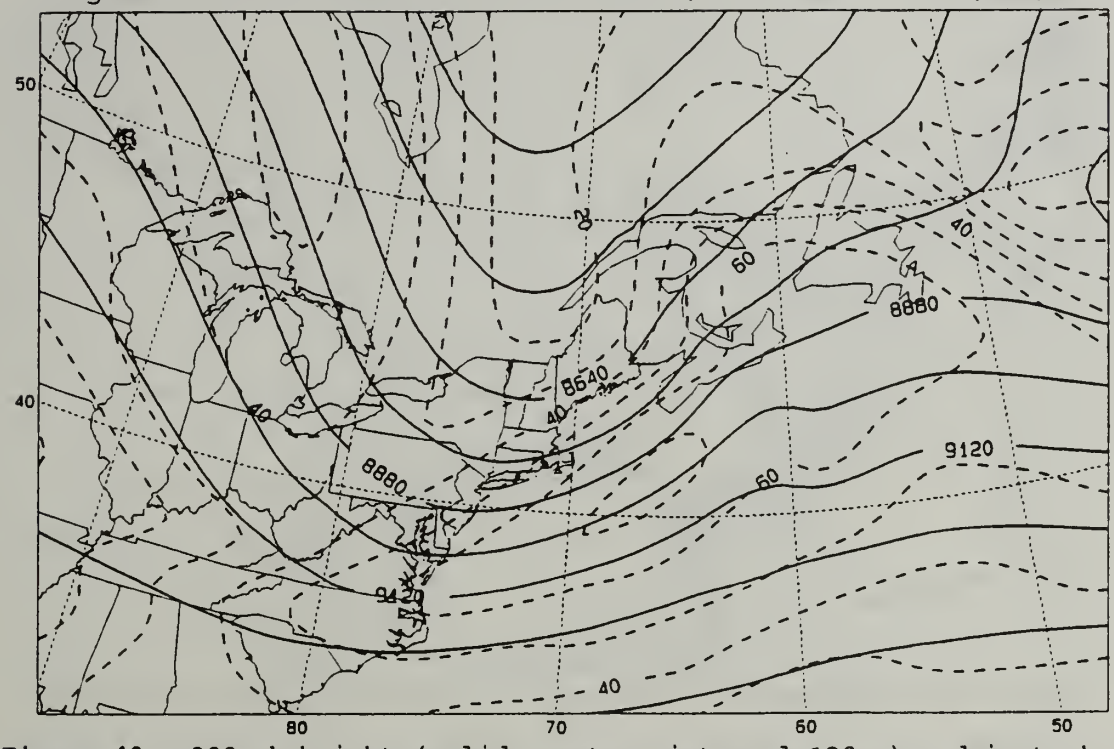

Figure 49. 300 mb height (solid, contour interval 120 m) and isotach (dashed, contour interval 10 m s^{-1}) forecast valid at 0600 UTC 21 January 1989.

indicates a slightly stronger jet maximum than was analyzed (not shown). At 1200/21, the (24-h) forecast intensity and location of the jet streak (not shown) closely resemble the analysis (Figure 27) for that time.

The 30-h forecast (Figure 50), valid at 1800/21, shows the jet streak further northeast on the eastern side of the upper-level trough than the analysis (not shown) indicates. The 60 m s^{-1} contour on the analysis extends further to the southwest than the forecast depicts. However, both fields indicate the same intensity of the maximum contour.

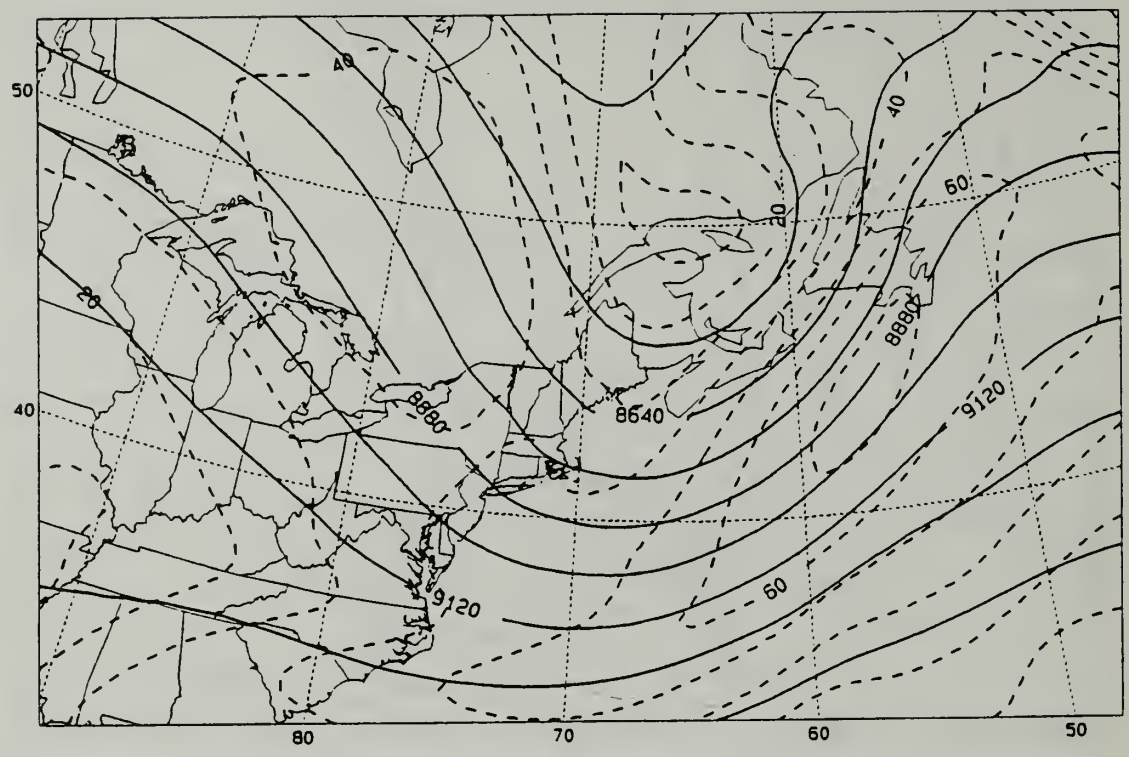

Figure 50. 300 mb height and isotach forecast as in Figure 49, except for 1800 UTC 21 January 1989.

A comparison of forecast versus analyzed 300 mb divergence was also conducted. At 1800/20, the 6-h forecast (not shown) and the analysis (Figure 11) both indicate a divergence value of 2×10^{-5} s^{-1} over the surface low and northeastward from the left exit region of the jet maximum. The 18-h forecast (Figure 51) shows much stronger divergence east of the surface low than indicated in the analysis (Figure 23). This forecast divergence correlates well with the intense cloud band that extends southward from east of the cyclone at this time. At 1200/21, the 24-h forecast (not shown) agrees much more closely with the analyzed divergence field (Figure 28).

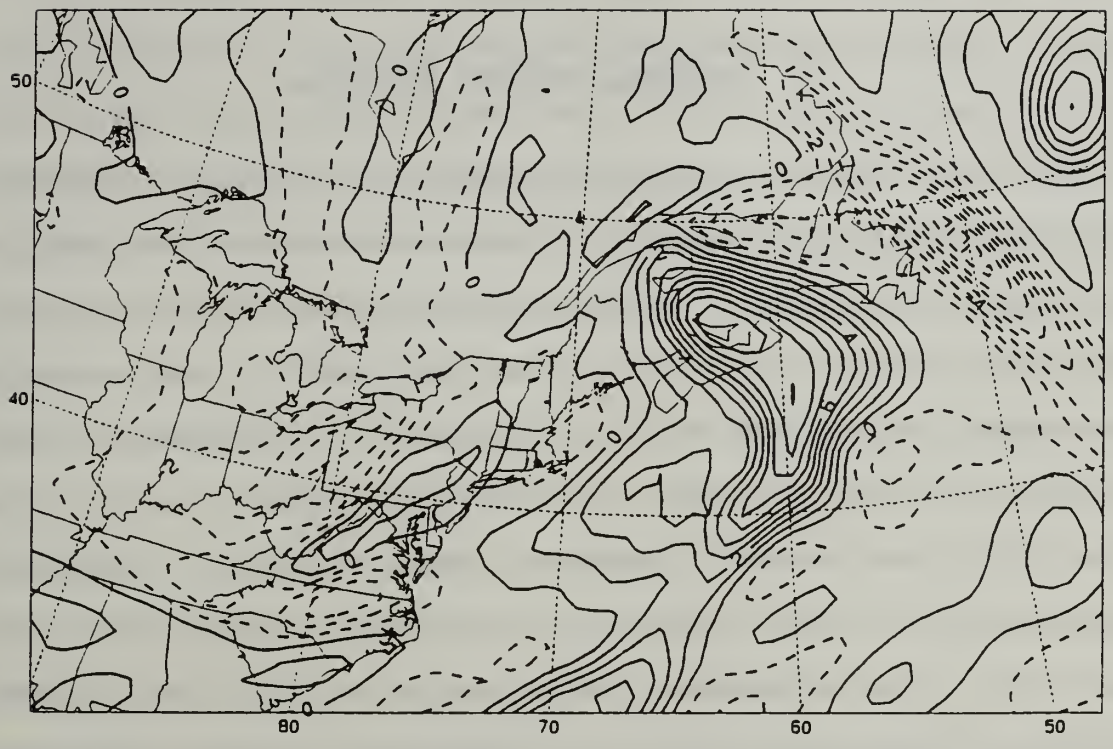

Figure 51. 300 mb divergence (solid, contour interval $1x10^{-5}$ s^{-1}) forecast valid at 0600 UTC 21 January 1989.

F. SUMMARY

From the above discussion, it is evident that the overall performance of NORAPS in predicting this case of rapid cyclogenesis was good. The major features such as the MSLP and thickness fields, 500 mb geopotential heights and absolute vorticity centers and 300 mb jet streak and divergence patterns were all well-represented by the forecast fields.

V. VERTICAL MOTION ANALYSIS

In this chapter, various estimates of vertical velocities will be examined in order to better understand the IOP-5A cyclone's development. While synoptic-scale vertical motions are usually small, they are an important tool in the study of processes associated with cyclogenesis. Knowledge of the vertical motion fields can provide insight as to the distribution of sensible weather elements such as clouds and precipitation (Dunn, 1991). A second objective of this section is to determine the accuracy of the NORAPS model forecast of vertical motions. A comparison of several methods of computing omega will be used to achieve this end.

A. METHODS OF CALCULATING VERTICAL VELOCITY

Three determinations of omega were used for the comparison of vertical velocity. The first omega depiction utilized in the examination was the NORAPS calculation of vertical velocity. In this method, the model vertical velocity is derived in sigma coordinates using an internal computational scheme for vertically integrating the continuity equation within NORAPS.

In the next method, omega was computed kinematically[1] (with $\omega(1000)=0$) from the NORAPS analyzed wind fields, which were based on observational data. The advantages of the kinematic method of computing omega are that it is simple mathematically and numerically, and it implicitly includes diabatic and ageostrophic effects. Unfortunately, a disadvantage is that the divergence calculation and the resulting vertical motions are error-prone. But if divergence errors are correlated vertically, then the O'Brien (1970) adjustment technique[2] can be used to reduce the effect of cumulative bias error. In order to perform the kinematic calculation, a bottom boundary condition for ω must be specified; while a top condition must be available to apply the O'Brien adjustment. In the O'Brien method, omega is assumed to be zero at the top of the column, so the difference between the kinematic vertical motion at the column top and zero is the amount of "error" upon which to base the adjustment. Normally, to satisfy the need for boundary conditions, $\omega(1000)$ and ω at the column top are set to zero.

The analysis-based kinematic omega fields in this study were modified using the O'Brien adjustment technique so that

---

[1]In the kinematic method of calculating omega, the continuity equation is vertically integrated with divergence computed from finite differences of gridded horizontal winds.

[2]The O'Brien correction method changes the vertical velocity profile by an amount that linearly depends on the distance from the lowest surface. The "error" in omega at the top of the column is distributed throughout the column to arrive at the adjusted profile. Thus, the largest correction occurs at the top level.

omega at 25 mb (the top level) was zero. The model-generated forecast omega fields were checked against the kinematically derived, analysis-based, adjusted omega fields, and significant differences were found. After various tests, it was determined that the top and bottom boundary conditions for the kinematic adjusted omega calculations were best specified by utilizing the NORAPS forecast omega fields (rather than assuming $\omega=0$ at the top and bottom, as discussed above).

To aid in the comparison of vertical motion, a third method of calculating omega was deemed necessary. As in the previous method, omega was computed kinematically, but this time using the NORAPS forecast winds (as opposed to using observed/analyzed winds as in the above method). As above, the O'Brien adjustment was applied to these omega fields to make them more physically reasonable. Again, the omega calculation utilized boundary conditions obtained from the NORAPS forecast omega fields, instead of assuming $\omega=0$ at the top and bottom.

Understandably, these kinematic omega fields based on the forecast wind fields more closely resembled the model's omega fields than they resembled the kinematic omega fields derived from analyzed wind fields (based on observational data). The forecast-based adjusted kinematic omega fields were compared to analysis-based adjusted kinematic omega fields in order to examine the vertical motions associated with the IOP-5A cyclone.

It has already been shown that the NORAPS forecasts from the 1200/20 model run were quite accurate in detailing the evolution of the IOP-5A cyclone event at low, middle and upper levels and at all synoptic times during the 36-h forecast period. Therefore, it should be expected that the vertical motion fields generated from the model forecasts would display at least a fair degree of accuracy.

The concept that a model-based, dynamically consistent data set could supplement and extend observational interpretation is not new. Keyser and Uccellini (1987) proposed that regional models could be useful and sophisticated objective-analysis tools in mesoscale research due to their high-resolution, four-dimensional, dynamically consistent data sets. Consequently, their contention is that mesoscale processes can be investigated under "controlled" conditions by utilizing model data combined with observations in conducting case studies of mesoscale phenomena.

B. COMPARISONS OF VERTICAL MOTION ESTIMATES

For the sake of simplicity the vertical motion fields will be defined as follows: method #1 = NORAPS model vertical velocities (MVV); method #2 = adjusted kinematic omega based on analyzed wind fields, and using NORAPS vertical velocities as top and bottom boundary conditions (OKA); method #3 = adjusted kinematic omega based on forecast wind fields, and

using NORAPS vertical velocities as top and bottom boundary conditions (OKF).

The 700 mb level was chosen for this examination due to the strength of the vertical motions at this level. It will afford the best opportunity to study the differences among the three comparison fields. The MVV and OKF vertical motion estimates are the forecast omega fields from the 1200/20 NORAPS model run. The OKA vertical motion estimates are from the NORAPS multi-variate optimum interpolation objective analysis scheme at each analysis time.

An attempt at assessing the accuracy of the various depictions of vertical motion will be made using satellite imagery. While it is possible to infer some sense of where ascent and descent are taking place from the appearance (brightness, location, cloud type and extent) of clouds in the imagery, this method does have its limitations. It is impossible to quantify the comparison, or to detect rising but unsaturated air, and it is difficult to ascertain the low-level cloud structure, especially in the case of a cirrus deck obscuring lower cloud layers in infrared imagery.

1. 1800 UTC 20 January 1989

Figure 52 shows the three vertical motion depictions for the 6-h forecast valid time. In general, the MVV and OKF panels are very similar in all respects. While the OKA panel does show an overall rising and sinking pattern as expected

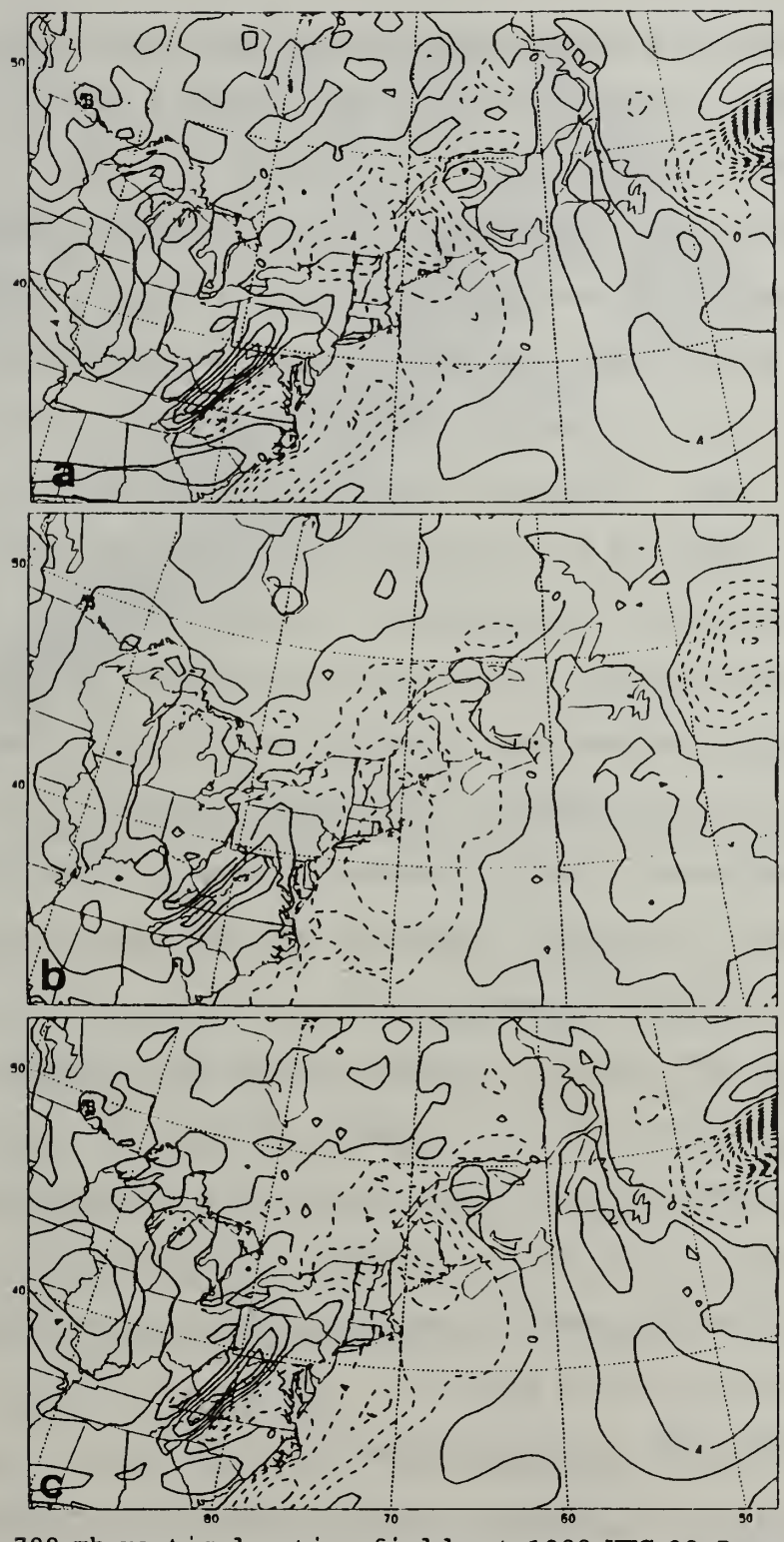

Figure 52. 700 mb vertical motion fields at 1800 UTC 20 January 1989. (a) is MVV, (b) is OKA, (c) is OKF. Positive (solid) for downward and negative (dashed) for upward motion. Contour interval is 2 $\mu b\ s^{-1}$.

with a developing cyclone, the magnitudes and concentration of the analyzed vertical motions were weaker and less detailed than the model forecasts.

Figure 53 shows the NORAPS terrain height field, delineating major orographic features within the model domain. Figure 52 also shows substantial vertical motion on all three panels in the vicinity of the mountains of Tennessee, Kentucky, West Virginia, North Carolina and Virginia at 1800/20. There is a cloud-free area in the satellite imagery (Figure 12) that corresponds to downward motion on the lee side of the mountains. All three fields show this subsidence, with sinking air over the general vicinity of the Appalachian mountains. On the MVV and OKF charts there is upward motion shown downstream of the mountains, over western North Carolina and Virginia extending eastward to Maryland which is not indicated in the IR imagery.

The MVV and OKF panels (based on forecasts) show a relatively narrow band of upward motion of -4 μb s^{-1} and stronger offshore from South Carolina to Massachusetts that corresponds to the bright frontal cloud area on satellite imagery. The OKA panel (based on the analysis) shows weaker upward motion in this area.

2. 0000 UTC 21 January 1989

Figure 54 presents the three vertical motion fields, valid at 0000/21, 12 h into the forecast. The MVV and OKF

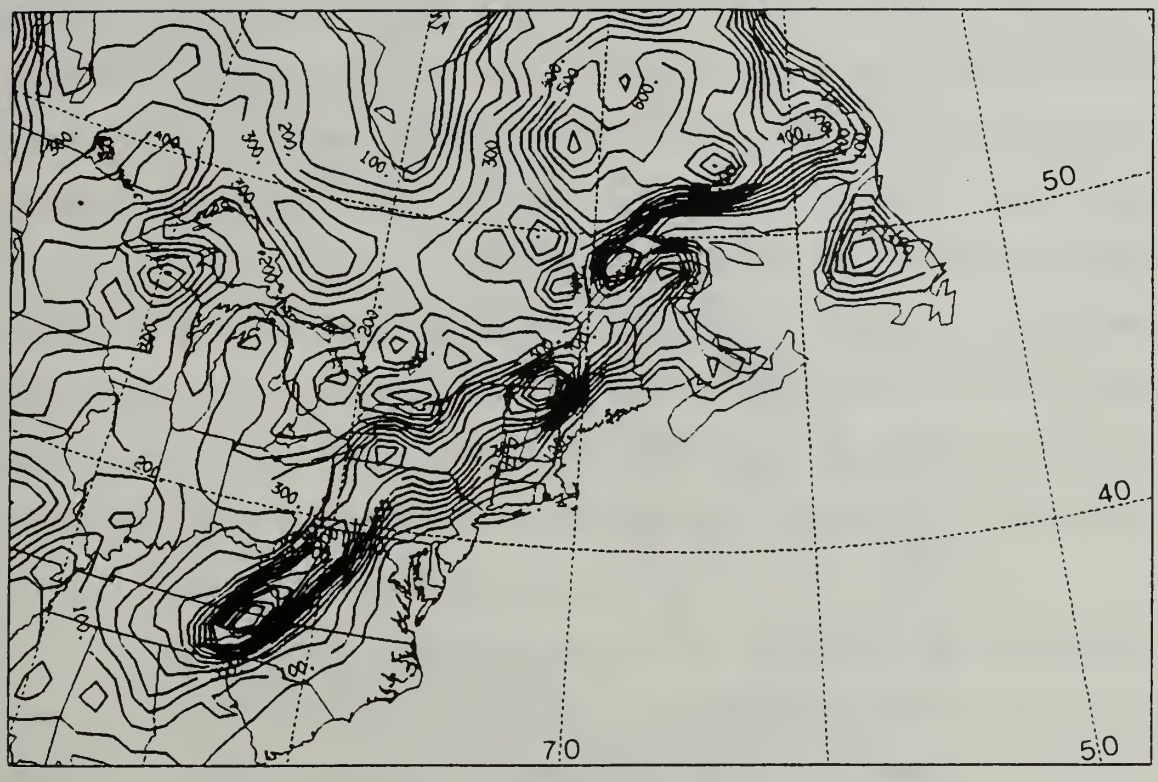

Figure 53. NORAPS surface terrain height (solid, contour interval 50 m) for January 1989.

fields remain very similar, with MVV showing the strongest overall vertical motions, but no more than 2 μb s^{-1} stronger than OKF. Intense forecast vertical motion (seen in the MVV and OKF fields) is found in a band south of the developing cyclone. The OKA field's upward motion area is broader and less intense than MVV and OKF, but is in the same general area. This area still corresponds to the bright cloud area in satellite imagery (Figure 17).

Northeast of the surface low (from the Saint Lawrence River to Lake Ontario), all three fields show rising motion of similar magnitudes. Over the Appalachians, the long and narrow 10 μb s^{-1} contour in the MVV and OKF fields shows the

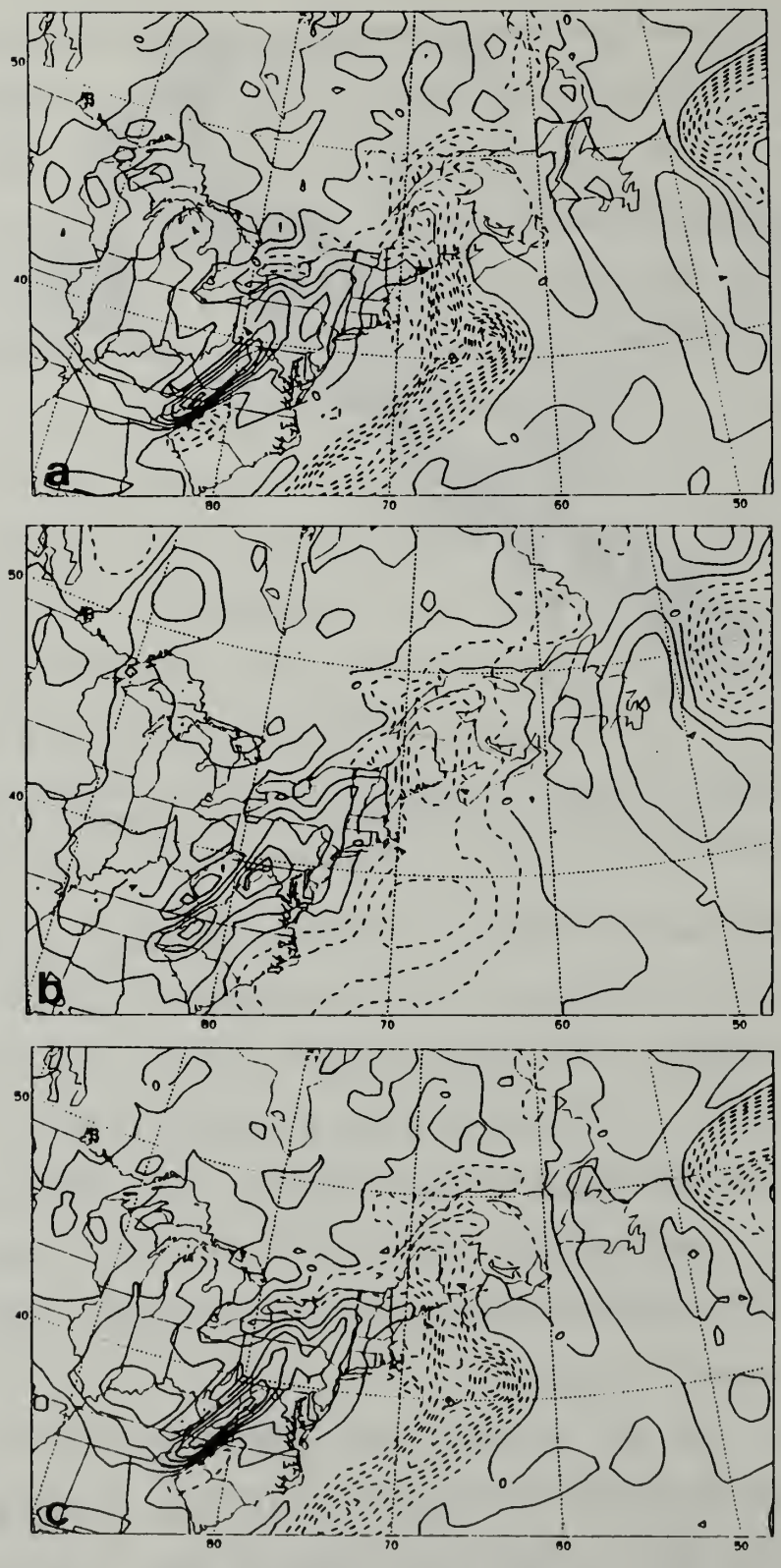

Figure 54. 700 mb vertical motion fields as in Figure 52, except for 0000 UTC 21 January 1989.

maximum subsidence right along the mountain peak. The dark cloud-free area on satellite imagery (Figure 17) extends over North Carolina and Virginia northeastward to offshore of Delaware and New Jersey. Directly next to the southeast edge of the subsidence is an area of weak ascent on the MVV and OKF charts. The OKA depiction shows weaker subsidence centered just east of the mountain peak, and weak rising motion to the northwest. There is evidence of low clouds over West Virginia in the satellite imagery to support the upslope rising motion.

3. 0600 UTC 21 January 1989

This is the 18-h forecast time, and rapid cyclogenesis has occurred over the last 6 h. The MVV and OKF fields are similar to each other, and indicate stronger vertical motion patterns associated with the IOP-5A storm and the orographic effects of the Appalachian mountains than are shown in the analysis (Figure 55). The maximum upward motion shown in the OKA field has a value of -16 $\mu b\ s^{-1}$, located east of the surface low, north of 40N. The MVV and OKF fields show much stronger ascent near 43N 61W, with a maximum value of -28 $\mu b\ s^{-1}$. Intense upward motion extends southwest along the cold front as well. All three panels continue to show the orographically induced vertical motions, with the subsidence along the mountain ridge-line and upstream (northwest) shown as being weaker and offset slightly further east on the OKA computation.

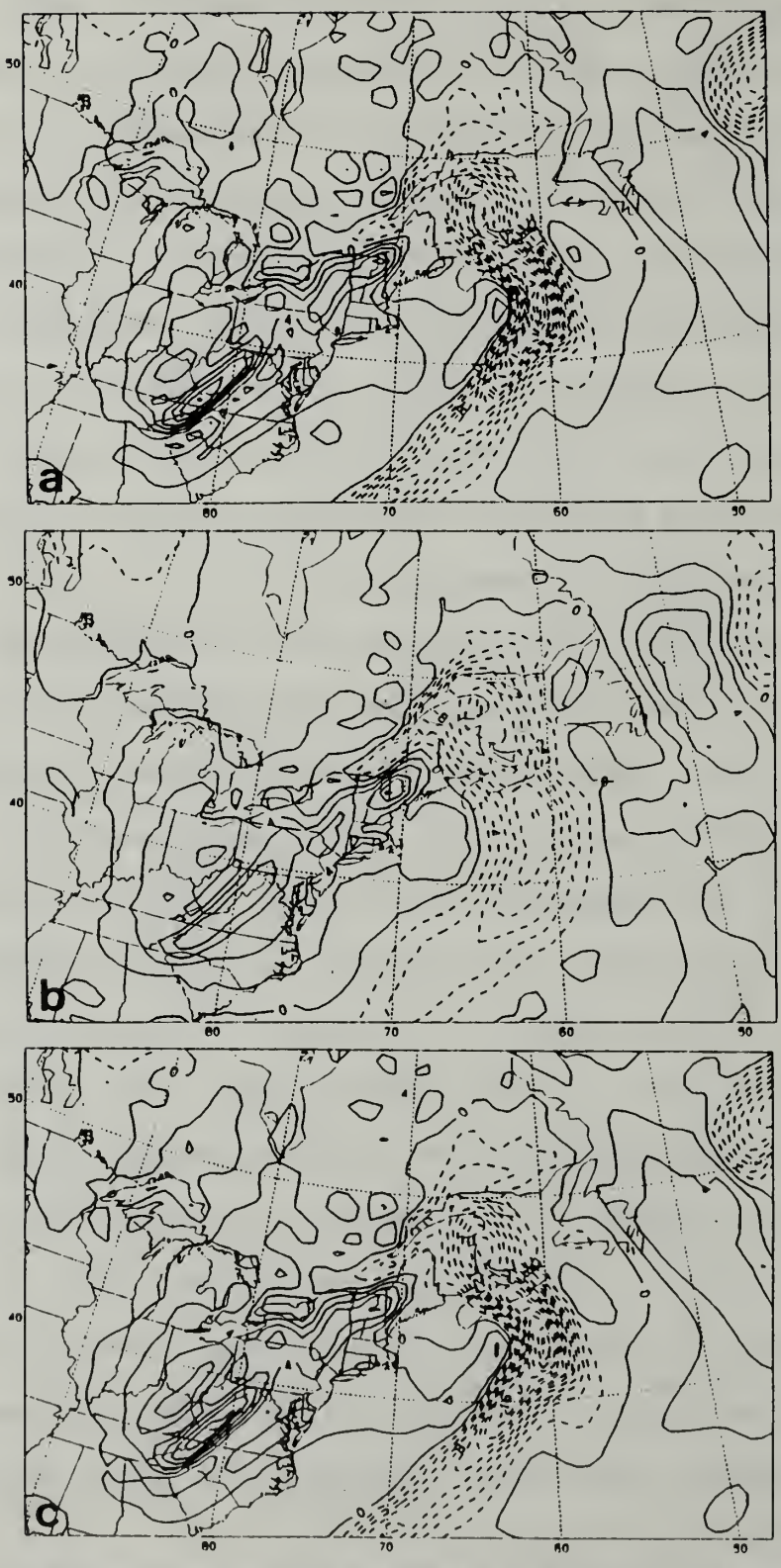

Figure 55. 700 mb vertical motion fields as in Figure 52, except for 0600 UTC 21 January 1989.

The IR satellite imagery (Figure 20) now shows clear skies east of the Appalachians correlating with the subsidence indicated on all three fields (Figure 55) over the Eastern Seaboard states. The comma cloud associated with the IOP-5A cyclone still has the brightest (coldest) clouds southeast of the low center, east of a line from 38N 67W to 47N 59W, which again correlates well with the location of the strongest vertical motions depicted in all three fields. North of 40N the clouds extend to approximately 53W. There are slightly warmer cloud-top temperatures indicated throughout the "comma head" area north of the surface low. Thus all three fields appear to indicate the proper location of the vertical motions.

4. 1200 UTC 21 January 1989

This is the 24-h forecast time, and the end of the rapid deepening period. Figure 56 continues to show the MVV and OKF vertical motions remaining much stronger than OKA's, particularly in the offshore region southeast of Newfoundland. The ascent area southeast of the surface low has decreased on all three charts, while the upward vertical motion maximum north of the surface low has intensified. The northern portion of the band of strong upward motion appears more cyclonically curved around the low. The upward vertical motion maximum on the OKA chart has shifted to the southeast of its previous position, now located halfway between the two

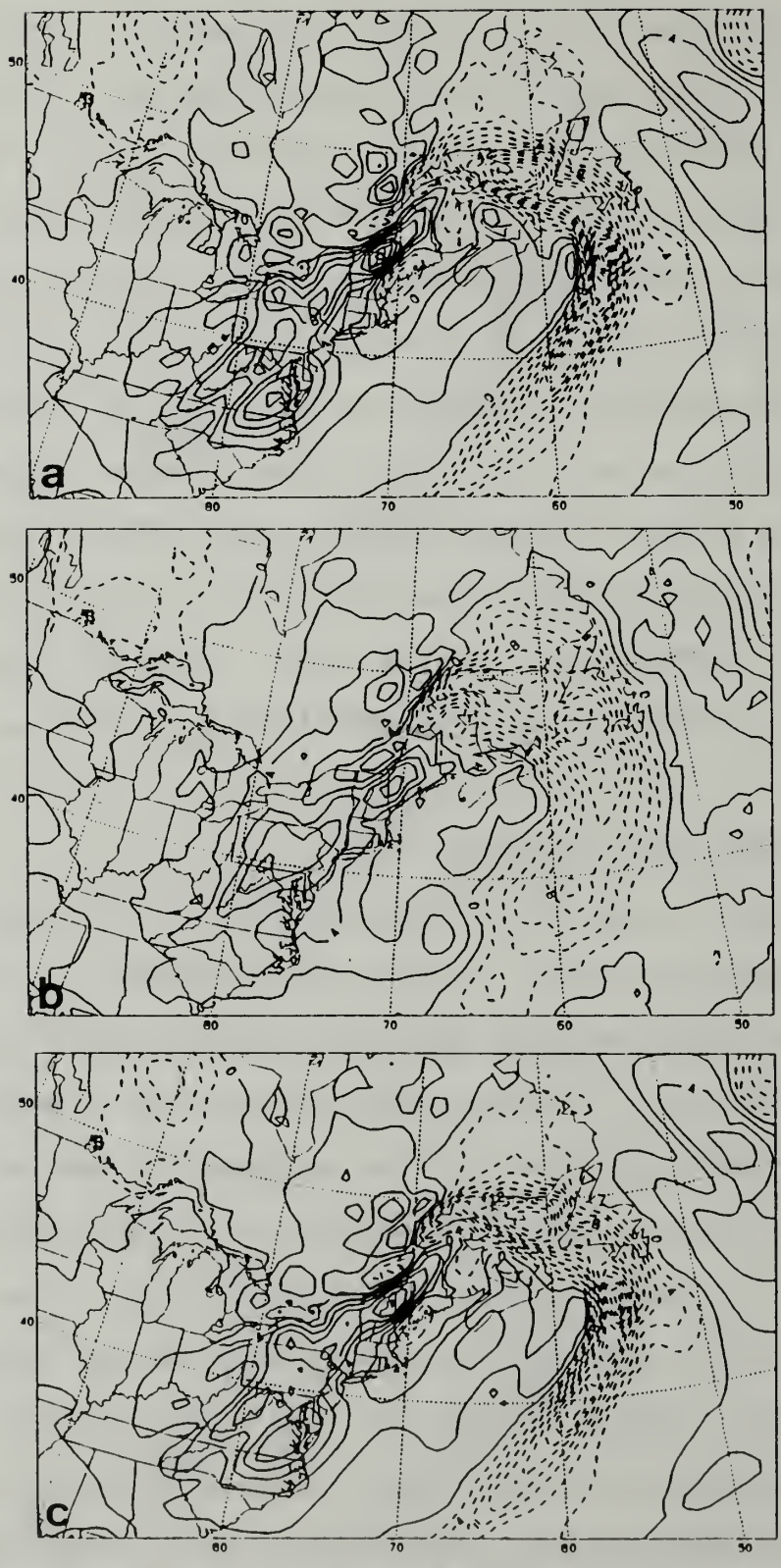

Figure 56. 700 mb vertical motion fields as in Figure 52, except for 1200 UTC 21 January 1989.

separate maxima on the MVV and OKF charts (north and east of the surface low). Orographic influences on the vertical motions over the mountains of northern Vermont and New Hampshire are evident on all three panels due to the strong northwesterly flow over the northern Appalachians.

Satellite imagery for this time (Figure 24) shows cold, high clouds wrapping around the north and west of the surface low, with evidence of the dry slot intruding to the southeast of the low center. The increased cyclonic curvature depicted in the vertical motion fields is supported by the cloud band appearance in the imagery. The coldest area on enhanced IR imagery remains near the area of maximum vertical motion. The southern end of the cold frontal cloud band seems to connect with the cloudy area further southwest (emanating from the Gulf of Mexico) so that cloudiness is continuous all the way across Florida. The OKF and MVV panels indicate much stronger upward motion over the southern portion of the cold front than the OKA panel does, in better agreement with the imagery. Lee-side subsidence is evident as the southern Maine coast and coastal plain are clear in the satellite picture.

5. 1800 UTC 21 January 1989

The magnitude of the upward motion in the comma cloud band has decreased slightly in all three panels (Figure 57). The MVV and OKF fields continue to show much stronger vertical motions than the OKA field shows, especially in the upward

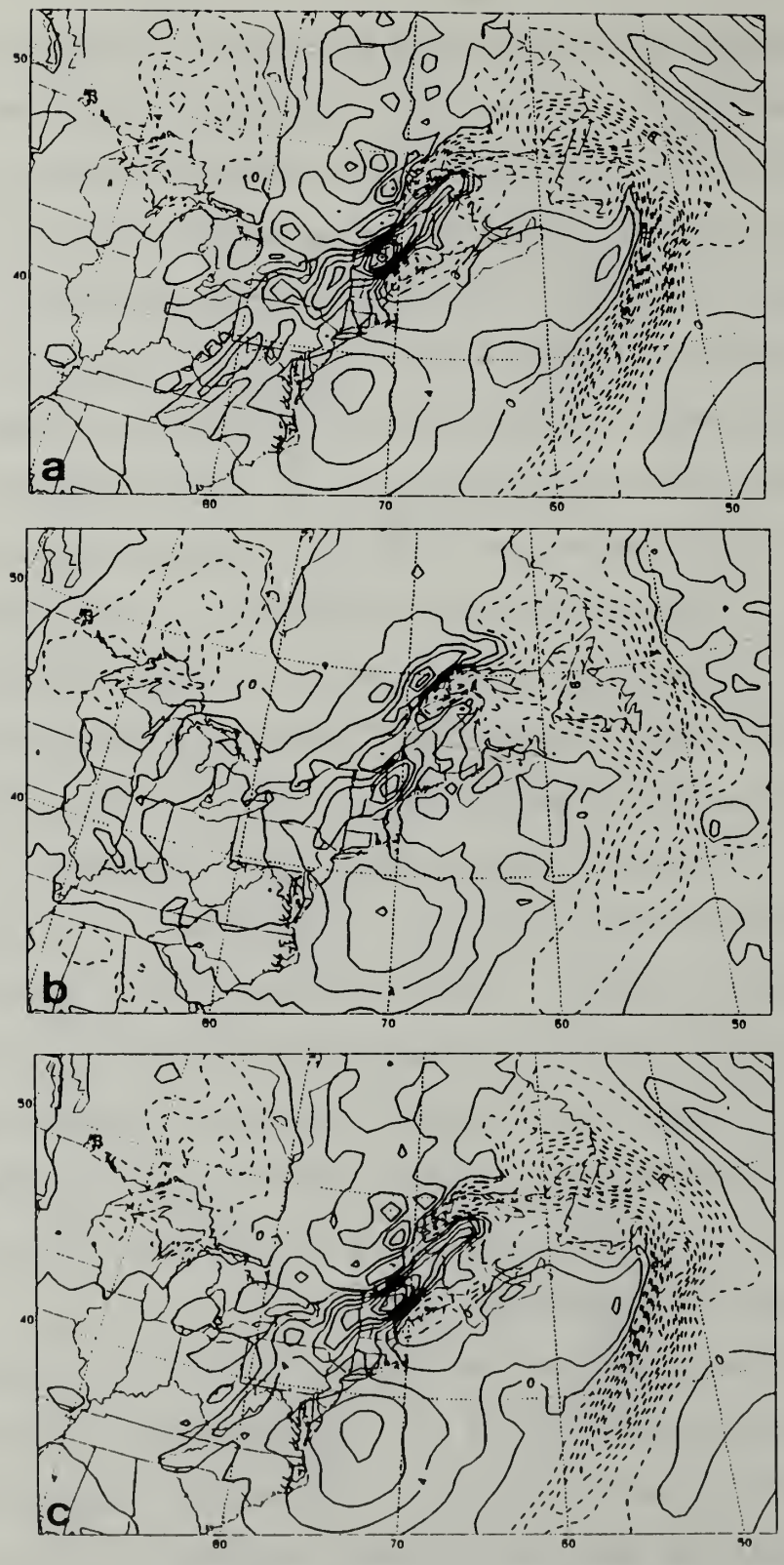

Figure 57. 700 mb vertical motion fields as in Figure 52, except for 1800 UTC 21 January 1989.

motion maximum southeast of Newfoundland and the southwestward extension of the cold-frontal cloud band. Stronger subsidence is also evident along the northern Appalachians.

The coldest and brightest clouds associated with the IOP-5A cyclone are now east of Newfoundland (Figure 33). The bright cloud band continues to wrap around the surface low, lending credence to the vertical motion depictions of all three fields. While the vertical motion fields indicate ascent south of Maine, satellite imagery shows this area as being clear. All three charts show rising motion at the mouth of the Saint Lawrence River and near 40N 62W, and cloudiness is evident over these areas in the imagery.

6. Summary

The observed and forecast fields appear to provide a suitably accurate estimate of vertical motion. The frontal cloud band associated with the IOP-5A cyclone is expected to be a region of intense upward motion, especially in the area of the warm conveyor belt as described by Carlson (1980). The vertical motion fields derived from the NORAPS forecast wind fields exhibited much more intense upward motion than those from the NORAPS analyses. The lack of over-ocean observations is probably responsible for the apparent weakness of the vertical motion fields derived from the analyses. The forecast vertical motion captured a secondary maximum southwest of the cyclone that correlated with the area of

coldest IR cloud-top temperatures. Distinct subsidence was found in the lee of the Appalachians to the west of the cyclone.

VI. CONCLUSIONS AND RECOMMENDATIONS

A. CONCLUSIONS

Analysis of the synoptic forcing associated with the development of the cyclone observed during ERICA IOP-5A revealed that a variety of processes made important contributions to the rapid deepening. Significant lower-tropospheric thermal advection was evident several hours preceding the rapid intensification. The thickness field evolved into the classic "S-shaped" pattern often observed during intense cyclogenesis. Favorable superposition of a mobile 500 mb trough over the frontal wave provided positive vorticity advection aloft, which aided the explosive development of the storm as well.

The presence of a jet streak on the eastern side of the 300 mb trough also had a significant influence on the evolution of the system. This jet streak, and the ageostrophic circulation associated with its exit region, was associated with focused upper-level divergence and enhanced vertical motions. Intense upward vertical motion was found throughout the cyclone's frontal cloud band, with an area of strong ascent originating in the warm conveyor belt that propagated northward to merge with the cyclone system during rapid development.

In order to examine the mesoscale structure of the IOP-5A cyclone, manually-produced subjective analyses were completed for the early period of rapid development. These analyses indicated that coastal cyclogenesis occurred prior to the onset of explosive deepening. The mesoscale coastal vortex, which may have formed as the result of topographic effects, developed south of the primary low, deepened and tracked along the Maine coast appearing to merge with the original low. An analysis of 500 - 1000 mb equivalent potential temperature prior to rapid deepening indicated that the New England coast and offshore region was markedly less stable than the interior of Maine. This aided the coastal development and subsequent rapid intensification of the "merged" system when it reached the near-coastal unstable environment.

On the synoptic scale, the NORAPS model forecasts produced a realistic simulation of the rapid cyclogenesis event. The important large-scale features such as location and intensity of the 500 and 300 mb troughs, vorticity centers, jet streak and upper-level divergence areas were represented well. Thus, the model forecasts of the IOP-5A cyclone's position and intensity were relatively accurate. A characteristic of numerical cyclone forecasts is that they tend to deepen and fill cyclones more slowly than is observed. This type of error, although small, was present in the NORAPS forecast of the IOP-5A cyclone.

Significant differences were found between the vertical motion fields derived from the model output wind fields and those derived from the analyzed winds. The vertical motion derived from the forecast wind fields indicated much stronger ascent in the frontal cloud regions of the storm system than did the analyzed vertical motion. Judging from the appearance (brightness or cloud-top temperature, location, cloud type and extent) of the major cloud features in the satellite imagery, the model-derived fields appear to be a more reasonable estimate of vertical motions associated with the system. The probable reason for the weakness of the analysis-based vertical motion fields is the lack of over-ocean data from which to calculate omega.

B. RECOMMENDATIONS

A significant result of this study is the verification of the development of a mesoscale coastal low that is not represented in the NORAPS analyses or forecasts. It is conceivable that the development of this coastal low affected the rapid cyclogenesis of the IOP-5A cyclone. Unfortunately, the details of these effects remain unclear. Further studies of the mesoscale processes involved in the deepening of the storm system are clearly needed. A more quantitative mesoscale study with the specific goal of analyzing the cyclogenetic effect of the static stability in the coastal region would also be worthwhile.

Due to the general accuracy of the NORAPS model's simulation, the model output data is ideally suited for use in more elaborate diagnostic studies. The model data could be utilized to:

(i) Compare an adiabatic or mountainless simulation with the full physics simulation utilized in this study to examine effects of latent heat release and topography on the IOP-5A storm;

(ii) Study trajectories in the warm conveyor belt; and

(iii) Compare the coastal development and track of the IOP-5A cyclone with other oceanic cases such as the IOP-5 and IOP-4 storms.

Finally, as this study was primarily a qualitative overview of the IOP-5A cyclone's development, future research efforts should concentrate on performing more quantitative studies of the ERICA observational data and numerical model data. Quantitative diagnostic studies focusing on specific features or processes will greatly increase our understanding of rapid cyclogenesis in general and the IOP-5A storm's life cycle in particular.

LIST OF REFERENCES

Anthes, R. A., Y-. H. Kuo, and J. R. Gyakum, 1983: Numerical simulations of a case of explosive marine cyclogenesis. *Mon. Wea. Rev.*, **111**, 1174-1188.

Bosart, L. F., 1981: The President's Day snowstorm of 18-19 February 1979: A subsynoptic-scale event. *Mon. Wea. Rev.*, **109**, 1542-1566.

Boyle, J. S., and L. F. Bosart, 1986: Cyclone-anticyclone couplets over North America. Part II: Analysis of a major cyclone event over the eastern United States. *Mon. Wea. Rev.*, **114**, 2432- 2465.

Carlson, T. N., 1980: Airflow through midlatitude cyclones and the comma cloud pattern. *Mon. Wea. Rev.*, **108**, 1498-1509.

Dirks, R. A., J. P. Kuettner, and J. A. Moore, 1988: Genesis of Atlantic Lows Experiment (GALE): An overview. *Bull. Amer. Meteor. Soc.*, **69**, 147-160.

Dunn, L. B., 1991: Evaluation of vertical motion: Past, present and future. *Wea. Forecasting*, **6**, 65-75.

Emanuel, K. A., 1983: On assessing local conditional symmetric instability from atmospheric soundings. *Mon. Wea. Rev.*, **111**, 2016-2033.

Hadlock, R., and C. W. Kreitzberg, 1988: The Experiment on Rapidly Intensifying Cyclones over the Atlantic (ERICA) field study: Objectives and plans. *Bull. Amer. Meteor. Soc.*, **69**, 1309-1320.

____, E. Hartnett, and G. Forbes, 1989: The Experiment on Rapidly Intensifying Cyclones over the Atlantic (ERICA) Field Phase Summary. [Available from ERICA Data Center, Department of Physics and Atmospheric Science, Drexel University, Philadelphia, Pennsylvania 19104.], 388 pp.

Hirschberg, P. A., and J. M. Fritsch, 1991a: Tropopause undulations and the development of extratropical cyclones. Part I: Overview and observations from a cyclone event. *Mon. Wea. Rev.*, **119**, 496-517.

____, and ____, 1991b: Tropopause undulations and the development of extratropical cyclones. Part II: Diagnostic analysis and conceptual model. *Mon. Wea. Rev.*, **119**, 518-550.

____, and R. H. Langland, 1992: The effects of a mesoscale tropopause undulation in a numerical simulation of the cyclogenesis event during ERICA IOP 5A. Fifth Conference on Mesoscale Processes January 5-10, 1992

Hodur, R. M., 1987: Evaluation of a regional model with an update cycle. *Mon. Wea. Rev.*, **115**, 2707-2718.

Hoskins, B. J., M. E. McIntyre, and A. W. Robertson, 1985: On the use and significange of isentropic potential vorticity maps. *Quart. J. Roy. Meteor. Soc.*, **111**, 877-946.

Keyser, D., and L. W. Uccellini, 1987: Regional models: Emerging research tools for synoptic meteorologists. *Bull. Amer. Meteor. Soc.*, **68**, 306-320.

Kocin, P. J., and L. W. Uccellini, 1990: *Snowstorms Along the Northeastern Coast of United States: 1955 to 1985.* Meteorological Monographs. American Meteorological Society, 280 pp.

Kuo, Y-. H., and S. Low-Nam, 1990: Prediction of nine explosive cyclones over the Western Atlantic ocean with a regional model. *Mon. Wea. Rev.*, **118**, 3-25.

____, R. J. Reed, and S. Low-Nam, 1991: Effects of surface energy fluxes during the early development and rapid intensification stages of seven explosive cyclones in the Western Atlantic. *Mon. Wea. Rev.*, **119**, 457-476.

Nuss, W. A., and S. I. Kamikawa, 1990: Dynamics and boundary layer processes in two Asian cyclones. *Mon. Wea. Rev.*, **118**, 755-771.

O'Brien, J. J., 1970: Alternative solutions to the classical vertical velocity problem. *J. Appl. Meteor.*, **9**, 197-203.

Pauley, P. M., and P. J. Smith, 1988: Direct and indirect effects of latent heat release on a synoptic-scale wave system. *Mon. Wea. Rev.*, **116**, 1209-1235.

Petterssen, S., 1956: *Weather Analysis and Forecasting*, 2nd ed., Vol. 1. McGraw-Hill, 428 pp.

Roebber, P. J., 1984: Statistical analysis and updated climatology of explosive cyclones. *Mon. Wea. Rev.*, **111**, 723-744.

Rogers, E., and L. F. Bosart, 1986: An investigation of explosively deepening oceanic cyclones. *Mon. Wea. Rev.*, **114**, 702-718.

Sanders, F., and J. R. Gyakum, 1980: Synoptic-Dynamic climatology of the "bomb". *Mon. Wea. Rev.*, **108**, 1589-1606.

____, 1986a: Explosive cyclogenesis in the west-central North Atlantic ocean, 1981-1984. Part I: Composite structure and mean behavior. *Mon. Wea. Rev.*, **114**, 1781-1794.

____, 1986b: Explosive cyclogenesis in the west-central North Atlantic ocean, 1981-1984. Part II: Evaluation of LFM model performance. *Mon. Wea. Rev.*, **114**, 2207-2218.

____, 1987: Skill of NMC operational dynamical models in predicting explosive cyclogenesis. *Wea. Forecasting*, **2**, 322-336.

Sinclair, M. R., and R. L. Elsberry, 1986: A diagnostic study of baroclinic disturbances in polar air streams. *Mon. Wea. Rev.*, **114**, 1957-1983.

Stewart, R. E., R. W. Shaw, and G. A. Isaac, 1987: Canadian Atlantic Storms Program: The meteorological field project. *Bull. Amer. Meteor. Soc.*, **68**, 338-345.

Uccellini, L. W., P. J. Kocin, R. A. Petersen, C. H. Wash, and K. F. Brill, 1984: The President's Day cyclone of 18-19 February 1979: Synoptic overview and analysis of the subtropical jet streak influencing the pre-cyclogenetic period. *Mon. Wea. Rev.*, **112**, 2540-2541.

____, 1990: Processes contributing to the rapid development of extratropical cyclones. *Extratropical Cyclones The Erik Palmén Memorial Volume*, C. Newton, and E. O. Holopainen, Eds., Amer. Meteor. Soc., 81-105.

Wash, C. H., J. E. Peak, W. F. Calland, and W. A. Cook, 1988: Diagnostic study of explosive cyclogenesis during FGGE. *Mon. Wea. Rev.*, **116**, 431-451.

INITIAL DISTRIBUTION LIST

		No. Copies
1.	Defense Technical Information Center Cameron Station Alexandria VA 22304-6145	2
2.	Library, Code 052 Naval Postgraduate School Monterey CA 93943-5002	2
3.	Chairman (Code MR/Hy) Department of Meteorology Naval Postgraduate School Monterey CA 93943-5000	1
4.	Professor Carlyle H. Wash (Code MR/Wx) Department of Meteorology Naval Postgraduate School Monterey CA 93943-5000	3
5.	Professor Paul A. Hirschberg (Code MR/Hs) Department of Meteorology Naval Postgraduate School Monterey CA 93943-5000	1
6.	LT Julia M. Spinelli NOCD Naval Air Station Alameda CA 94501-5011	1
7.	Director Naval Oceanography Division Naval Observatory 34th and Massachusetts Avenue NW Washington DC 20390	1
8.	Commander Naval Oceanography Command Stennis Space Center MS 39529-5001	1
9.	Commanding Officer Fleet Numerical Oceanography Center Monterey CA 93943-5005	1
10.	Commanding Officer Naval Oceanographic and Atmospheric Research Laboratory	1

Stennis Space Center
MS 39529-5004

11. Chief of Naval Research 1
800 N. Quincy Street
Arlington VA 22217

Thesis
S66853 Spinelli
c.1 An investigation of the
ERICA IOP-5A cyclone.